

# INTEGRATED COMPONENT-SPECIFIC MEASUREMENTS TO DEVELOP EMISSION FACTORS FOR COMPRESSORS AND GAS GATHERING LINES

**FINAL REPORT**

**DE-FE0029084**



**Issued: 1 October 2018**

**Prepared for:** Department of Energy - National Energy Technology Laboratory  
(DOE NETL)



**GSI Environmental Inc.**

9600 Great Hills Trail, Suite 350E, Austin, TX 78759  
Tel: 512.346.4474  
[www.gsi-net.com](http://www.gsi-net.com)

**Utah State University Bingham Research Center**

320 N. Aggie Blvd., Vernal, UT 84078  
[www.binghamresearch.usu.edu](http://www.binghamresearch.usu.edu)

**Houston Advanced Research Center**

8801 Gosling Road, The Woodlands, TX 77381  
[www.harcresearch.org](http://www.harcresearch.org)

**Colorado State University**

Fort Collins, CO 80523  
[www.colostate.edu](http://www.colostate.edu)

## Table of Contents

<b>EXECUTIVE SUMMARY .....</b>	<b>1</b>
<b>1.0 INTRODUCTION .....</b>	<b>1</b>
1.1 Background .....	1
1.1.1 Regulations & Current Literature .....	1
1.1.2 General Equipment at G&B Stations .....	2
1.2 Overall Project Approach .....	3
<b>2.0 METHODS .....</b>	<b>4</b>
2.1 Participating Field Sites .....	4
2.2 Overview of Field Campaigns .....	4
2.3 Component Classification and Count .....	7
2.3.1 Equipment Type .....	7
2.3.2 Component Type .....	7
2.4 Technologies .....	9
2.4.1 Optical Gas (FLIR) Imaging .....	9
2.4.2 High Volume Sampling System .....	10
2.4.3 High Volume Field Measurements .....	11
2.4.4 Open Path – Fourier Transform Infrared Spectrometer .....	11
2.5 Screening and Measurements Summary .....	12
2.6 Data Analysis .....	13
2.6.1 High Volume Emission Rates and Non-Detects .....	13
2.6.2 Statistical Analyses .....	14
2.6.3 Emission Factor Calculations .....	14
2.6.4 OP-FTIR Tracer Analysis .....	15
2.7 Plume Visualization Model .....	16
<b>3.0 RESULTS AND DISCUSSION .....</b>	<b>17</b>
3.1 Component Population Counting Methodology .....	17
3.2 Appropriateness of Component Categories in the GHGRP .....	19
3.3 Emission Rate Variability by Site and Operational Parameters .....	22
3.4 Temporal Variability in Emission Rates .....	24
3.4.1 Quarterly Emission Rate Variability .....	25
3.4.2 Emission Rate Variability During Sample Measurements .....	27
3.5 Emissions Comparison – Measured vs. Estimated .....	32
3.6 Data Visualization .....	33
<b>4.0 TECHNOLOGY TRANSFER .....</b>	<b>35</b>
<b>5.0 CONCLUSIONS AND RECOMMENDATIONS .....</b>	<b>37</b>
<b>6.0 REFERENCES .....</b>	<b>38</b>

## TABLES

<b>Table 2-1.</b> Summary of project field campaigns.....	5
<b>Table 2-2.</b> Equipment counts for participating field sites.....	5
<b>Table 2-3.</b> Component categories and subcategories from the component classification protocol.....	8
<b>Table 2-4.</b> Screened population and measurement counts.....	13
<b>Table 3-1.</b> Emission factors currently included in the GHGRP.....	20
<b>Table 4-1.</b> List of TASC Participants .....	35
<b>Table 4-2.</b> Technology Transfer Events.....	36

## FIGURES

<b>Figure 1-1.</b> Example schematic of a G&B station from this study.....	3
<b>Figure 2-1.</b> Operational compressors by site and field campaign.....	6
<b>Figure 2-2.</b> Field method summary for component emissions.....	6
<b>Figure 2-3.</b> Major equipment types at G&B Stations: a) compressor, b) separator, c) dehydrator, d) yard piping, e) coalescer, f) slug catcher, g) tanks, and h) gathering lines .....	7
<b>Figure 2-4.</b> Major component types: a) connector, b) valve, c) pressure relief valve, d) meter, e) gauge, f) regulator, g) pneumatic device, h) compressor vent. ....	8
<b>Figure 2-5.</b> a) Screening a pneumatic device with the FLIR OGI Camera, b) compressor rod packing vent, c) FLIR view of compressor rod packing vent.....	9
<b>Figure 2-6.</b> a) USU sampling trailer with high volume tubing connected, b) interior of trailer, c) bagged pneumatic device for sampling .....	10
<b>Figure 2-7.</b> OP-FTIR spectrometer .....	12
<b>Figure 2-8.</b> OP-FTIR/tracer sampling schematic .....	12
<b>Figure 3-1.</b> Average component count by equipment type, including gas and liquid lines .....	18
<b>Figure 3-2.</b> Average component count by equipment type, gas lines only.....	18
<b>Figure 3-3.</b> Measured methane emission rates by component type and site.....	21
<b>Figure 3-4.</b> Distance piece vent emissions vs. emission rate rank .....	23
<b>Figure 3-5.</b> Distance piece vent emissions by site plotted against compressor age .....	24
<b>Figure 3-6.</b> Component leak/malfunction and vent rates by site and field campaign .....	25
<b>Figure 3-7.</b> Component leak and vent rates by individual compressor and field campaign.....	26
<b>Figure 3-8.</b> High-flow 20 second emission rate measurements on a distance piece vent .....	28
<b>Figure 3-9.</b> Within measurement variability vs. high-flow sample duration for all components and field campaigns .....	28
<b>Figure 3-10.</b> Comparison of within measurement variability between pneumatic device vents and all other component types .....	29
<b>Figure 3-11.</b> Measured site-wide leaks compared to leaks calculated using USEPA leaker and population factors.....	33

**Figure 3-12.** *Hypothetical estimated methane plume for measured methane emissions from Compressors 13, 14, and 15 at Site 1 during Field Campaign 2* ..... 34

## APPENDICES

**Appendix A.** *Fugitive Emissions Screening Procedures, Equipment, and Specifications*  
**Appendix B.** *High Volume Sampling Procedures, Equipment, and Specifications*  
**Appendix C.** *Component Classification and Count Protocol*  
**Appendix D.** *OP-FTIR Spectrometry Procedures, Equipment, and Specifications*  
**Appendix E.** *Plume Visualize Tool*  
**Appendix F.** *Emission Factors*  
**Appendix G.** *Additional Component Count Results*

## ACRONYMS AND ABBREVIATIONS

cf	cubic feet
CFR	Code of Federal Regulations
CH <sub>4</sub>	methane
d	diameter
DL	detection limit
DOE	Department of Energy
DPV	distance piece vent
EF	emission factor
ER	emission rate
ESD	emergency shut-down
ft <sup>3</sup>	cubic feet
g/hr	grams per hour
GHGI	Greenhouse Gas Inventory
GHGRP	Greenhouse Gas Reporting Program
G&B	gathering and boosting
GRI	Gas Research Institute
IR	infrared
KS	Kolmogorov-Smirnov
LGR	Los Gatos Research
m	meter
MCF	thousand cubic feet
MET	meteorological
MQI	method quality indicator
n/a	not applicable
NETL	National Energy Technology Laboratory
OGI	optical gas imaging
OP-FTIR	open path – Fourier transform infrared
PMP	project management plan
PRV	pressure relief valve
RPV	rod packing vent
RRPR	Research Performance Progress Report
scf/hr	standard cubic feet per hour
SF <sub>6</sub>	sulfur hexafluoride
TCS	Transmission Compressor Stations
USEPA	United States Environmental Protection Agency
USU	Utah State University

## EXECUTIVE SUMMARY

The Department of Energy (DOE) National Energy Technology Laboratory (NETL) and other critical stakeholders (e.g., U.S. Environmental Protection Agency (USEPA), state regulators, and industry) seek to more accurately characterize and quantify methane emissions from compressors and gathering lines within the Gathering and Boosting (G&B) segment of the natural gas system network. These efforts will reduce uncertainties in estimates of these emissions in USEPA's current Green House Gas Inventory (GHGI) under their Greenhouse Gas Reporting Program (GHGRP; EPA, 2016). These estimates are primarily based on data from other types of pipeline segments and may not accurately reflect the different characteristics of emissions from G&B compressors and gathering lines. For example, emission factors used to estimate methane emissions from the G&B segment are the same factors used for onshore natural gas production (USEPA, 2015 and 2016). A robust and representative dataset of emissions from G&B station components will inform future enhancements to the current GHGI.

For this study, four G&B stations in the Gulf Coast Area were visited four times over the course of one year. Components were classified according to equipment and component type and emissions from select components were measured based on initial screening procedures. The following major equipment types were considered:

- compressors,
- separators,
- dehydrators,
- coalescers,
- slug catchers,
- yard piping,
- tanks, and
- gathering lines.

Individual components on each equipment type were further divided into the following main categories:

- connectors,
- valves,
- pressure relief valves (PRV),
- meters,
- gauges,
- regulators,
- pneumatic device vents, and
- compressor vents (e.g., distance piece vents [DPVs] and rod packing vents [RPVs]).

Components were screened for the presence of leaks and venting emissions with an optical gas imaging (OGI) camera, and methane emission rates were measured using a microdilution high volume sampler. Downwind emissions were measured using an Open Path Fourier Transform Infrared (OP-FTIR) Spectrometer. Data were evaluated to assess variability related to site, equipment, time, operational variables (e.g., pressure, flowrate, temperature), equipment characteristics (e.g., age, type), and sampling duration. Key findings and recommendations from the study include:

- **Component Population Counting Methodology:** Different counting methodologies can result in vastly different component counts, thus influencing total emissions calculations

using Subpart W population EFs. A standard methodology should be adopted for classifying and counting components in order to minimize inconsistencies across studies and instruct stakeholders responsible for GHGI reporting.

- **Appropriateness of Component Categories in the GHGRP:** Results support current component subcategories listed in USEPA Subpart W, including the subdivision of connectors (flanged and “other”) and pneumatic device vents (intermittent, continuous low bleed, and continuous high bleed). Results warrant further study of emissions from compressor vents, meters, gauges, and regulators.
- **Emission Rate Variability by Site and Operational Parameters:** There is variation of emissions rates across sites and a relationship between higher emissions and compressor age for some components. More measurements should be taken on additional compressor components to further assess emissions rate variability by site and operational parameter.
- **Temporal Variability in Emission Rates:** Component emission rates varied between field campaigns. The type of components contributing to overall measured emissions also varied among field campaigns. However, the emission rate variability was larger between different components (of the same category) than the variability in one component over the four field campaigns. Therefore, when calculating emission factors, it is not necessary to take repeat measurements to capture component variability. Visiting many sites once is likely to capture more variability in emission rates than visiting sites multiple times.
- **Emission Rate Variability During Sampling Measurements:** Measuring the emission rate of a sample for an extended period of time is not necessary to capture the average component emission rate. Pneumatic devices, which are designed to actuate and/or throttle, did not show greater variability than other component types. This may indicate the sampling time was not sufficient for pneumatic devices; further investigation is recommended.
- **Emission Comparison – Gas vs Liquid Lines:** For reporting purposes, excluding liquid lines from site-wide screening may have a negligible effect on component-related emissions. However, from a site management perspective, malfunctioning components were not uncommon on liquid lines and contributed substantially to fugitive emissions at some sites.
- **Emissions Comparison - Measured vs. Estimated:** Population EFs, whether including or excluding liquid lines, were a conservative estimate of fugitive emissions. Leaker EFs consistently underestimated emissions at the field sites. Measurements at more sites, particularly sites in other areas of the country, need to be completed before determining the accuracy of EFs.

The results of this study are useful to regulators for updating the GHGI and GHGRP, highlighting areas of additional research, such as 1) developing a standard counting and classification protocol for components, 2) determining the importance of emissions from liquid lines, and taking additional measurements from compressors in the G&B segment to provide stronger statistical support for proposed updates to Subpart W EFs.



## 1.0 INTRODUCTION

Methane emissions from natural gas gathering and boosting (G&B) stations are reportable under the United States Environmental Protection Agency (USEPA) Greenhouse Gas Reporting Program (GHGRP) and tracked nationwide under the Greenhouse Gas Inventory (GHGI). Methane is a potent greenhouse gas that has a global warming potential of 28 (IPCC, 2014), which means that methane can store 28 times more heat in the atmosphere than carbon dioxide over a 100-year period. The U.S. Department of Energy (DOE) National Energy Technology Laboratory (NETL) has ongoing research efforts to accurately characterize and quantify methane emissions from compressors and gathering lines within the G&B segment of the natural gas system network. As defined in Title 40 of the Code of Federal Regulations (CFR) Part 98 Subpart W, onshore natural gas G&B means:

*Gathering pipelines and other equipment used to collect natural gas from onshore production gas wells and used to compress, dehydrate, sweeten, or transport the natural gas to a natural gas processing facility, a natural gas transmission pipeline or to a natural gas distribution pipeline. Gathering and boosting equipment includes, but is not limited to gathering pipelines, separators, compressors, acid gas removal units, dehydrators, pneumatic devices/pumps, storage vessels, engines, boilers, heaters, and flares. (40 CFR1.98.230(9) [2016]).*

At present, methane emission estimates for G&B stations are primarily based on data from other sectors of the natural gas inventory, such as production and transmission, rather than emissions specifically from G&B stations. Consequently, efforts are needed to reduce uncertainties in estimates of these emissions in the current GHGI. A robust and representative dataset of emissions from G&B station components will ultimately inform future enhancements to the current GHGI.

This report describes the results from DOE Project DE-FE0029084: *Integrated Component-Specific Measurements to Develop Emission Factors for Compressors and Gas Gathering Lines*. For this study, component characterization and emissions measurements were performed using a suite of leak detection and measurement technologies at four G&B stations in the Gulf Coast area. Four G&B stations were visited four times over the course of one year (February 2017-March 2018). The technical approach, analyses, and results of this study are discussed in the following sections, with references to appendices for additional details and supporting information.

## 1.1 Background

### 1.1.1 Regulations & Current Literature

USEPA addresses methane emissions from natural gas production, processing, transmission, storage, and distribution segments under Subpart W (Petroleum and Natural Gas Systems) of the 2016 GHGRP, covered under Title 40 of the CFR. Emissions reported to the GHGRP support the accounting of total methane emissions from man-made sources to USEPA's GHGI.

The USEPA and Gas Research Institute (GRI) published the first comprehensive study to quantify methane emissions from the natural gas industry in 1996 (Harrison et al., 1996) as part of the GHGI. Since the *Mandatory Reporting of Greenhouse Gases Rule* was signed in 2009 (40 CFR §98, Subpart C and Subpart W), the emission factors (EF) published in 1996 have come under increased scrutiny and undergone several revisions (Clearstone Engineering, 2002; USEPA,



2006; Harrison et al., 2011; Marchese et al., 2015). Though the GHGI is updated and improved annually, recent studies have pointed to the inadequacies of GHGI methane emissions estimates, particularly in the G&B segment.

A study by Marchese et al. (2015) found that G&B operations contributed approximately 30% of total methane emissions in the natural gas systems GHGI. Results of the study invoked the 2016 update to the GHGRP, and prompted further study of the G&B segment as a significant source of methane emissions.

As of 2016, methane emissions from natural gas G&B stations are reportable under the USEPA GHGRP and tracked nation-wide under the GHGI. Further, emissions from process components (e.g., valves, connectors, pressure relief valves) at such stations are estimated using EFs in accordance with Subpart W of the GHGRP. Therefore, it is critical that data in the GHGI accurately represent the full range of expected field conditions, including temporal and operational variability in the G&B station segment.

USEPA is currently considering improving GHGI emissions estimates in the G&B segment by requesting “feedback on how to consider regional and temporal variability specifically for G&B (USEPA, 2018) as well as incorporating data collected in recent studies (Vaughn et al., 2017; Yacovitch et al., 2017; and Zimmerle et al., 2017). The results of this study can help to address the temporal variability of emissions highlighted in the USEPA memo.

### **1.1.2 General Equipment at G&B Stations**

As natural gas moves long distances through pipelines, the pressure of the gas decreases. G&B stations are strategically placed along transfer pipelines to boost the gas pressure. This helps to maintain gas flow through the pipelines and ensures gas is at the proper pressure for end users. A general schematic of a G&B station is shown in **Figure 1-1**. Natural gas enters the station through the receiving side of the gathering lines and passes through a series of equipment that reduces moisture and/or filters impurities from the gas (e.g. slug catchers, dehydrators, separators, and coalescers). Slug catchers and large vertical separators, for example, are designed to remove high volumes of liquid from the gas stream using gravity. Equipment such as coalescers and filter separators are designed to remove additional liquids, as well as any particulate matter, oily liquids and condensate, and other impurities from the gas. Liquids that are removed from the gas are typically sent to holding tanks. Note that the type, number, and configuration of liquid handling equipment varies between stations, and depends on the moisture content and quality of the incoming gas and the facility gas throughput. Following gas conditioning, the pressure of the gas is then increased by the compressors and sent out of the facility through the discharge pipes of the gathering lines.

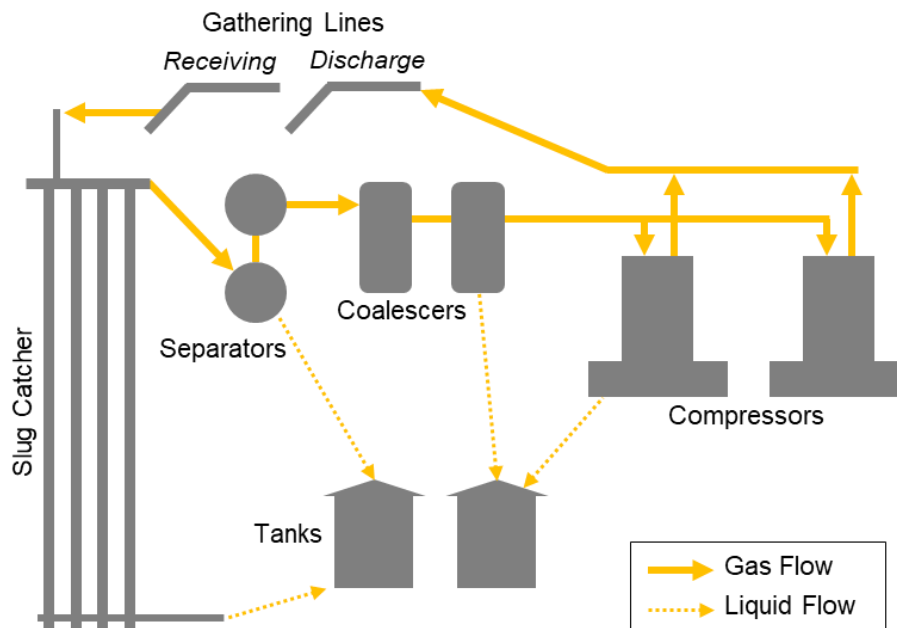


**Figure 1-1.** Example schematic of a G&B station from this study

## 1.2 Overall Project Approach

The objective of this study is to characterize methane emissions from G&B station components within the G&B segment to improve the quantification of methane emission factors included in Subpart W of the USEPA's GHGRP. Main project tasks included: i) measuring methane emission rates from a variety of equipment components (e.g., connectors, valves, compressor vents) at multiple G&B stations using a suite of measurement and leak detection technologies (e.g., OGI camera, high volume sampler, OP-FTIR spectroscopy), ii) assessing the temporal variability of methane emission rates from equipment and components by returning to the same sites multiple times, and iii) evaluating the effect of operational parameters (e.g., throughput, gas composition) on emission rates. Key research questions and project activities are summarized below.

Key research questions addressed by this study include:

1. How are component populations counted on different equipment types and how are counts affected by counting methodology?
2. Do methane emissions data support component categories and subcategories currently identified in the GHGRP?
3. Do emission rates vary from site to site? Do site operational parameters (e.g., gas throughput, gas composition, compressor age) correlate with emission rates?
4. Do emissions from the same site or piece of equipment vary over time?
5. What effect does sample duration have on the measured emission rate?
6. How do measured emissions compare to estimated emissions calculated from published Subpart W emission factors?

The project consists of two major phases, with two field campaigns conducted in each phase (four total field events). Methane emission rates were collected from disaggregated components (e.g., connectors and valves) at different time periods, reflecting changes in operational and temporal conditions at G&B sites. The temporal variability in methane emission rates was assessed and will aid in the development of refined EFs for G&B stations. The following specific activities were performed:

- **Component Classification.** Developed a detailed protocol to classify and count components at G&B stations.
- **Emissions Measurement.** Employed a suite of measurement and leak detection technologies (i.e., optical gas imaging (OGI) camera, high-flow, Open path – Fourier transform infrared (OP-FTIR) spectroscopy) to characterize methane emissions from components at G&B stations.
- **Temporal Variability Assessment.** Evaluated temporal variability of emission rates by measuring components over multiple field campaigns. Assessed the magnitude of variability in emissions rates over varying sample durations (from 3 to 70 minutes).
- **Emission Factors.** Calculated EFs with a small data set from four sites, and used variability results to determine the importance of repeat measurements in EF calculation.
- **Data Visualization.** Developed a data visualization tool that uses a Gaussian dispersion model to estimate the methane plume associated with measured emissions. The model was also used to visualize how the methane plume changed throughout the day based on meteorological data collected in the field.
- **Technical Advisory Steering Committee.** As part of technology transfer activities, a Technical Advisory Steering Committee (TASC) was assembled to receive feedback on project scope and results from industry, regulatory, and academic participants. Presentations were given to the TASC at multiple times during the study and feedback from the committee was incorporated into the study.

## 2.0 METHODS

### 2.1 Participating Field Sites

In December 2016, 16 G&B station facilities located in the Gulf Coast area housing a total of 47 reciprocating compressors, were offered by operators as candidate field sites. Four facilities were randomly selected in which to perform the field activities, consisting of a total of 15 compressors and associated equipment (slug catchers, separators, coalescers, dehydrators, and yard piping) (**Table 1-2**). For confidentiality purposes, the four facilities are referred to as Sites 1-4.

### 2.2 Overview of Field Campaigns

Four field campaigns were conducted between February 2017 and March 2018. The dates of each field campaign for each site under the two project phases are provided in **Table 2-1**.

**Table 2-1. Summary of project field campaigns**

	Phase I		Phase II	
	Campaign 1	Campaign 2	Campaign 3	Campaign 4
Site 1	March 2-3, 2017	June 6, 2017	October 26-27, 2017	March 5-6, 2018
Site 2	March 1, 2017	June 8, 2017	October 24, 2017	March 8, 2018
Site 3	February 28, 2017	June 7, 2017	October 25, 2017	March 7, 2018
Site 4	February 27, 2017	June 7, 2017	October 23, 2017	March 9, 2018

Field sampling events were performed at the same facilities to capture variability in operational parameters, such as compressor operational modes, facility gas throughput, and gas composition. The field sites had throughputs that ranged from 5,000 to 250,000 thousand cubic feet per day (MCF/day). The sites also had different numbers and configurations of equipment (**Table 2-2**).

**Table 2-2. Equipment counts for participating field sites**

Equipment	Site 1	Site 2	Site 3	Site 4
Compressors *	5-6	4	2	2-3
Operational Compressors	2-3	1	1	1
Separators	2	3	3	4
Coalescers	2	1	1	2
Dehydrators	0	1	2	0
Slug Catchers	1	0	0	1

\* Total number of compressors at a given site (Note: not all compressors were operational during all sampling campaigns). Counts for other equipment types represent operational equipment only.

It is important to note that operation schedules of compressor units varied over the four field campaigns (**Figure 2-1**). For example, at Site 4, Compressor 93 was operational during Field Campaigns 1 and 4, Compressor 95 during Field Campaign 2, and Compressor 94 during Field Campaign 3. Also, Compressor 95 was removed from the site between campaigns 2 and 3. In one instance, a new compressor was installed (Site 1, Field Campaign 4). The substitution of operating compressors over time resulted in limited repeat measurements that could be taken on compressor components. Only two compressors, located at Site 1, were operational during all four campaigns (1301 and 1501). On Figure 2-1, green boxes represent compressor units at Sites 1-4. Operational compressors at the time of sampling during the four field campaigns are outlined in dark green; remaining compressors were not operating. Compressors that were removed from the field sites during the study are denoted with red X's.

	Campaign 1			Campaign 2			Campaign 3			Campaign 4		
Site 1	1301	1401	1501	1301	1401	1501	1301	1401	1501	1301	1401	1501
	1601	1701	1801	1601	1701	1801	1601	1701	<del>1801</del>	1601	1701	NEW
Site 2	ENG-1	ENG-2		ENG-1	ENG-2		ENG-1	ENG-2		ENG-1	ENG-2	
	ENG-3	ENG-4		ENG-3	ENG-4		ENG-3	ENG-4		ENG-3	ENG-4	
Site 3	Unit 1	Unit 2		Unit 1	Unit 2		Unit 1	Unit 2		Unit 1	Unit 2	
Site 4	93	94		93	94		93	94		93	94	
	95			95			<del>95</del>			<del>95</del>		

**Figure 2-1.** Operational compressors by site and field campaign.

Field campaigns at the four sites consisted of three major steps: i) component classification and counting, ii) identification of leaks from equipment components using an OGI camera (FLIR GF320), and iii) measurement of methane emissions using a high volume sampler (**Figure 2-2**). In addition, during Field Campaign 1, an OP-FTIR spectrometer was employed to quantify methane concentration downwind of the compressors units. Operational parameters were provided by G&B station operators (facility gas throughput, gas composition, etc.).



**Figure 2-2.** Field method summary for component emissions

To the extent possible, equipment leaks and vents that were identified and measured at a given component were measured during subsequent field campaigns. Detailed descriptions of the component classification and leak detection/measurement technologies are provided in Sections 2.3 and 2.4, respectively.



## 2.3 Component Classification and Count

A protocol was developed to classify and count disaggregated components of G&B stations. Counting and classification can be interpreted differently depending on the field personnel, making consistency difficult to achieve between field campaigns. A detailed classification protocol, provided in Appendix C, was developed to ensure consistent counts between field sites. Key components of the protocol are briefly described below.

### 2.3.1 Equipment Type

G&B stations were separated into eight main equipment types: compressors, separators, dehydrators, coalescers, slug catchers, yard piping, tanks, and gathering lines (**Figure 2-3**). Components associated with each equipment type were classified and counted. The purpose of classification by both component and equipment type was to more accurately quantify methane emissions from individual pieces of equipment at G&B stations rather than a facility wide component count and emission rate. Organizing the count in this manner may reduce uncertainty, as pieces of equipment are often operated under varying conditions from day to day, are relocated from site to site, and/or are decommissioned and removed from the G&B process entirely. Additionally, G&B stations are uniquely configured depending on station operational parameters such as gas throughput and gas moisture content. For example, a G&B station receiving wet gas will require more separation and possibly installation and management of slug catchers; tanks will flash more, and liquid level pneumatic controllers will actuate more, creating additional emissions.

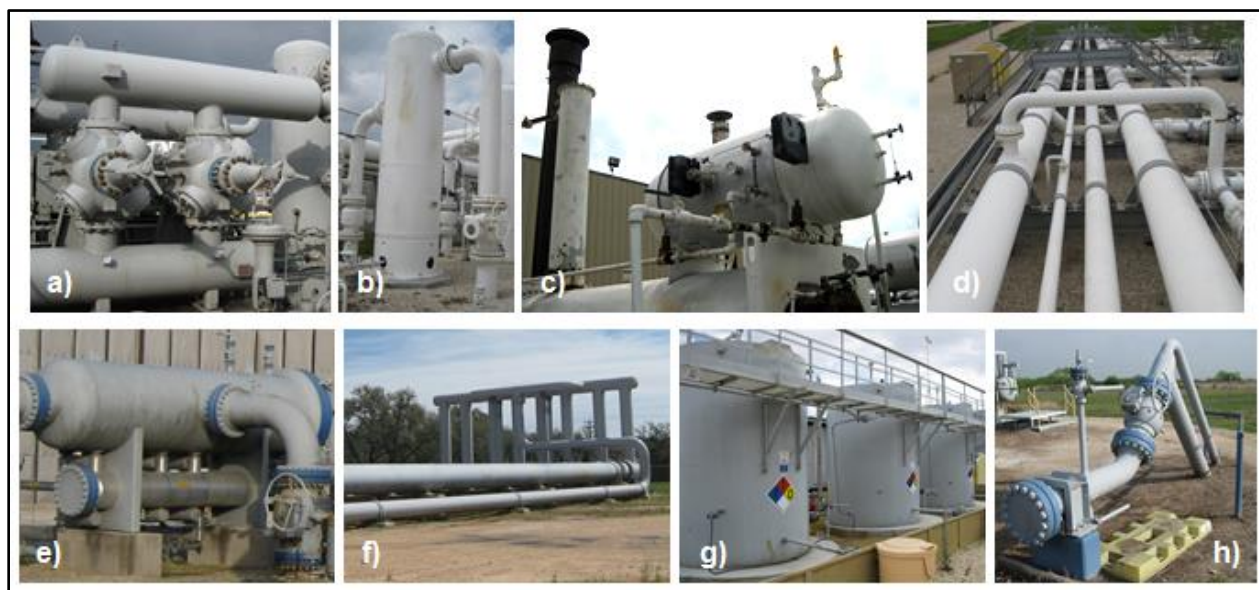


**Figure 2-3.** Major equipment types at G&B Stations: a) compressor, b) separator, c) dehydrator, d) yard piping, e) coalescer, f) slug catcher, g) tanks, and h) gathering lines

### 2.3.2 Component Type

Components were classified into eight major categories: connectors, valves, pressure relief valves, meters, gauges, regulators, pneumatic devices, and compressor vents. Where possible, these categories were subdivided into smaller groups and the function of the component was noted (**Table 2-3**). For example, connectors could be flanged or other (e.g., threaded, compression), and the function of a pneumatic device could be to control pressure, liquid level, or flow. Component counts for each piece of equipment were started and stopped at the

equipment's isolation valve. Components moving liquid (e.g., liquid lines from separators to tanks) were differentiated from lines moving gas. Photos of each of the component types are shown on **Figure 2-4**. Pneumatic devices are used to operate mechanical devices, like valves, with compressed air or natural gas. When a signal is sent to the pneumatic device controller that a change in system parameters (e.g., pressure, level, or flow) is needed, the device will reposition a valve (open/close, throttle) to achieve the desired system condition. Compressed gas contained in the actuator diaphragm is released, or actuates, to operate the valve. A detailed description of the component count methodology for this project is provided in Appendix C.

**Table 2-3.** Component categories and subcategories from the component classification protocol

Major Component Categories	Major Component Subcategories	Component Specifics
Connector	Other or flanged; Size of other connector ( $d < 6"$ , $6" \leq d < 12"$ , $d \geq 12"$ ); Size of flanged connector ( $d=0.5"$ , $0.5" < d < 6"$ , $d \geq 6"$ )	<ul style="list-style-type: none"> <li>Equipment category and location</li> <li>Liquid or gas line</li> <li>Within pneumatic loop?</li> <li>Venting, leaking, or both</li> <li>Function (e.g. level, pressure, temperature, ESD, etc.)</li> <li>Make, model, age</li> <li>Operational parameters (e.g. inlet and discharge pressure)</li> <li>Other (visibility limitations)</li> </ul>
Valve	Size (small, large); type (ball, gate, needle); and operating mechanism (manual, pneumatic, electronic)	
Pressure Relief Valve	n/a	
Meter	n/a	
Gauge	n/a	
Regulator	n/a	
Pneumatic Device Vent	Intermittent, continuous low-bleed, continuous high-bleed	
Compressor Vent	Rod packing, distance piece, pocket	

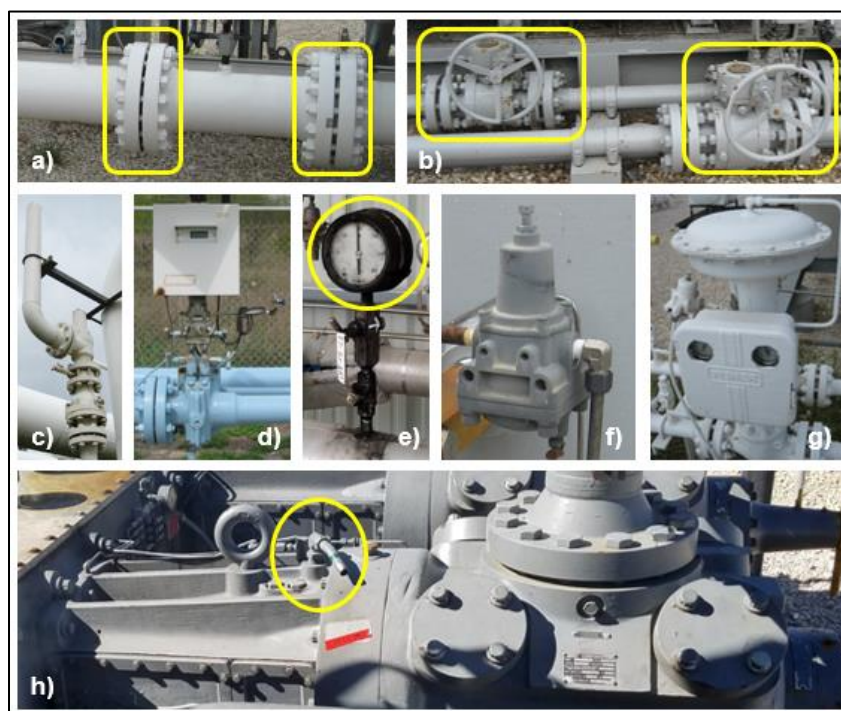


**Figure 2-4.** Major component types: a) connector, b) valve, c) pressure relief valve, d) meter, e) gauge, f) regulator, g) pneumatic device, h) compressor vent.



## 2.4 Technologies

### 2.4.1 Optical Gas (FLIR) Imaging

A FLIR GF320 infrared (IR) imaging OGI camera was used as a screening tool to visually locate (but not quantify) leaking and venting components of G&B stations. The FLIR GF320 creates images within a narrow range of the mid-IR spectrum (3.3-3.4  $\mu\text{m}$  wavelength) within which methane and other light hydrocarbons actively absorb (FLIR, 2011; **Figure 2-5**). Measurements using the FLIR were performed in accordance with 40 CFR Part 60, Subpart A, §60.18 of *Alternative Work Practice for Monitoring Equipment Leaks*. The detection limit of the FLIR GF320 is 60 grams per hour (g/h) (3.1 standard cubic feet per hour [scf/hr]) or less, which is consistent with the requirements of 40 CFR Part 60, Subpart A, Table 1: Detection Sensitivity Levels. The minimum detected leak rate for methane in FLIR lab testing is 0.8 g/hr. In the field, the FLIR is usually able to detect natural gas emissions in the range of 1 scf/hr or larger from 3 m away (Ravikumar et al., 2018). A spec sheet for the FLIR GF320 is provided in Appendix A.



**Figure 2-5.** a) Screening a pneumatic device with the FLIR OGI Camera, b) compressor rod packing vent, c) FLIR view of compressor rod packing vent

FLIR cameras utilize specialized spectral detectors that measure radiant energy incident within the field of view. This radiant energy, in a leak-detection setting, comes from four principal sources: (1) direct radiance from the methane plume, (2) transmitted radiance from the scene (background), (3) scene-reflected cold-sky radiance, and (4) direct atmospheric radiance. Radiance is a function of the temperature emissivity of a given source (e.g., object or substance).

Imaging is affected by factors such as viewing distance, wind velocity, and temperature contrast, depending upon the factors described above. For best survey results, equipment leak detection is performed under favorable conditions, such as during daylight hours in the absence of precipitation, in the absence of high wind (if possible), and in front of appropriate reflective backgrounds within the detection range of the instrument. Temperature contrast is essential for effective gas imaging. Imaging in High Sensitivity Mode (HSM) is utilized to detect emissions in less favorable conditions.

Facilities were surveyed for gas emissions using the FLIR camera by systematically examining process equipment and components in infrared mode. Video images of gas emissions from leaks and vents were recorded for reference, and each was identified with the date, site, and component type. Components identified during screening were classified as venting, leaking, or malfunctioning according to the following criteria:

- **Vent** – Component designed to emit gas (e.g., compressor vent, pneumatic device), and functioning properly
- **Leak** – Component not designed to emit gas (e.g., connector, valve)
- **Malfunction** – Component designed to emit gas, but not functioning properly (e.g., pneumatic device vent stuck open).

The FLIR was used in Field Campaigns 1, 3, and 4. A FLIR was not used in Field Campaign 2, which focused on high volume measurements on compressor vents.

#### 2.4.2 High Volume Sampling System

Where individual equipment components (valve, connector, etc.) were identified as leaking or venting by the FLIR team, emission rates were quantified using a customized, microdilution high volume sampling system, built and operated by Utah State University (USU). This system was designed to distinguish between methane and other organics - a limitation of typical high volume sampling systems. The customized sampling system, which is housed in a generator-powered trailer (**Figure 2-6**), includes a Los Gatos Research (LGR) Ultraportable Greenhouse Gas Analyzer to measure methane concentrations in sample gas and a Fox Thermal Instruments Model FT1 mass flow meter to measure total flow. The field detection limit at G&B stations is 0.09 scf/hr (see details in Appendix B).

The trailer also houses a custom-built air scrubber system to generate methane-free air and a GPS system to record the location of the weather station measuring atmospheric conditions. An explosion-proof blower, attached to the trailer, generates flow from the bagged component to the trailer. All components of the high volume system are grounded to the trailer, which is attached to a ground rod to dissipate buildup of static electricity.



**Figure 2-6.** a) USU sampling trailer with high volume tubing connected, b) interior of trailer, c) bagged pneumatic device for sampling

### 2.4.3 High Volume Field Measurements

Methane emissions from G&B facility equipment and associated components were measured directly using the high volume sampling system in accordance with 40 CFR Part 98 Subpart W. Individual components were either taped with antistatic tape or bagged off with an antistatic polymer bag to ensure all emissions were captured (**Figure 2-6**). A hose was then inserted into the bag or taped around the component to sample the leak, and the blower pulled a high volume of gas from the partitioned component through antistatic ducting, into a flow measurement tube, and to the analyzer for sample collection and analysis. The background air concentrations were measured by a sample port that was positioned next to each partitioned component to ensure an accurate background concentration measurement. If a known leak was near the background port, caution was taken to ensure the sample was of ambient air and not of the elevated concentrations from the nearby leak.

Methane concentrations were measured, on average, in 10-minute intervals. This allowed for 2-3 minutes of calibration between sampled components, and about 8 minutes of usable data. Data was collected in 15- or 20-second intervals, and the average emission rate was reported (see Appendix B for details). The variability in the 15- and 20-second intervals is discussed in Section 3.6.2. During sampling, a set of pumps continuously pulled air from the sample hose and ambient air port through Teflon lines. An automated switching unit allowed the methane analyzer to alternately measure concentrations from the sample and background lines. A Fox Thermal Instruments Model FT1 mass flow meter measured total system flow; flow was corrected for temperature, pressure, water vapor, and methane concentration. A data logger recorded methane concentration, sample flow rate, and sample temperature as well as meteorological conditions (wind speed and direction, air temperature, barometric pressure, relative humidity).

The LGR Greenhouse Gas Analyzer was able to detect methane concentrations of up to 10% in air. However, if methane concentrations exceeded this threshold, a mass flow controller was used to dilute the analyzer flow with methane-free air to keep within the analyzer's range. This methane-free air was generated with a custom-built air scrubber system. Dilution was necessary for 12 samples.

During all gas measurements with the high volume sampler, field technicians ensured that data were complete and component location and type were accurately documented and backed up as soon as practical (no less frequently than daily). To confirm sample locations and IDs on field notes, photos were taken at each component showing a labeled whiteboard listing sample ID and time next to the sampled component. Further details on the high volume sampling system and methods are located in Appendix B.

### 2.4.4 Open Path – Fourier Transform Infrared Spectrometer

Methane concentrations downwind of operating compressor units were measured with OP-FTIR spectroscopy. Path-integrated gas concentrations were measured by Kassay Field Services, Inc., using a OP-FTIR spectrometer (**Figure 2-7**) and retroreflector. A controlled stream of inert sulfur hexafluoride ( $\text{SF}_6$ ) tracer gas was released following protocols recommended by Lamb et al. (1995). Methane emission rates were determined based on the ratio of the measured methane and  $\text{SF}_6$  concentrations during measurement periods with favorable atmospheric conditions. The general layout of the OP-FTIR and tracer release configuration at each wellhead is shown on **Figure 2-8**. The OP-FTIR was employed during Field Campaign 1, and due to the poor correlations

**Figure 2-7.** OP-FTIR spectrometer





between the methane plume and tracer gas, was not used in subsequent field campaigns. A detailed description of OP-FTIR methods is in Appendix D.

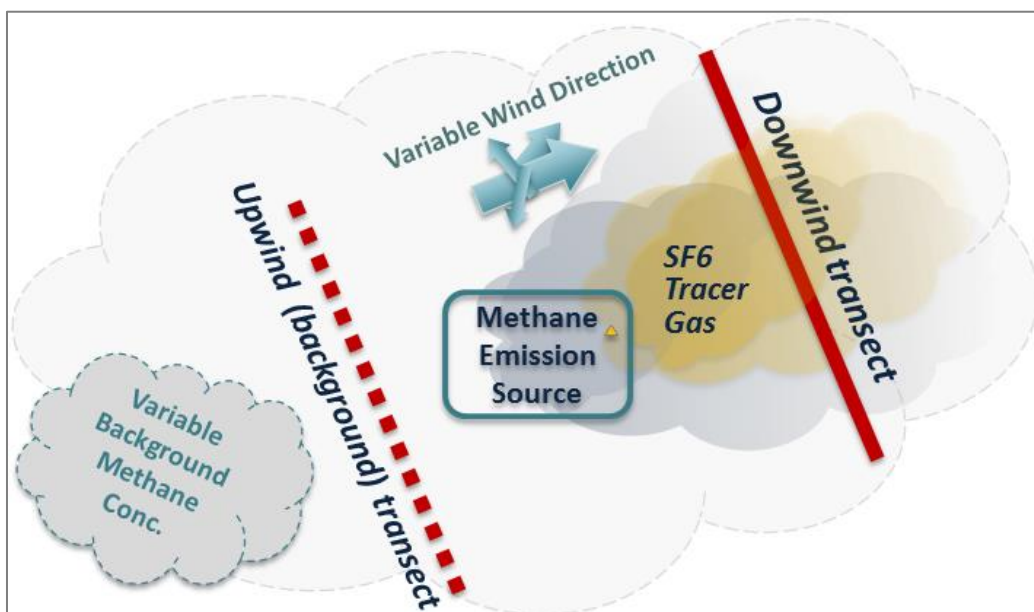


**Figure 2-8.** OP-FTIR/tracer sampling schematic

#### 2.4.5 OP-FTIR and Tracer Release Field Measurements

Ambient upwind and downwind measurement data were collected using the RAM2000 monostatic OP-FTIR spectrometer with a corner cube retroreflector (**Figure 2-7**). This optical spectroscopy technology was adapted to perform real-time monitoring of gaseous compounds in ambient air. The OP-FTIR spectrometer was used to detect and quantify the mixed plumes of SF<sub>6</sub> and methane.

Measurements were averaged over 5-minute intervals and path lengths ranging from 50 to 130 meters (165 – 430 ft). Path-integrated concentrations of methane and SF<sub>6</sub>, were determined using standard infrared spectra of known concentrations for these gases and converted to ppm by dividing by the path length. The onboard computer software and a spectral library allowed for real time determination of concentrations for each compound. On-site data including start time, end time, weather, location of reflector, location of OP-FTIR, site conditions, and other field parameters were recorded during sampling. The spectrometer was calibrated in accordance with manufacturer specifications. Synchronous meteorological data, including wind speed, wind direction, and ambient temperature, were collected at 5-minute intervals during OP-FTIR sampling at all transect locations. These data were collected using a portable, tower-mounted weather station positioned 6 m above ground level (affixed to the high volume sampler trailer). All meteorological and tracer release data were logged in conjunction with the high volume sampling data collected by USU.

### 2.5 Screening and Measurements Summary

A total of 52,500 components were screened with the FLIR during Field Campaigns 1, 3, and 4 (**Table 2-4**). A FLIR was not used for screening in Field Campaign 2, rather the campaign was focused on taking measurements from compressor vents. A total of 307 components were

sampled with the high volume system over the four field campaigns, and an additional 15 field blanks were also sampled.

**Table 2-4. Screened population and measurement counts**

Component Type	Screened <sup>a</sup> Population	Measurement <sup>b</sup> Count
Valve	6,281	28
Connector, Flanged	6,457	8
Connector, Other	37,118	24
Pressure Relief Valve	385	8
Meter	86	1
Gauge	972	5
Regulator	762	10
Actuator	275	3
Distance Piece Vent	80	80
Rod Packing Vent	34	27
Pneumatic Device Vent	297	101
Other <sup>c</sup>	--	12
<b>TOTAL</b>	<b>52,744</b>	<b>307</b>

<sup>a</sup> Screening with a FLIR was conducted during field campaigns 1, 3, and 4. <sup>b</sup> Total measurement count for all 4 field campaigns. <sup>c</sup> "Other" category contains filters, thief hatches, pump vents, and compressor pocket vents.

Component screening with the FLIR was performed only on operational and pressurized equipment, therefore the number and type of equipment screened was subject to change between field events, as discussed in Section 2.2 (see **Figure 2-1**). Alternatively, equipment that was operational or pressurized during more than one field event was screened multiple times (e.g. compressor vents).

## 2.6 Data Analysis

### 2.6.1 High Volume Emission Rates and Non-Detects

The methane emission rate was calculated as the methane concentration in sampled air ( $C_{CH_4, sample}$ ) minus methane concentration in background air ( $C_{CH_4, background}$ ) (hereafter referred to as "effective sample concentration") multiplied by flow rate ( $Q$ ) (**Equation 2-1**). Results were averaged over the measurement period and converted to units of scf/hr to align with component-level EFs currently found in 40 CFR Part 90 Subpart W.

$$ER_i = (C_{CH_4, sample} - C_{CH_4, background}) \times Q \quad (2-1)$$

In some cases, negative effective sample concentrations were measured (methane concentration in background air was larger than methane in the sampled air), resulting in calculation of a negative emission rate. Although negative effective sample concentrations are possible in some rare cases (e.g., if the component being measured is located next to a second, higher emitting component, the emissions from the second component could be pulled into the background measurement for the first), for purposes of this study, negative emission rates were considered as non-detect.

The high volume sampling field detection limit (DL) was determined to be 0.09 scf/hr based on field blank measurements after removing outliers. Outliers were removed due to highly variable background methane concentrations or high methane concentrations in the sample line before the blank measurement was performed (details in Appendix B). Emission rates less than the field DL were classified as non-detects.

### **2.6.2 Statistical Analyses**

A variety of statistical tests were used to analyze the collected data.

#### **Component Category Comparison**

The Kolmogorov-Smirnov (KS) test was used to identify statistical differences in emission rates between: i) two compressor vent subcategories – RPV and DPV, and ii) two connector subcategories – flanged and other (e.g., threaded, compression). The KS test is a nonparametric test used to determine if sample sets come from different distributions; it is sensitive to differences in shape, spread, and median of the sample sets.

The Mann-Whitney test with Bonferroni correction was used to identify statistical differences in emission rate distributions between more than two sample categories. The Mann-Whitney test is a nonparametric test used to compare sample distributions. The Bonferroni correction was used to counteract the increased rate of Type 1 errors (incorrectly rejecting the null hypothesis) that can occur when making multiple comparisons. Data sets that were compared using Mann-Whitney were the three pneumatic device vents categories (intermittent, high-, and low-bleed), and component emissions by site.

#### **Emission Rate Correlations**

Spearman's Rho was used to evaluate correlations between component emission rates and site parameters, including compressor age, inlet and discharge pressures, facility throughput, energy throughput, and gas composition (i.e., % methane). Spearman's Rho is a nonparametric test that measures the rank correlation between two sample sets. A value of 1 or -1 is a perfect correlation; a value of 0 is no correlation.

### **2.6.3 Emission Factor Calculations**

Population and leaker EFs were calculated using **Equations 2-2, 2-3, and 2-4**. Population EFs are used to estimate methane emissions by multiplying the EF by the total component counts. Leaker EFs are used to estimate methane emissions by multiplying the EF by the number of components identified as leaking (e.g., with OGI).

Emission factors were calculated from a small data set (four G&B stations). As such, the factors presented are likely not representative of national emissions. The data collected in this study is being incorporated into emission factor calculations being conducted by Colorado State University. Emission factors associated with data from this study, and the number of samples used for calculations, are presented in Appendix F.

#### **Population Emission Factor**

Population EFs are calculated differently for components that are leaking compared to venting. For leaking components (e.g., connectors), it was assumed that all leaks were detected and measured during the field campaigns. The population EF for leaking components was calculated as the total emissions from component type  $i$  normalized by the screened population of component type  $i$ :

$$\text{Population } EF_{i,leak} = \frac{\sum ER_{i,measured}}{N_{i,screened \text{ population}}} \quad (2-2)$$

Where:

$ER_{i, measured}$  = Methane emission rate if component type  $i$  measured with high volume (scf/hr)

$N_{i, screened \text{ population}}$  = Total number of component type  $i$  screened with the FLIR during field campaigns

The same equation could not be used for venting components (compressor vents, pneumatic device vents), because not all vents were measured during the field work. It was assumed that all components designed to vent (on operational equipment) were venting; the screened population was equal to the emitting population. The population EF for venting components was calculated as the average measured emission rate:

$$\text{Population } EF_{i,vent} = \text{Average}(ER_{i,measured}) \quad (2-3)$$

For the pneumatic device population EFs, there was some bias in the field toward measuring pneumatic devices that were actively emitting methane. This may have resulted in pneumatic device vent population EFs that are more likely leaker EFs, since the sample set includes a potentially biased number of actuating and/or malfunctioning devices.

### Leaker Emission Factor

The leaker EF for component type  $i$  was calculated as the average leaking emission rate measured with high volume ( $ER_{i, measured, leak}$ ):

$$\text{Leaker } EF_i = \text{Average}(ER_{i,measured,leak}) \quad (2-4)$$

Leaker EFs were not calculated for components designed to vent.

### 2.6.4 OP-FTIR Tracer Analysis

Methane emission rates were calculated using tracer correlations, based on downwind methane and tracer concentrations and controlled tracer release rates. Tracer correlations were performed using three independent methods adapted from previous studies (USEPA, 2014; Galle et al., 2001; Mønster et al., 2014; Schuetz et al., 2011; and Foster-Wittig, 2015): (i) time-series plume integration, (ii) unconstrained slope, and (iii) mixing ratio methods. The plume integration method provides the most accurate estimate of emission rate given its effective consideration of an entire time series of measurements. However, to ensure the validity of these estimates several method quality indicators (MQIs, described below) were applied based on the agreement of emission rates estimates among the three methods. When MQIs were satisfied, the result of the plume integration method was adopted as the final calculated value for methane emission rate.

Due to the nature of tracer correlation methods, several precautions were taken to ensure that the recorded data was appropriately interpreted; most importantly, the methane and tracer plumes needed to be well mixed. Tracer correlation methods are not considered reliable for measurement periods during which downwind methane and tracer concentrations are poorly correlated or when there is substantial non-agreement among the three emission rate estimation methods described above. Such conditions suggest instability in either the methane or tracer plume, which may be caused by low wind speeds (causing pooling of the tracer, which is much heavier than methane),



highly variable wind direction, variable upwind (background) methane concentrations during periods of downwind measurements, and other possible factors.

Foster-Wittig et al. (2015) propose that the coefficient of determination ( $R^2$ ) between methane and tracer concentrations should be greater than 80% over five or more consecutive measurement intervals. Additionally, Foster-Wittig et al. (2015) recommend that i) the relative difference in emission rates calculated by the plume integration and mixing ratio methods be less than 20% and ii) the relative difference in emission rates calculated by the plume integration and unconstrained slope methods be less than 55%.

Overall, only a small portion of all downwind OP-FTIR measurement periods satisfied the MQIs required for these data to be relied on for total emissions quantification. Specific factors contributing to this condition include limitation of a single tracer release point (located adjacent to the running compressor/s at each site) to adequately represent a spatially distributed array of significant methane emissions, when OP-FTIR measurements are practicably attainable only within the boundaries of the participating facilities. Due to the limited amount of data that satisfied MQIs, OP-FTIR measurements were not continued after Field Campaign 1.

## 2.7 Plume Visualization Model

The Gaussian air dispersion model was used to visualize the methane plume associated with compressor component emissions measured with the high volume system (**Equation 2-5**). This model is a steady-state model, and therefore is a conservative estimate of the plume.

$$C(x, y, z) = \frac{Q}{2\pi u \sigma_y \sigma_z} \times \left[ \exp - \left( \frac{y^2}{2\sigma_y^2} \right) \right] \left[ \exp \left( \frac{-(z-H)^2}{2\sigma_z^2} \right) + \exp \left( \frac{-(z+H)^2}{2\sigma_z^2} \right) \right] \quad (2-5)$$

Where:

C = Concentration of methane in the air (mg/m<sup>3</sup>)

Q = Rate of chemical emission (mg/s)

u = Wind speed in the x-direction (m/s)

$\sigma_y$  = Standard deviation in the y-direction (m)

$\sigma_z$  = Standard deviation in the z-direction (m)

y = Distance along axis horizontal to wind direction (m)

z = Distance along vertical axis (m)

H = Effective stack height (m)

The visualization tool calculates  $\sigma_y$ ,  $\sigma_z$ , and H based on input parameters including date and time, site location, sky cover, and land surface cover. Up to three different emission sources can be input into the tool, and the resulting plume is calculated and plotted. Note that Q was set equal to the sum of measured emissions from a single compressor, and included compressor vents, pneumatic device vents, and leaking components. Details are provided in Appendix E.

### 3.0 RESULTS AND DISCUSSION

Results and key findings are summarized in the sections below. Research questions, relevant findings, and potential implications are highlighted in blue boxes, followed by a detailed summary of key results and recommendations.

#### 3.1 Component Population Counting Methodology

##### **Research Question 1**

***How are component populations counted on different equipment types and how are counts affected by counting methodology?***

##### **Key Findings**

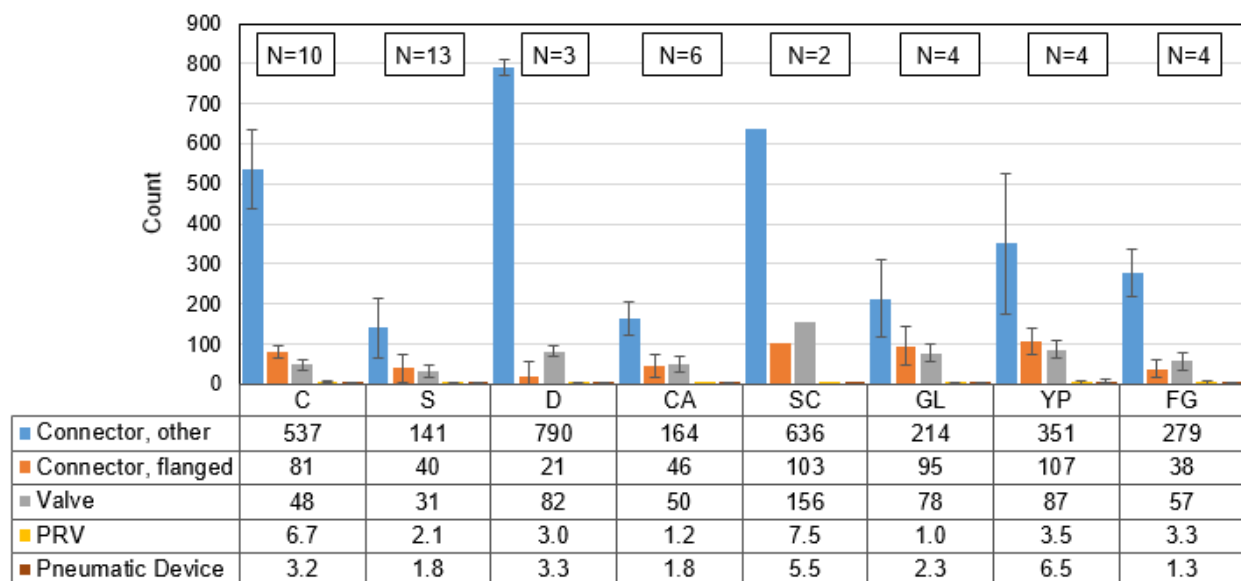
1. Component counts vary substantially based on classification and counting methodology (e.g., including/excluding components on liquid lines and pneumatic device loops).
2. Connectors and valves comprised the largest population of components at compressor sites.
3. Dehydrators and slug catchers had the highest total component counts when liquid lines were included in equipment component counting.
4. Yard piping, compressors, and gathering lines had the highest total component counts when components on liquid lines were *not* included in equipment component counting (i.e., only components on gas lines were included).
5. Eliminating components within pneumatic loops from component counts reduced the count on slug catchers, coalescers, separators, and gathering lines.

##### **Summary**

Different counting methodologies can result in vastly different component counts, thus influencing total emissions calculations using Subpart W population EFs. A standard methodology should be adopted for classifying and counting components in order to minimize inconsistencies across studies and instruct stakeholders responsible for GHGI reporting.

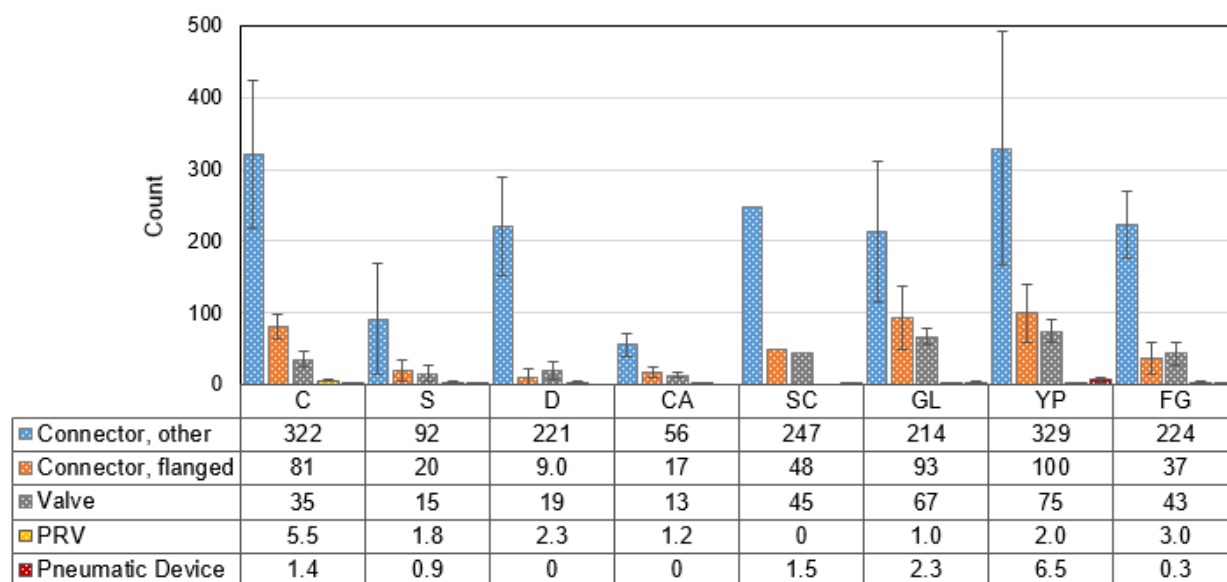
During the 4<sup>th</sup> field campaign conducted during March 2018, >22,000 components from 10 G&B equipment types were classified and counted according to the procedures discussed in Section 2.2 and Appendix C. Average component counts for both liquid and gas lines from 5 component categories that fall under Subpart W for G&B stations are presented in **Figure 3-1**. Average component counts for gas lines only (i.e., liquid line components excluded) are shown in **Figure 3-2**. Components on pneumatic device loops are included in total counts on both figures. Additional categories, such as compressor vents, meters, and regulators, were also classified and counted. Component count results for these additional categories are located in Appendix G.

When liquid lines were included in equipment component counting, dehydrators and slug catchers had the highest number of individual components per piece of equipment (**Figure 3-1**). Yard piping, compressors, and gathering lines had the highest number of components per piece of equipment when liquid lines were *not* included (**Figure 3-2**). For both counting scenarios, the components with the highest counts were: “other” connectors; flanged connectors; and valves.



The number of each equipment type that was counted is given as N. Error bars are standard deviations. Abbreviations: PRV = pressure relief valve, C = compressor, S = separator, D = dehydrator, CA = coalescer, SC = slug catcher, GL = gathering line, YP = yard piping, FG = fuel gas skid.

**Figure 3-1.** Average component count by equipment type, including gas and liquid lines



Error bars are standard deviations. Abbreviations: PRV = pressure relief valve, C = compressor, S = separator, D = dehydrator, CA = coalescer, SC = slug catcher, GL = gathering line, YP = yard piping, FG = fuel gas skid.

**Figure 3-2.** Average component count by equipment type, gas lines only

There was a substantial difference in total counts when liquid lines were excluded. The total count dropped from >22,000 components to just over 14,000. In specific, “other” connectors reduced from an average of 537 to 322 when liquid lines were excluded from the count, as shown on **Figures 3-1** and **3-2**. As expected, this reduction was most notable for equipment designed to handle liquids (e.g. liquid separation). Since the majority of natural gas process equipment have

some degree of liquid handling capabilities, the counts were also reduced on equipment that handle less liquid, such as compressors and fuel gas skids.

There was a further reduction in component count (<12,000 components) when components in pneumatic loops (regulators, small valves, connectors) were removed from the gas line counts. The average component count on slug catchers was affected the most, with a 46% reduction in the average count. Slug catchers were followed by coalescers (30% reduction), separators (29% reduction), and gathering lines (28% reduction). Components that were the most affected were regulators, gauges, and other connectors, which are the most common components in pneumatic loops.

The differences between these counts highlight the need for a consistent counting protocol, as different counting methodologies can result in vastly different component counts, thus influencing total emissions calculations using Subpart W population EFs.

### 3.2 Appropriateness of Component Categories in the GHGRP

#### **Research Question 2**

***Do methane emissions data support component categories and subcategories currently identified in the GHGRP?***

#### **Key Findings**

1. There is a significant difference ( $p < 0.05$ ) between leaking emission rate distributions of flanged and other connectors in the current GHGRP.
2. There is a significant difference ( $p < 0.05$ ) between venting emission rate distributions of different types of pneumatic devices in the current GHGRP.
3. There is a significant difference between compressor vent (DPVs, RPVs) emission rate distributions, and the current EF may not be representative for compressor venting.
4. Limited data sets for meters, gauges, and regulators did not allow for statistical analysis to determine if they should be added to the GHGRP.

#### **Summary**

Results support current component subcategories listed in USEPA Subpart W, including the subdivision of connectors (flanged and “other”) and pneumatic device vents (intermittent, continuous low bleed, and continuous high bleed). Results warrant further study of emissions from compressor vents, meters, gauges, and regulators.

### **Current Subpart W Subcategories**

Under Subpart W of the GHGRP for G&B stations, the USEPA published population and leaker emission factors based on various component subcategories (**Table 3-1**). For example, pneumatic device vents are subdivided into low continuous, high continuous, and intermittent bleed vents. Further, connectors are separated into flanged and other (e.g. threaded, compression). As discussed in Section 2.4, statistical analyses were performed to evaluate the methane emission rate distributions among subcategories currently listed in Subpart W. The results of these analyses are discussed below.

**Table 3-1. Emission factors currently included in the GHGRP**

Subpart W Population EF Component Categories (USEPA, 2015)	Subpart W Leaker EF Component Categories (USEPA, 2016)
Valve	Valve
Connector <sup>a</sup>	Flange
Open-Ended Line	Connector (other) <sup>b</sup>
Pressure Relief Valve	Open-Ended Line
Low Continuous Bleed Pneumatic Device Vent	Pressure Relief Valve
High Continuous Bleed Pneumatic Device Vent	Pump Seal
Intermittent Bleed Pneumatic Device Vent	Other <sup>c</sup>
Pneumatic Pump	

<sup>a</sup> Includes all types of connectors (i.e., flanged and other), <sup>b</sup> Includes all non-flanged connectors (e.g., threaded and compression), <sup>c</sup> Includes any equipment leak emission not specifically listed in the table

The Kolmogorov-Smirnov (KS) test was used to determine whether emission rates for two component categories were significantly different. The KS test showed distributions of flanged and other connectors were significantly different ( $p = 0.047$ ). The Mann-Whitney pairwise test with Bonferroni correction was also used to determine if more than two component categories had significantly different distributions. The Mann-Whitney test results showed:

- Distributions of continuous low-bleed and continuous high-bleed pneumatic device vents were significantly different ( $p = 0.003$ )
- Distributions of continuous high-bleed and intermittent pneumatic device vents were significantly different ( $p = 0.001$ )
- Continuous low-bleed and intermittent pneumatic device vents may have come from the same distribution ( $p = 0.80$ )

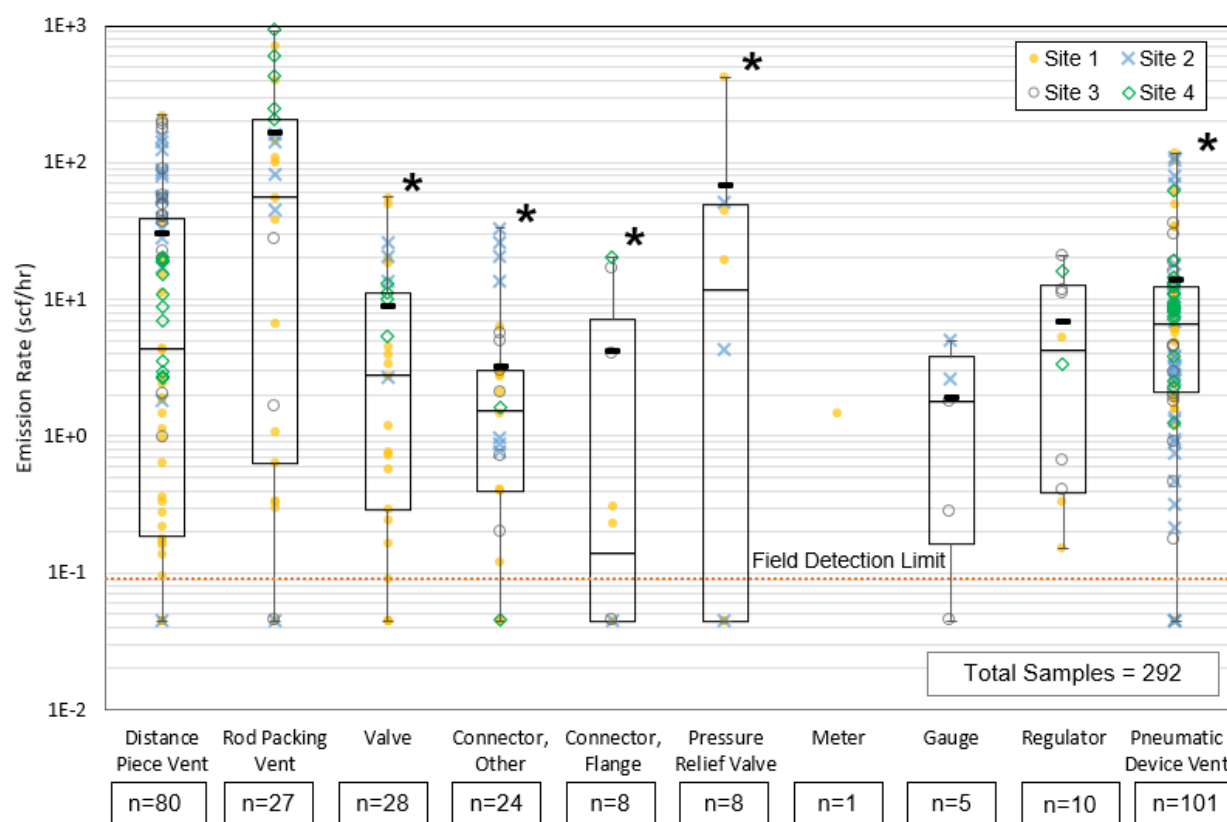
Although it could not be shown that continuous low-bleed and intermittent pneumatic device vents came from different distributions, the significant differences between continuous low- and high-bleed, and continuous high-bleed and intermittent support the current subcategorization of pneumatic device vents in the population factor table from the 2015 update (USEPA, 2015), and the division of connectors into flanged and other in the 2016 leaker factor addition (USEPA, 2016).

### Potential Subpart W Categories/Subcategories

General trends in emission rates showed venting components, such as DPVs, RPVs, and pneumatic device vents, had higher emission rates than leaking components (e.g., connectors, gauges, valves). All components had emission rates that ranged at least two orders of magnitude. RPVs and pressure relief valves (PRVs) had the largest emission range, with approximately four orders of magnitude difference between minimum and maximum emission rates. However, the large emission range for PRVs was due to one measurement (424 scf/hr) from Field Campaign 1, which was repaired by the operator prior to Field Campaign 2. Leaking components (valves, connectors, gauges, regulators) had a smaller overall range of emissions than venting components.

Although compressor vents (DPVs, RPVs) are not currently sub-classified in Subpart W, they exhibited relatively wide ranges of emission rates (**Figure 3-3**) and the highest average emissions (i.e., 30.4 and 165 scf/hr, respectively) of the major categories. Results of the KS test showed the emission rate distributions of RPVs and DPVs to be significantly different ( $p = 0.0083$ ), warranting consideration of compressor venting sub-classification, as opposed to a single EF. Further, in Subpart W a single EF of  $9.48 \times 10^3$  scf/yr/compressor (1.1 scf/hr/compressor; Harrison et al., 1996) is currently used for compressor venting at G&B stations (USEPA, 2011). This EF may not accurately represent (i.e., may be significantly lower than) measured compressor venting rates.

It should be noted that compressor vent emissions rates measured for this study, however, are based on a small data set (10 compressors; 4 G&B stations in Gulf Coast area) and are not representative of national averages. A more robust dataset of emission measurements of compressor vents, including sites outside the Gulf Coast area would be needed to properly add compressor venting components and develop specific emission factors for DPVs and RPVs.



**Notes:**

\* Component categories currently included in leaker and/or population emission factors in the GHGRP

Measured rates less than the detection limit were assigned the value of  $\frac{1}{2}$  the field detection limit.

For comparison, a standard cubic foot is approximately 7.5 gallons, or the size of a small kitchen-sized trash bag. A typical water heater pilot light has a flow rate between 0.25 and 1 scf/hr (Energuide 2018).

**Figure 3-3.** Measured methane emission rates by component type and site

Measured emission rates for additional component categories are presented in **Figure 3-3**. Due to the limited sample size of valves, additional subcategorization (e.g., by size or type as outlined in **Table 2-3**) could not be analyzed. Additionally, the limited data sets for meters, gauges, and



regulators did not allow for statistical analysis to determine if these component types should be incorporated as new categories in the GHGRP.

### 3.3 Emission Rate Variability by Site and Operational Parameters

#### **Research Question 3**

***Do emission rates vary from site to site? Do site operational parameters (e.g., gas throughput, gas composition, compressor age) correlate with emission rates?***

#### **Key Findings**

1. Emission rates from DPVs are significantly different by site.
2. Emissions rates from pneumatic devices and RPVs showed no significant difference by site due to the intermittent nature of leaking components.
3. Compressor age does not appear to play a statistically significant role in emission rate; however greater variability in emission rates (including higher emissions) from DPVs was observed on older (e.g., >10 years) compressors.
4. Site inlet pressure had a statistical correlation with emission rates on compressor RPVs.
5. Other site operational parameters, including gas throughput, composition, discharge pressure and energy throughput, did not have statistically significant correlations with emission rates from DPVs and RPVs.

#### **Summary**

There is variation of emissions rates across sites and a relationship between higher emissions and compressor age for some components. More measurements should be taken on additional compressor components to further assess emissions rate variability by site and operational parameter.

### **Emission Rate Variability by Site**

The number and type of malfunctioning/leaking components at a site and point in time appear to be random, and in general, had a low frequency of occurrence. As a result, the sample size of leaking components was insufficient for identifying statistically significant trends among sites. Distance piece vents (DPVs) were the only component with a sufficient number of detected emissions (n=80) that showed a diversity of emissions across 2 or more sites. Other venting components with sufficient observations of emissions (e.g., RPVs and pneumatic device vents) showed no significant difference in methane emissions by site typically due to the intermittent nature of leaking components.

DPV emissions for all sites and field campaigns were ranked in order by magnitude of emission rate, with the rank plotted against the corresponding emission rate (**Figure 3-4**). Data from the four sites were plotted with different symbols to support evaluation of site-related trends. There appears to be a link between DPV emission rates and site, as indicated by “groupings” of emission rates. For example, Site 1 emission rates were consistently lower (<50 scf/hr) than Sites 3 and 4 (50-200 scf/hr). It is important to note, however, that each site had occasional DPV emission rates that were on the low and high ends of the observed emission rate range. This implies that



emissions from compressor DPVs are not necessarily uniform, and may be dependent upon site and compressor specific operational conditions (e.g., maintenance, vent configuration).

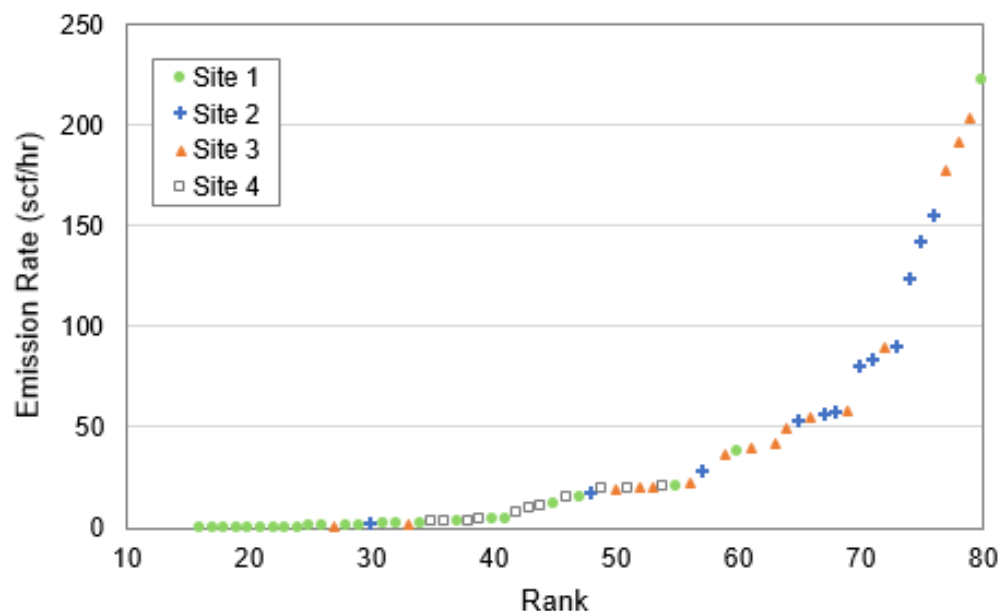


**Figure 3-4.** Distance piece vent emissions vs. emission rate rank

DPV emission rates by site were compared using the Mann-Whitney pairwise test with Bonferroni correction. Results showed a significant difference ( $p < 0.05$ ) between all site pairs except between Sites 2 and 3. The similarity between Sites 2 and 3 is noticeable in **Figure 3-4** by the apparent overlap in the data points compared to other sites.

RPVs and pneumatic device vent data were also evaluated using the Mann-Whitney pairwise test. Test results showed no significant difference in pneumatic device emissions by site. For RPVs, the only potential difference in emissions was between Sites 1 and 4; however statistical significance cannot be concluded as the p-value (0.0499) is nearly equal to the significance level of 0.05 for a 95% confidence level. Emission rates from pneumatic device vents may be influenced by operational conditions of the equipment the device is located on rather than the site. It is recommended that more measurements be taken at components on additional compressors to assess emissions rate variability of a greater population of components by site.

### Emission Rate Correlation by Operational Parameter

As mentioned above, the number of malfunctioning/leaking components observed during our repeat field investigations had a low frequency of occurrence. As a result, the sample size of most leaking components was insufficient for identifying statistically significant trends by operational parameter. For those components that produced sufficient data populations (rod packing vents and distance piece vents), Spearman's rho was used to evaluate correlations between component emission rates and operational parameters, including compressor age, inlet and discharge pressures, gas throughput, energy throughput, and gas composition (i.e., % methane). A correlation was identified between compressor RPV emissions and increased site inlet pressure (Spearman's rho = 0.72). However, this result was based on a limited data set (site inlet pressure was not available for Site 1). The correlation makes sense conceptually, as increased pressures around rod packing seals could increase the amount of gas vented from the rod packing units.

No significant correlation was observed between emission rate and compressor age for DPVs ( $R^2=0.22$ ; Spearman's  $\rho=0.34$ ). However, as shown in **Figure 3-5**, the highest emission rates were from older compressors and there was an increase in emission rate variability with compressors 10 years and older. Other site operational parameters, including gas throughput, composition, discharge pressure and energy throughput, did not have statistically significant correlations with emission rates with DPVs and RPVs. A greater dataset of emissions measurements from additional compressor components is needed to assess emissions rate variability of components by operational parameter.

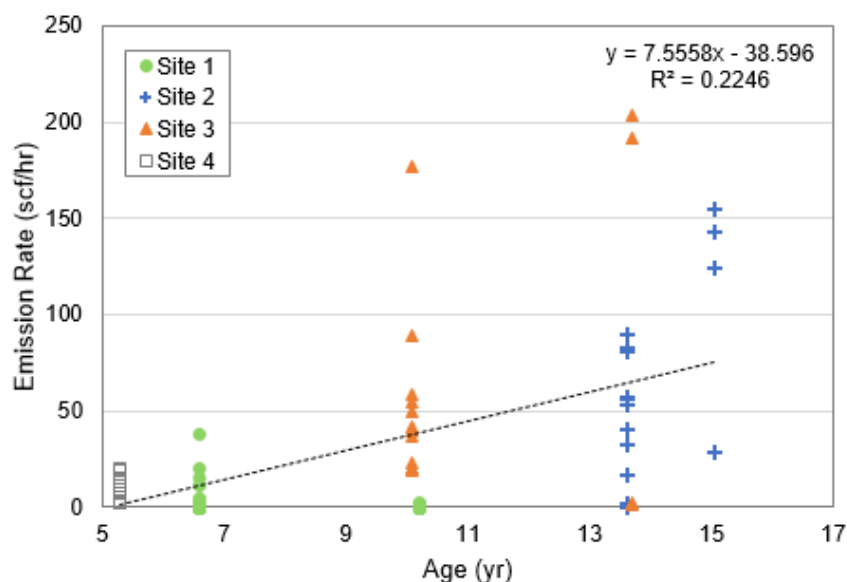


**Figure 3-5.** Distance piece vent emissions by site plotted against compressor age

### 3.4 Temporal Variability in Emission Rates

#### Research Question 4

*Do emissions from the same site or piece of equipment vary over time?*

#### Key Findings

1. Variation in site and compressor component emissions was significant between field campaigns.
2. The type and proportion of component(s) contributing to compressor emissions also varied across field campaigns.

#### Summary

Component emission rates varied between field campaigns, especially on compressors. The type of components contributing to overall measured emissions also varied among field campaigns. However, the emission rate variability was larger between different components (of the same category) than the variability in one component over the four field campaigns.

Variability in emission rates was analyzed under two scenarios: i) variability across four quarterly field campaigns and ii) measurement variability during 3- to 72-minute high-flow measurements. Results are presented in the following sections.

### 3.4.1 Quarterly Emission Rate Variability

Emission rates from compressor vents, other vents (i.e., pneumatic device vents), and leaks for each site and field campaign are plotted in **Figure 3-6**. Note that leaking or malfunctioning components are not designed to emit methane (e.g., connectors), or are designed to vent methane but are not functioning properly (e.g., pneumatic device vent that is stuck open). It is evident that emissions vary over time among field campaigns. For example, compressor-vented emissions at Site 1, Field Campaign 1 were 3 times higher than Field Campaign 2, 90 times higher than Field Campaign 3, and 15 times higher than Field Campaign 4. Leaks also varied substantially between field campaigns. One leaking component measured at Site 1 during Field Campaign 1 (a PRV at 424 scf/hr) was fixed prior to returning to the site, and was not leaking during subsequent field campaigns. Similarly, Site 4 had minimal leaks during Field Campaigns 1, 2, and 4; however, a malfunctioning RPV was measured during Field Campaign 3.

Using the density of methane (19.17 g/ft<sup>3</sup>), the measured methane emissions from the four facilities can be converted from volumetric flow rate (scf/hr) to mass flow rate (kg/hr). The mass flow rate ranged from 3.11 kg/hr (Site 3, FC2) to 36.2 kg/hr (Site 1, FC1).

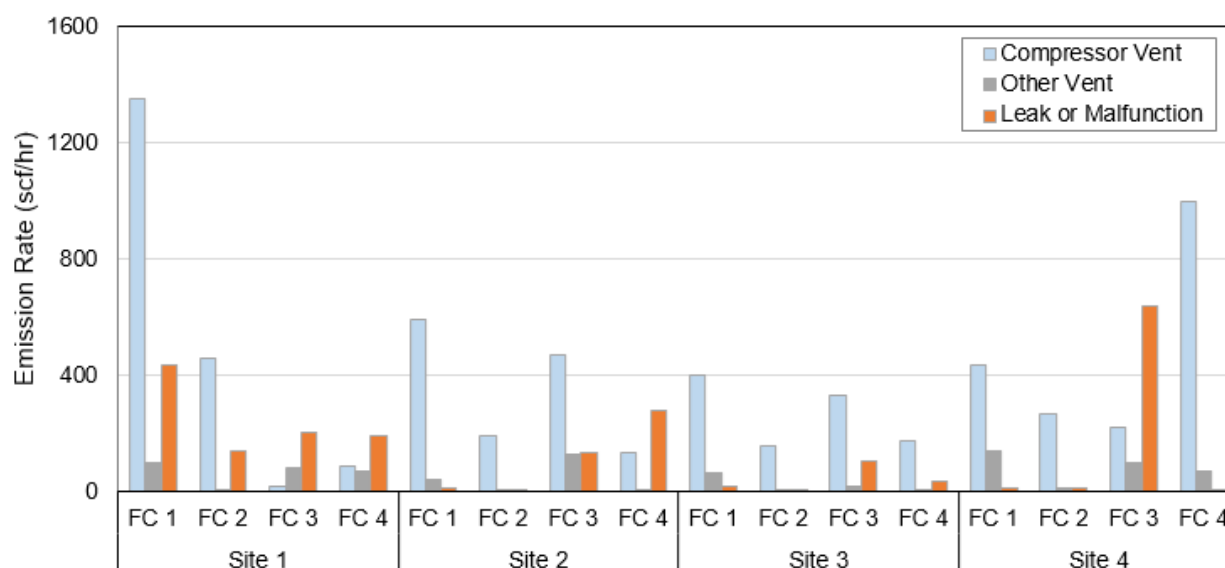
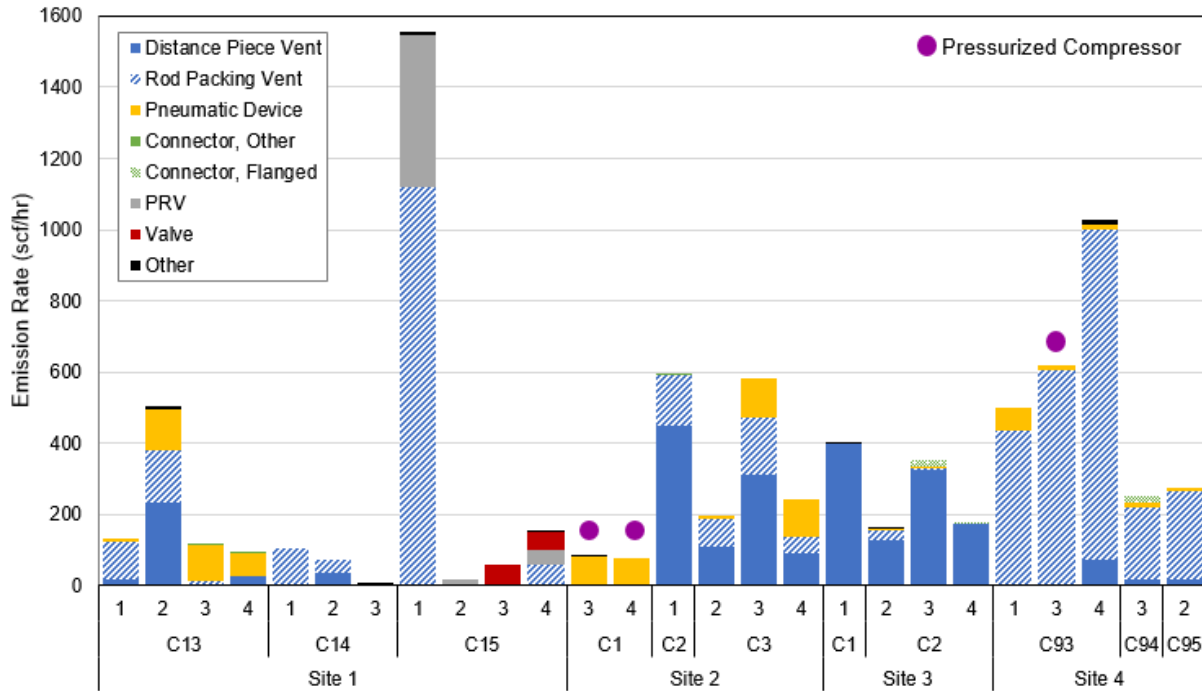


**Figure 3-6.** Component leak/malfunction and vent rates by site and field campaign

Emissions from specific equipment varied among field campaigns, as shown for compressor components in **Figure 3-7**. For example, Site 1, Compressor 15 (C15) emissions were approximately 2 orders of magnitude higher in Field Campaign 1 compared to Field Campaigns 2 and 3. At Site 4, Compressor 93 (C93) emissions doubled from Field Campaign 1 to Field Campaign 4.



Note: The order of the x-axis from bottom to top is Site ID, compressor ID, field campaign. Components in the "Other" category: actuator, regulator, gauge, meter, filter, other vents.

**Figure 3-7. Component leak and vent rates by individual compressor and field campaign**

Not only did the magnitude of total measured emission rates from specific equipment vary between field campaigns, but the type of components contributing to overall equipment emissions also varied. To illustrate, emissions from Compressor 13 (C13) at Site 1 during Field Campaign 1 resulted predominantly from RPVs (see **Figure 3-7**). In Field Campaign 2, this transitioned to DPVs, and ultimately was dominated by pneumatic controllers in Field Campaigns 3 and 4. Further, at Site 2, Compressor 3 (C3), the ratio of pneumatic controller emissions increased to nearly half of total C3 emissions from Field Campaigns 2 to 4.

Note that the emission rate variability was larger between different components (of the same category) than the variability in one component over the four field campaigns. This finding suggests that when calculating emission factors, it is not necessary to take repeat measurements on the same component to capture variability.

### 3.4.2 Emission Rate Variability During Sample Measurements

#### **Research Question 5**

**What effect does sample duration have on the measured emission rate?**

#### **Key Findings**

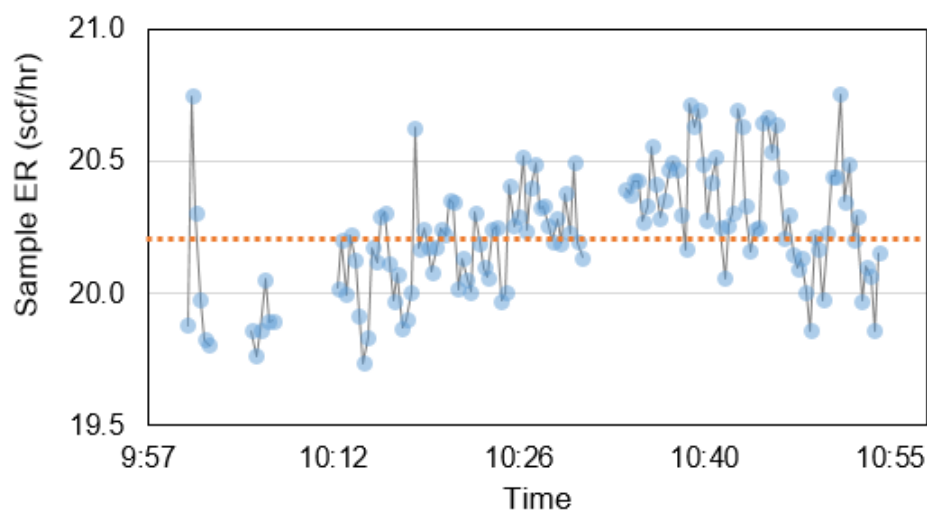
1. Longer sample duration did not result in greater variability within the sample measurement; short sample durations (~10 minutes) adequately capture variability within measurements for most components.
2. Pneumatic device vents did not have greater variability than other types of components, which is unexpected considering the throttling and actuation of pneumatic devices.

#### **Summary**

Measuring the emission rate of a sample for an extended period of time is not necessary to capture the average component emission rate. Pneumatic devices, which are designed to actuate and/or throttle, did not show greater variability than other component types. This may indicate the sampling time was not sufficient for pneumatic devices; further investigation is recommended.

Throughout the field campaigns, samples were measured for ~4 to 72 minutes, with the average high-flow sample duration equal to ~12 minutes. To determine whether prior sample periods were adequate to capture the variability that occurs *during* those periods, longer measurement durations were implemented.

Emission rate variability was evaluated on select components (i.e., components that had sufficient datasets and data from at least 3 multiple events) using the high flow system. The system measured methane concentrations in sample air and air flowrate in 15 or 20 second intervals. In other words, an emission rate was logged every 15 or 20 seconds throughout the measurement duration. For example, a 20-second interval emission measurements on a DPV that was measured for approximately 55 minutes is shown in **Figure 3-8**. This figure highlights the variability in emission rate during sample collection.



**Note:** The orange line represents the average emission rate

**Figure 3-8.** High-flow 20-second emission rate measurements on a distance piece vent

To conclude that an average sample duration of 12 minutes is not sufficient to capture variability, longer duration (30-72 minutes) samples should exhibit greater variability (i.e., larger standard deviation) than shorter duration samples. To test this theory, variability *within* a sample measurement (i.e., standard deviation) was plotted against sample duration (see **Figure 3-9**). As shown, a few of the longer duration samples had relatively high “within-measurement” variability; however, some of the short duration samples also exhibited wide variability. Conversely, the majority of both the short and long duration samples had relatively low within measurement variability (standard deviation <5 scf/hr). Based on these observations, within measurement variability does not appear to trend with sample duration. These results imply that measuring the emission rate of a sample for an extended period of time is not necessary to capture the average component emission rate.

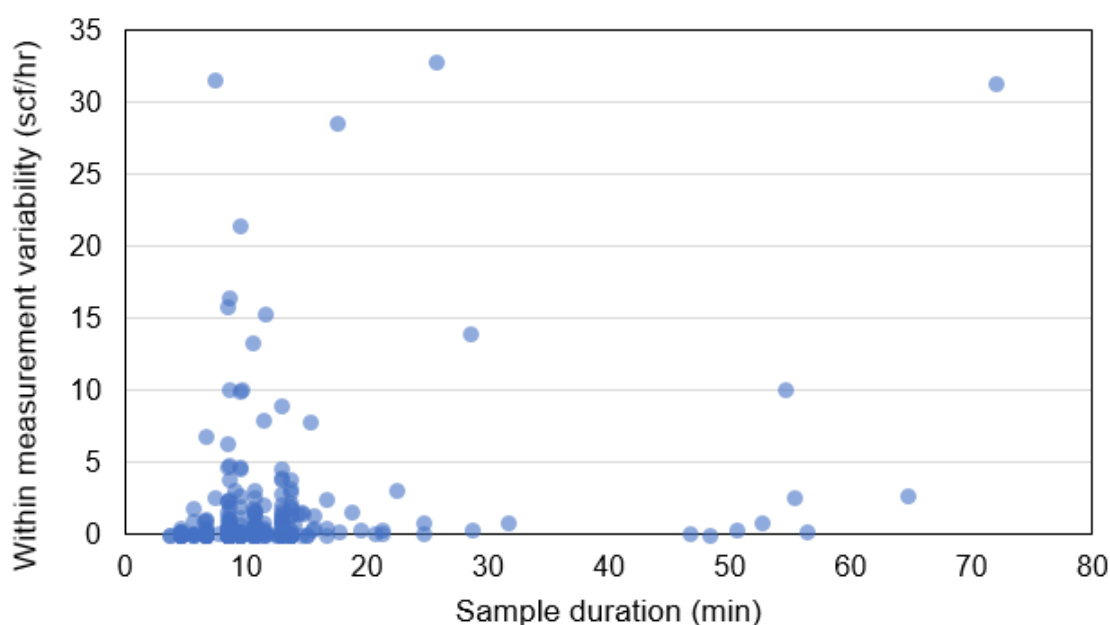


**Figure 3-9.** Within measurement variability vs. high-flow sample duration for all components and field campaigns

Note that the emission rate from many pneumatic devices is designed to vary, for example, during actuation or throttling. Therefore, it would be consistent with the component’s designed function for emissions rates to be more variable. To determine if pneumatic device emissions had greater variability than other types of components variability in measurements of pneumatic device vents were separated from the rest of the data (**Figure 3-10**).

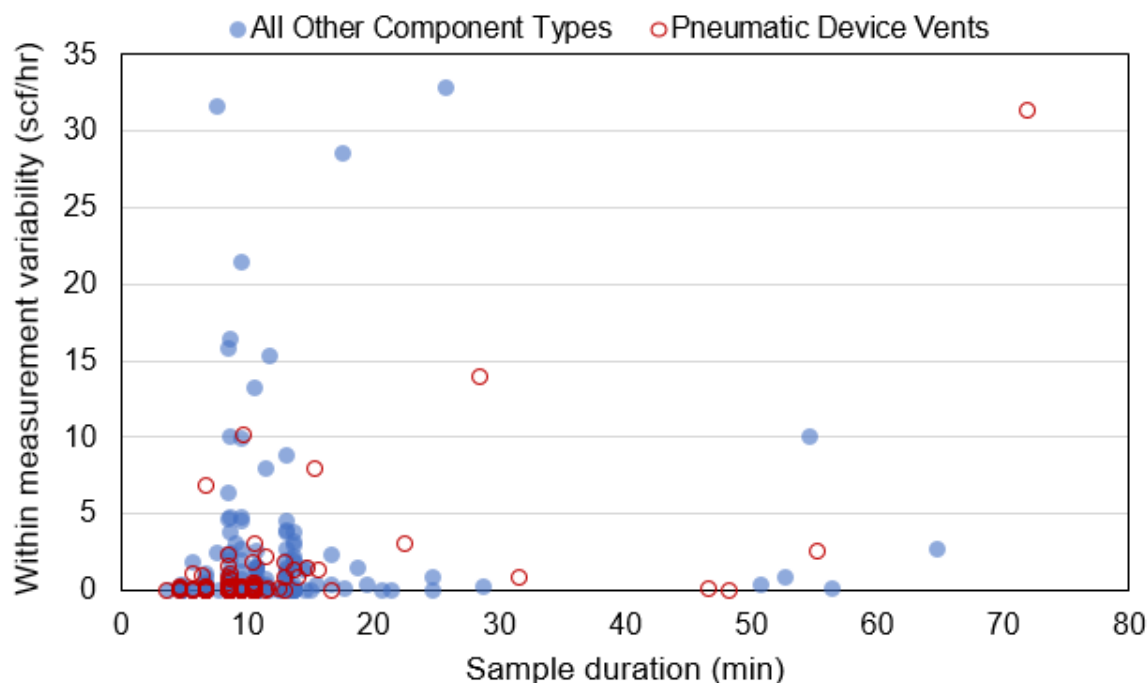


**Figure 3-10.** Comparison of within measurement variability between pneumatic device vents and all other component types

As shown in **Figure 3-10**, greater within measurement variability was not observed for pneumatic device vents compared to other component types. A possible explanation is that measured devices may not have actuated during the sampling period. A pneumatic device that actuates during the measurement period is expected to have greater within measurement variability due to spikes in emissions during actuation. As a result, an average sample duration of 10 minutes may not be sufficient to capture pneumatic device variability, and further research on emission variability of pneumatic device vents is recommended.

### 3.4.3 Temporal Emission Rate Variability Comparison

#### **Research Question 6**

**When calculating emission factors, is it important to take repeat measurements on the same component to capture variability?**

#### **Key Findings**

1. “Within” measurement variability is small compared to quarterly (repeat) sampling or component variability.
2. In general, quarterly sampling variability is smaller than component variability.



### **Summary**

When calculating emission factors, it is not necessary to take repeat measurements to capture component variability. Visiting many sites once is likely to capture more variability in emission rates than visiting sites multiple times.

When possible, repeat measurements were taken on the same component during the field campaigns. Leaking components were often random between field campaigns, which resulted in few repeat measurements on components such as connectors, valves, and PRVs. Operational compressors often changed between field campaigns, which also reduced the number of repeat DPV and RPV measurements. Eleven components were measured during all four field campaigns (4 repeat measurements), and 34 components were measured at three field campaigns (3 repeat measurements). The variability over field campaigns for these repeat measurements is summarized in **Table 3-2**. Since field campaigns were conducted three months apart, these repeat measurements are referred to as quarterly measurements. The quarterly sampling variability was compared to “within” measurement variability (see Research Question 5) and component variability (e.g., variability among all RPVs).

In general, component variability was larger than quarterly (repeat) sampling variability, with the exception of PRVs. However, the relatively large quarterly sampling variability for PRVs was based on one PRV. This PRV had a large emission rate during Field Campaign 1 (424 scf/hr) and was repaired prior to subsequent field campaigns.

Within measurement variability was consistently much smaller than quarterly sampling and component variability, indicating variations in emission rates during the sampling event were insignificant compared to variability between components and between field campaigns.

**Table 3-2: Emission rate variability comparison by component type**

Component Type	Average ER, all data (scf/hr)	“Within” measurement variability (scf/hr)	Quarterly sampling variability (scf/hr)	Component variability, all data (scf/hr)
Distance Piece Vent	30.40	1.40	21.70	51.12
Rod Packing Vent	165.14	5.60	143.22	244.76
Pneumatic Device Vent	14.06	1.07	14.64	24.21
Connector, Other	3.21	0.17	n/a	6.65
Connector, Flange	5.26	0.06	n/a	8.44
Valve	9.86	0.38	3.43	14.64
PRV	67.99	3.30	201.91	145.16

**Note:** Variability was calculated as the average of the standard deviations of multiple samples

Additional comparisons were done between quarterly sampling variability and component variability within field campaigns. The variability within a field campaign (spatial) was generally larger than the quarterly variability (temporal). In other words, variability between a unique component over time was less than the variability between two unique components from the same category. This indicates that emission factors calculated from emission rates measured from single visits to multiple site will likely capture temporal emission variability.

### 3.5 Emission Comparison – Gas vs. Liquid Lines

#### **Research Question 7**

***Should liquid lines be included in the population count? How much do liquid lines contribute to measured emissions?***

#### **Key Findings**

1. Emissions from liquid lines accounted for an average of 1.3% of the total emissions measured.
2. On average, 16% of fugitive emissions came from liquid lines.

#### **Summary**

For reporting purposes, excluding liquid lines from site-wide screening may have a negligible effect on component-related emissions. However, from a site management perspective, malfunctioning components were not uncommon on liquid lines and contributed substantially to fugitive emissions at some sites.

As discussed in Section 3.1 (Component Counts), including liquid lines had a substantial effect on the component counts (~36%). Emissions from gas lines were compared to emissions from liquid lines to determine if liquid lines should be included in component counting and screening. Pneumatic devices that controlled liquid level were counted as part of the gas line because these devices are operated using site gas. The percent of total emissions that were measured from liquid lines is presented in **Table 3-3**. On average, emissions from liquid lines accounted for 1.3% of the total emissions measured at the sites.

**Table 3-3. Percent of total emissions from liquid lines**

Field Campaign	Site 1	Site 2	Site 3	Site 4
1	0.1%	2.3%	0.04%	0%
3	1.2%	2.8%	0%	0%
4	1.5%	7.4%	0%	0%

Field Campaign 2 not included because a FLIR was not used to screen liquid lines for emissions

It should be noted that not all pneumatic device vents were measured during the field events. Therefore, it is expected that emissions from gas lines (i.e., pneumatic devices not sampled) may be higher than measured values. Based on the sites in this study, excluding emissions from liquid lines will likely have a negligible effect on total component-related methane emissions.

Although emissions from liquid lines were small when compared to emissions from all components measured at the sites, emissions from liquid lines made up a larger portion of fugitive emissions. As shown in **Table 3-4**, there was large variability in fugitive emissions from liquid lines. Site 2 had the largest relative amount of fugitive emissions from liquid lines (36-100% depending on field campaign), while Site 4 had none. On average, fugitive emissions from liquid lines accounted for 16% of all fugitive emissions. From a site management perspective, operators may want to include liquid lines in screening protocols as it is possible that malfunctioning components are located on liquid lines.

**Table 3-4. Percent of fugitive emissions from liquid lines**

Field Campaign	Site 1	Site 2	Site 3	Site 4
1	0.4%	100%	10%	0%
3	3.5%	36%	0%	0%
4	4.0%	36%	0%	0%

Field Campaign 2 not included because a FLIR was not used to screen liquid lines for emissions

### 3.6 Emissions Comparison – Measured vs. Estimated

#### **Research Question 8**

***How do measured emissions compare to estimated emissions calculated from published Subpart W emission factors?***

#### **Key Findings**

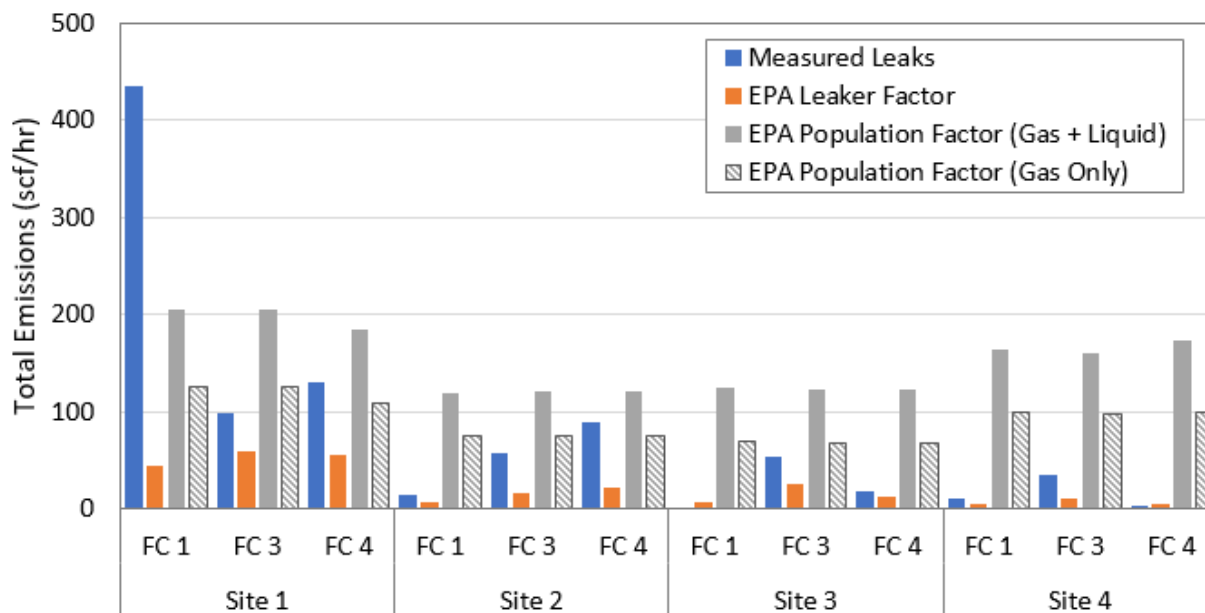
1. Total emissions based on leaks identified with a FLIR camera and leaker EFs underestimated emissions calculated using USEPA Subpart W EFs.
2. Total emissions based on component population counts and population EFs generally overestimated emissions calculated using USEPA Subpart W EFs.
3. Including liquid lines in the site-wide population counts substantially increased the estimated leaking emission rates compared to rates calculated with counts only from gas lines.

#### **Summary**

Population EFs, whether including or excluding liquid lines, were a conservative estimate of fugitive emissions. Leaker EFs consistently underestimated emissions at the field sites. Measurements at more sites, particularly sites in other areas of the country, need to be completed before determining the accuracy of EFs.

Leaker and population emission factors were calculated using emission results from the 4 field campaigns and compared against USEPA Subpart W EFs. For leaker EFs, total measured emission rates were calculated using the number and types of leaks identified in the FLIR survey and compared against calculated emissions (**Figure 3-11**). Field Campaign 2 was not included because a site-wide FLIR survey was not performed. For population EFs, emission rates were calculated using the component counts for each site, which typically varied by field campaign since different compressors were in operation.

Component categories included in the comparison were connectors (other and flanged), valves, and PRVs since these components had both population and leaker EFs available in Subpart W. Connectors were separated into other and flanged with leaker EFs, but kept as one category with population EFs. All other component types were excluded for this analysis.



Leaker and population factors from Tables W-1E and W-1A in the Mandatory Greenhouse Gas Reporting Subpart W (USEPA 2015; USEPA 2016). Population factor estimations calculated using population counts including both gas and liquid lines, as well as only gas lines.

**Figure 3-11.** Measured site-wide leaks compared to leaks calculated using USEPA leaker and population factors

Total emissions based on leaks identified with a FLIR camera and *leaker* EFs underestimated emissions calculated using USEPA Subpart W EFs. Results indicate that the study sites had fewer leaks than sites used to develop current Subpart W population EFs. However, leaks measured at each of the study sites had larger emission rates than those used to develop the current Subpart W leaker EFs.

Total emissions based on component population counts and *population* EFs generally overestimated emissions calculated using USEPA Subpart W EFs. Even when components on liquid lines were removed from the population count, which reduced calculated emissions by 41%, the population factor estimates were generally higher than the measured leaks. This could be due to population factors accounting for emissions that were below the detection limit of the FLIR. For example, a leak from a valve that was too small to be seen by the FLIR would not be measured by the high-flow system. The emissions from that valve would contribute to the total leaking emissions from the site, but would not be included in measured emissions. Measurements at more sites, particularly sites in other areas of the country, need to be completed before determining the accuracy of EFs.

### 3.7 Data Visualization

A data visualization tool was developed to conservatively estimate the extent of the plume generated by the measured emissions from a hypothetical compressor(s). The results of the visualization package for Site 1, Field Campaign 2 were exported to Python to generate contour plots (**Figure 3-12**). Three input sources were included in the model which were summed emissions from Compressors 13, 14, and 15. Since the model was designed for a steady-state source, compressor emissions were assumed to be constant throughout the day.

The data visualization tool was designed to be user friendly. It can be used to generate steady state plumes for gaseous chemicals or to determine the stability class of specific atmospheric conditions. Details of the tool are in Appendix D, and it can be downloaded as < url >.

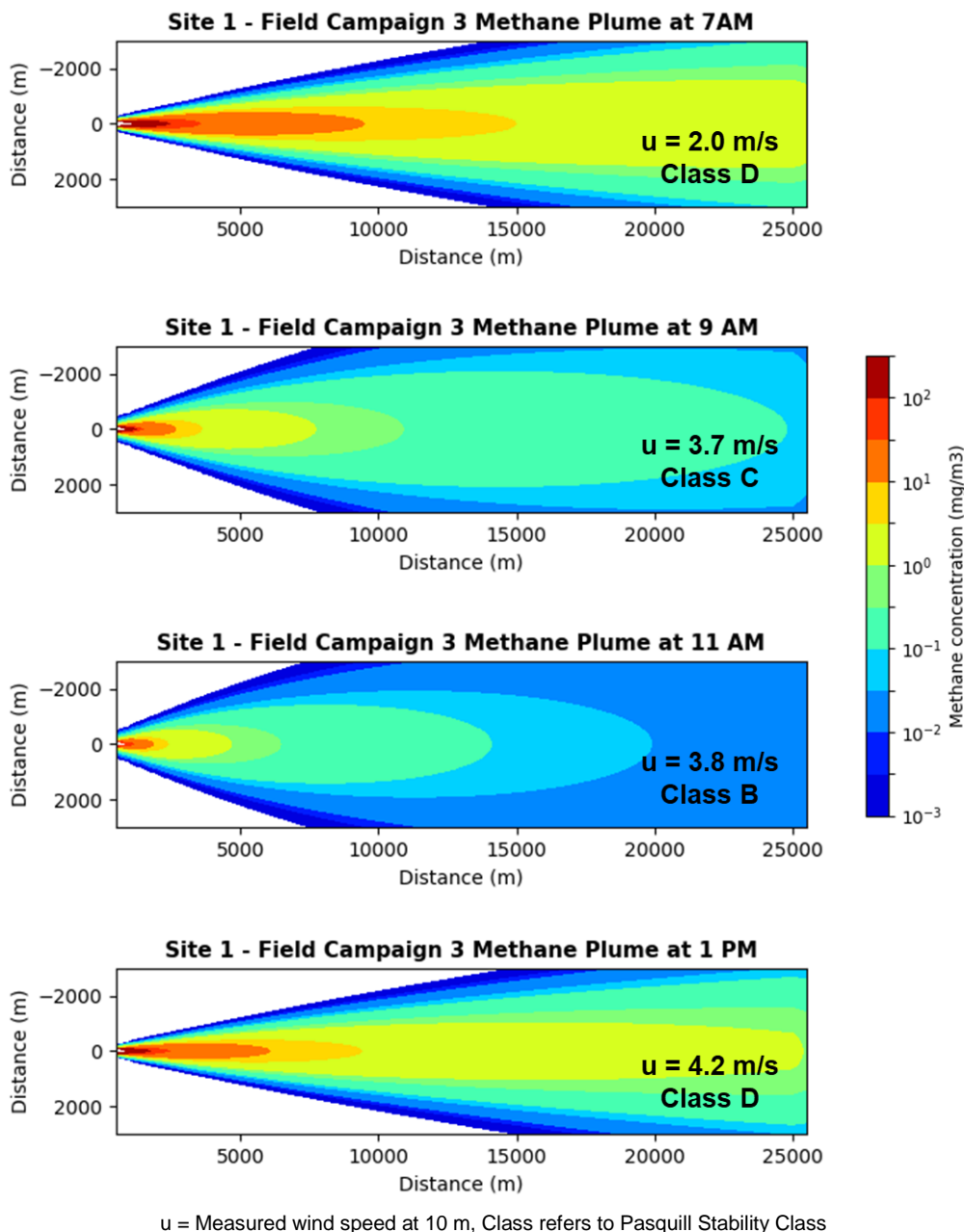


**Figure 3-12.** Hypothetical estimated methane plume for measured methane emissions from Compressors 13, 14, and 15 at Site 1 during Field Campaign 2

## 4.0 TECHNOLOGY TRANSFER

The high level of interest and participation on this project from industry and regulatory stakeholders concerned with methane emissions from G&B stations and updates to Subpart W increased its value to GSI and DOE NETL. Technical Advisory Steering Committees (TASCs) consisting of participants from industry, regulatory agencies, non-governmental organizations, academia, and consulting were assembled to provide recommendations and feedback on project activities over the two-year program. A list of TASC participants is provided in **Table 4-1**.

**Table 4-1. List of TASC Participants**

Industry			
Anadarko	Dominion	GE	Pioneer
Apache	Enbridge	Gulf Coast Green Energy	QEP Resources
Chevron	Energy Transfer	Haliburton	Shell
Devon	FLIR	Kinder Morgan	Spectra
Regulatory Agencies			
BLM	KGS	PA DEP	UT DEW
CADOC	MDE	TRRC	WVDEP
COGCC	MI DEQ	USEPA	
DOE NETL	NDIC	USEPA Region 6	
IL DNR	NY DEC	UT DAQ	
Non-Governmental Organizations			
AGA	EDF	HARC	PHMSA
API	GTI	INGAA	
Academia & Consulting			
Colorado State University	Indaco Air Quality Services, Inc.	University of Colorado-Boulder	University of Utah
GHD	University of Cincinnati	University of Kentucky	

TASCs formed for this project represented two-way exchanges of information. This open communication provided an excellent opportunity for GSI to inform TASC participants of recent project findings, and for TASC participants to increase project efficiency by giving GSI real-time feedback on sampling protocols and data analysis. GSI and our teaming partners hosted twelve conference calls under this project to solicit feedback from TASC participants. During one of the TASC calls, for example, API representatives expressed concern over explosive atmospheres associated with elevated methane flow rates (e.g., 100+ scfm). During that call, our Utah State University partner was able to quell those fears by outlining explosion-proof components that were built into their high volume sampler. An industry participant asked how our team will address episodic challenges associated with EF's, which are difficult to measure or predict. To address that concern, we ensured that we considered activity data (e.g., facility throughput, material types, maintenance/blowdowns) while performing EF calculations.

In addition, a memo with preliminary results was issued to coincide with the final set of TASC calls to inform TASC members in advance of project findings and encourage input and discussion. Specific feedback from participants was compiled and considered as GSI planned and implemented next steps throughout the project. Knowledge gained from this program was also disseminated through technical presentations at conferences (as shown in **Table 4-2**) and development of public education brochures and fact sheets summarizing project highlights and findings.



**Table 4-2. Technology Transfer Events**

Event Title	Date	Organization	Description
API Technical Meeting	February-2017	American Petroleum Institute	Susan Stuver, Ann Smith and Richard Bowers presented project scope and objectives to industry representatives and solicited participation in the I-TASC
Environmentally Friendly Drilling (EDF) Sponsors Meeting	April-2017	Houston Advanced Research Center	Susan Stuver and Richard Bowers presented project accomplishments and challenges.
AUVSI XPONENTIAL 2017	May-2017	Association for Unmanned Vehicle Systems International	Susan Stuver and Richard Bowers presented information on sampling technologies used in field programs and how automation could improve the accuracy of data collected.
TCEQ Tradefair	May-2017	Texas Commission on Environmental Quality	Susan Stuver attended meetings with TCEQ Commissioners regarding the value of the project.
KOGA Annual Meeting	July-2017	Kentucky Oil and Gas Association	Susan Stuver and Ann Smith presented preliminary results obtained from Field Campaign 1 Sampling Events 1 and 2.
SPE Annual Technical Conference and Exhibition	October-2017	Society of Petroleum Engineers	Susan Stuver disseminated brochures and fact sheets highlighting project findings.
O&G Environmental Conference	November-2017	Environmental Training Institute	Susan Stuver disseminated brochures and fact sheets highlighting project findings.
CH4 Connections Conference	December-2017	Groundwater Technology Inc.	Susan Stuver disseminated brochures and fact sheets highlighting project findings.

## 5.0 CONCLUSIONS AND RECOMMENDATIONS

Key findings and *recommendations* for the project are summarized below:

### Component count and classification

- Adjusting the component counting methodology (e.g., including components on liquid lines or pneumatic loops) impacts component population counts. *A standard methodology should be adopted for classifying and counting components in order to minimize inconsistencies across studies and instruct stakeholders responsible for GHGI reporting.*
- Results support current component subcategories listed in USEPA Subpart W, including the subdivision of connectors (flanged and “other”) and pneumatic device vents (intermittent, continuous low bleed, and continuous high bleed). *Results warrant further study of emissions from compressor vents, meters, gauges, and regulators.*

### Emission Rate Variability by Site, Operation and Time

- There is variation of emissions rates across sites and a relationship between higher emissions and compressor age for some components. *More measurements should be taken on additional compressor components to further assess emissions rate variability by site and operational parameter.*
- Site inlet pressure had a statistical correlation with emission rates on compressor RPVs. Other site operational parameters, including gas throughput, composition, discharge pressure and energy throughput, did not have statistically significant correlations with emission rates from DPVs and RPVs.
- Variation in site and compressor component emissions was significant between field campaigns. The type and proportion of component(s) contributing to compressor emissions also varied across field campaigns.
- Measuring the emission rate of a sample for an extended period of time is not necessary to capture the average component emission rate.

### Liquid Lines Contribution to Measured Emissions

- For reporting purposes, excluding liquid lines from site-wide screening may have a negligible effect on component-related emissions. However, from a site management perspective, malfunctioning components were not uncommon on liquid lines and contributed substantially to fugitive emissions at some sites.

### Comparisons to Current EPA EFs

- Population EFs, whether including or excluding liquid lines, were a conservative estimate of fugitive emissions. Leaker EFs consistently underestimated emissions at the field sites. *Measurements at more sites, particularly sites in other areas of the country, need to be completed before determining the accuracy of EFs.*

## 6.0 REFERENCES

- Clearstone Engineering, 2002. Identification and Evaluation of Opportunities to Reduce Methane Losses at Four Gas Processing Plants. internal report prepared under U.S. EPA Grant No. 827754-01-0 for Gas Technology Institute, Des Plaines, IL.
- Energuides, 2018. Just how much does the pilot light of a gas appliance consume exactly? Sibelga.
- FLIR, 2011. Gas-Find 320. FLIR Systems Inc.: Wilsonville, OR.
- Foster-Wittig, T.A., Thoma, E.D., Green, R.B., Hater, G.R., Swan, N.D., Chanton, J.P., 2015. Development of a mobile tracer correlation method for assessment of air emissions from landfills and other area sources. *Atmospheric Environment* 102, 323-330.
- Galle, B., Samuelsson, J., Svensson, B.H., Börjesson, G., 2001. Measurements of Methane Emissions from Landfills Using a Time Correlation Tracer Method Based on FTIR Absorption Spectroscopy. *Environmental Science & Technology* 35, 21-25.
- Harrison, M.R., Shires, T.M., Wessels, J.K., Cowgill, R.M., 1996. Methane Emissions from the Natural Gas Industry. Gas Research Institute and U.S. Environmental Protection Agency, Washington, DC.
- Harrison, M.R., Galloway, K.E., Shires, T.M., Allen, D., 2011. Natural Gas Industry Methane Emission Factor Improvement Study Final Report. U.S. Environmental Protection Agency, p. 53.
- Lamb, B.K., McManus, J.B., Shorter, J.H., Kolb, C.E., Mosher, B., Harriss, R.C., Allwine, E., Blaha, D., Howard, T., Guenther, A., Lott, R.A., Siverson, R., Westburg, H., Zimmerman, P., 1995. Development of Atmospheric Tracer Methods To Measure Methane Emissions from Natural Gas Facilities and Urban Areas. *Environmental Science & Technology* 29, 1468-1479.
- IPCC, 2014. Climate Change 2014: Synthesis Report. Contribution of Working Groups I, II and III to the Fifth Assessment Report of the Intergovernmental Panel on Climate Change. In: Core Writing Team, Pachauri, R.K., Meyer, L. (Eds.). IPCC, Geneva, Switzerland, p. 151.
- Marchese, A.J., Vaughn, T.L., Zimmerle, D.J., Martinez, D.M., Williams, L.L., Robinson, A.L., Mitchell, A.L., Subramanian, R., Tkacik, D.S., Roscioli, J.R., Herndon, S.C., 2015. Methane Emissions from United States Natural Gas Gathering and Processing. *Environmental Science & Technology* 49, 10718-10727.
- Mønster, J.G., Samuelsson, J., Kjeldsen, P., Rella, C.W., Scheutz, C., 2014. Quantifying methane emission from fugitive sources by combining tracer release and downwind measurements – A sensitivity analysis based on multiple field surveys. *Waste Management* 34, 1416-1428.
- Ravikumar, A.P., Wang, J., McGuire, M., Bell, C.S., Zimmerle, D., Brandt, A.R., 2018. “Good versus Good Enough?” Empirical Tests of Methane Leak Detection Sensitivity of a Commercial Infrared Camera. *Environmental Science & Technology* 52, 2368-2374.
- Scheutz, C., Samuelsson, J., Fredenslund, A.M., Kjeldsen, P., 2011. Quantification of multiple methane emission sources at landfills using a double tracer technique. *Waste Management* 31, 1009-1017.

- USEPA, 2006. Cost-Effective Directed Inspection and Maintenance Control Opportunities at Five Gas Processing Plants and Upstream Gathering Compressor Stations and Well Sites. National Gas Machinery Laboratory, Cleanstone Engineering Ltd., Innovative Environmental Solutions, Inc., p. 74.
- USEPA, 2011. Mandatory Reporting of Greenhouse Gases: Technical Revisions to the Petroleum and Natural Gas Systems Category of the Greenhouse Gas Reporting Rule; Final Rule. 40 CFR Part 98.
- USEPA, 2014. Draft Other Test Method 33A: Geospatial Measurement of Air Pollution, Remote Emissions Quantification - Direct Assessment (GMAP-REQ-DA). p. 91.
- USEPA, 2015. Mandatory Greenhouse Gas Reporting Subpart W - Petroleum and Natural Gas Systems.
- USEPA, 2016. Mandatory Greenhouse Gas Reporting Subpart W - Petroleum and Natural Gas Systems.
- USEPA, 2018. Inventory of U.S. Greenhouse Gas Emissions and Sinks 1990-2017: Updates Under Consideration for Incorporating GHGRP Data. p. 27.
- Vaughn, T.L., Bell, C.S., Yacovitch, T.I., Rosciolo, J.R., Herndon, S.C., Conley, S., Schwietzke, S., Heath, G.A., Pétron, G., Zimmerle, D., 2017. Comparing facility-level methane emission rate estimates at natural gas gathering and boosting stations. *Elementa Science of the Anthropocene* 5.
- Yacovitch, T.I., Daube, C., Vaughn, T.L., Bell, C.S., Rosciolo, J.R., Knighton, W.B., Nelson, D.D., Zimmerle, D., Pétron, G., Herndon, S.C., 2017. Natural gas facility methane emissions: measurements by tracer flux ratio in two US natural gas producing basins. *Elementa Science of the Anthropocene* 5.
- Zimmerle, D., C.K., P., Bell, C.S., Heath, G.A., Nummedal, D., Pétron, G., Vaughn, T.L., 2017. Gathering pipeline methane emissions in Fayetteville shale pipelines and scoping guidelines for future pipeline measurement campaigns. *Elementa Science of the Anthropocene* 5.

---

# **APPENDIX A**

## **Fugitive Emissions Screening Procedures, Equipment, and Specifications**

---

## APPENDIX A

### FUGITIVE EMISSIONS SCREENING PROCEDURES, EQUIPMENT, AND SPECIFICATIONS

#### 1.0 TECHNOLOGY BACKGROUND

As a component of field investigation activities, a FLIR™ GF320 infrared imaging camera was used as a screening tool to visually locate (but not quantify or speciate) losses and leaks from components of compressors and other equipment (e.g., separators, dehydrators). Optical gas imaging instruments were used in accordance with 40 CFR Part 60, Subpart A, §60.18 of the *Alternative Work Practice for Monitoring Equipment Leaks*. Field personnel operating the FLIR™ GF320 received training and certification for proper operation of the camera for optical gas imaging prior to use.

Infrared cameras convert thermal signatures to optical images. The GF320 camera is lightweight with features designed to detect gas emissions in field applications, resulting in efficient screening of large areas. The GF320 is capable of detecting methane emissions with temperatures up to 350 °C and within  $\pm 1$  °C accuracy. The spectral response is in the range of 3.2-3.4  $\mu\text{m}$  with a resolution of 320x240. Total pixels is 76,800. Minimum acceptable accuracy is  $\pm 1^\circ\text{C}$  for temperature ranges of 0 °C to 100 °C or  $\pm 2\%$  of reading for temperature range  $>100$  °C. The minimum detected leak rate for methane in FLIR lab testing is 0.8 g/hr. In the field, the FLIR is usually able to detect natural gas emissions in the range of 1 scf/hr or larger from 3 m away (Ravikumar et al., 2018)

#### 1.1 Field methods

When imaging an object during field activities that was of a temperature similar to the surroundings, such contrast was not evident. In order to compensate for this, a background material of differing thermal properties was placed behind the object to create contrast. The camera was also moved to different angles to find a background with sufficient thermal contrast. Shifting through the various color palettes also afforded better images.

At the beginning of daily field activity, the FLIR camera was powered up, commencing an automatic startup sequence. This sequence included cooling of the internal spectral detector and other electronic system checks. After the automatic startup sequence was concluded, a Non-Uniformity Correction (NUC) check was performed to assure that the camera was functioning properly prior to conducting gas imaging activities.



## 2.0 FLIR GF320 SPEC SHEET

### Specifications

Model	GF300 / GF320
Detector Type	FLIR Indium Antimonide (InSb)
Spectral Range	3.2 – 3.4 $\mu\text{m}$
Resolution	320 x 240 pixels
Detector Pitch	30 $\mu\text{m}$
NETD/Thermal Sensitivity	<15 mK @ +30°C (+86°F)
Sensor Cooling	Stirling Microcooler (FLIR MC-3)
Electronics / Imaging	
Image Modes	IR Image, visual image, high sensitivity mode (HSM)
Frame Rate (Full Window)	60 Hz
Dynamic Range	14-bit
Video Recording / Streaming	Real-time non-radiometric recording: MPEG4/H.264 (up to 60 min./clip) to memory card Real-time non-radiometric streaming: RTP/MPEG4
Visual Video	MPEG4 (25 min./clip) to memory card
Visual Image	3.2 MP from integrated visible camera
GPS	Location data stored with every image
Camera Control	Remote camera control via USB
Measurement	
Standard Temperature Range	-20°C to +350°C (-4°F to +662°F)
Accuracy*	$\pm 1^\circ\text{C}$ ( $\pm 1.8^\circ\text{F}$ ) for temperature range 0°C, to +100°C; +32°F to +212°F or $\pm 2\%$ of reading for temperature range > +100°C; > +212°F
Optics	
Camera f/number	f/1.5
Available Fixed Lenses	14.5" (38 mm), 24" (23 mm)
Focus	Automatic (one touch) or manual (electric or on the lens)
Image Presentation	
On-Camera Display	Built-in widescreen, 4.3 in. LCD, 800 x 480 pixels
Automatic Gain Control	Continuous/manual, linear, histogram
Image Analysis*	10 spotmeters, 5 boxes with max./min./average, profile, delta temperatures, emissivity & measurement corrections
Color palettes	Iron, Gray, Rainbow, Arctic, Lava, Rainbow HC
Zoom	1-8x continuous, digital zoom
General	
Operating Temperature Range	-20°C to +50°C (-4°F to +122°F)
Storage Temperature Range	-30°C to +60°C (-22°F to +140°F)
Encapsulation	IP 54 (IEC 60529)
Bump / Vibration	25 g (IEC 60068-2-27) / 2 g (IEC 60068-2-6)
Power	AC adapter 90-260 VAC, 50/60 Hz or 12 V from a vehicle
Battery System	Rechargeable Li-ion battery
Weight w/ Battery & Lens	1.94 kg (4.27 lbs)
Size (L x W x H) w/ Lens	305 x 169 x 161 mm
Mounting	Standard, 1/4"-20

\* GF320 model only



FLIR Systems, Inc.  
9 Townsend West  
Nashua, NH 03063  
USA  
PH: +1 866.477.3687

PORTLAND  
Corporate Headquarters  
FLIR Systems, Inc.  
27700 SW Parkway Ave.  
Wilsonville, OR 97070  
USA  
PH: +1 866.477.3687

EUROPE  
FLIR Systems  
Luxemburgstraat 2  
2321 Meer  
Belgium  
PH: +32 (0) 3665 5100

www.flir.com/ogi  
NASDAQ: FLIR

CANADA  
FLIR Systems, Ltd.  
920 Sheldon Court  
Burlington, ON L7L 5L6  
Canada  
PH: +1 800.613.0507

CHINA  
FLIR Systems Co., Ltd  
Rm 1613-16, Tower II  
Grand Central Plaza  
138 Shatin Rural  
Committee Road Shatin  
New Territories  
Hong Kong  
PH: +852 2792 8955

LATIN AMERICA  
FLIR Systems Brasil  
Av. Antonio Bardella, 320  
Sorocaba, SP 18052-852  
Brasil  
PH: +55 15 3238 7080

Equipment described herein may require US Government authorization for export purposes. Diversion contrary to US law is prohibited. Imagery for illustration purposes only. Specifications are subject to change without notice. ©2015 FLIR Systems, Inc. All rights reserved. (Updated 11/03/15)

www.flir.com



The World's Sixth Sense™

---

# **APPENDIX B**

## **High-Flow Sampling Procedures, Equipment, and Specifications**

---

# APPENDIX B

## HIGH-FLOW SAMPLING PROCEDURES, EQUIPMENT, AND SPECIFICATIONS

### 1.0 INTRODUCTION

High flow samplers have been used in the oil and gas industry to detect natural gas leaks for decades, have been used in a number of scientific studies (Allen et al., 2013; Johnson et al., 2015) and are approved by USEPA for leak quantification (CFR, 2016). However, only one commercial high flow sampler exists, the backpack-mounted Bacharach HI FLOW, and it suffers from several biases. The Bacharach sampler uses detectors that do not distinguish between methane and other organics, and that do not detect all organic compounds with the same sensitivity, leading to uncertainty in measurements, especially for sources for which non-methane organics make up a high percentage of total emissions. Because of the size of its pump, the Bacharach sampler is limited to leaks smaller than about 1,000 standard cubic feet per hour (SCFH). Most importantly, the sampler uses two detectors, and its software doesn't switch from the low-range to the high-range detector reliably, leading to a low bias in measurements (Howard et al., 2015; Ravikumar et al., 2018). Bacharach has stopped manufacturing the HI FLOW, and the instrument is difficult to obtain from equipment rental companies.

Alternatives to high flow sampling exist for measuring emissions from oil and gas infrastructure. Traditional bag sampling techniques (EPA, 1995) are more complicated, take longer to set up, and only work for low flows. Bag-filling techniques (CFR, 2016; Subramanian et al., 2015) suffer from poor accuracy, especially at low and high flows. Methods that directly measure actual emission flow rates from exhaust streams (Hendler et al., 2009) can provide as much or more accuracy than high flow sampling methods but are only applicable for equipment with an exhaust pipe to which a flow measurement tube can be attached. For most fittings, valves, meters, or other small components of gas infrastructure, high flow sampling provides the simplest and most versatile method to quantify emission rates.

A custom high-flow sampling system was constructed by Utah State University (USU) Bingham Research Center to quantify methane leaks from gas infrastructure. This system is similar to that developed by Johnson et al. (2015). The following sections describe this system and report on its performance.

### 2.0 SYSTEM DESCRIPTION

#### 2.1 System Overview

A diagram of the high flow sampling system is shown in **Figure B-1**, and photographs of the system are shown in **Figure B-2**. The system operates by:

1. Pulling sample gas from a leaking component into a sampling duct.
2. Precisely measuring the total flow rate of sample gas through the sampling duct.
3. Analyzing the sample gas to determine the methane concentration.
4. Correcting sample gas concentrations for the methane concentrations in ambient air near the leaking component.

The methane emission rate is calculated as:

$$E = C \times F \quad \text{(Equation C-1)}$$

where  $E$  is the methane emission rate ( $\text{g s}^{-1}$ ),  $C$  is the concentration of methane in the sample gas ( $\text{g m}^{-3}$ ; corrected for the concentration in ambient air), and  $F$  is the flow rate of sample gas ( $\text{m}^3 \text{s}^{-1}$ ). The ideal gas law was used to convert  $E$  to the commonly-used units of SCFH at standard temperature of  $60^\circ \text{F}$ .

The system was mounted in a generator-powered trailer and included 40 m of sample ducting, which allowed for a large area to be sampled without moving the trailer. The entire flow path was intrinsically safe or conductive and grounded to the trailer, which was grounded to the earth.

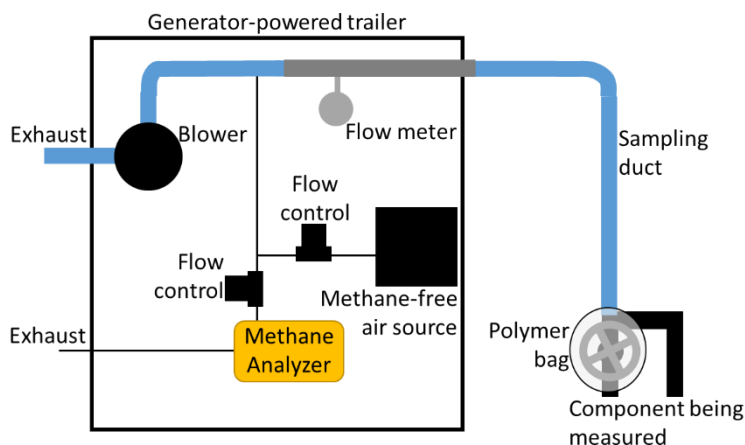


**Figure B-1.** Diagram of high flow sampling system.

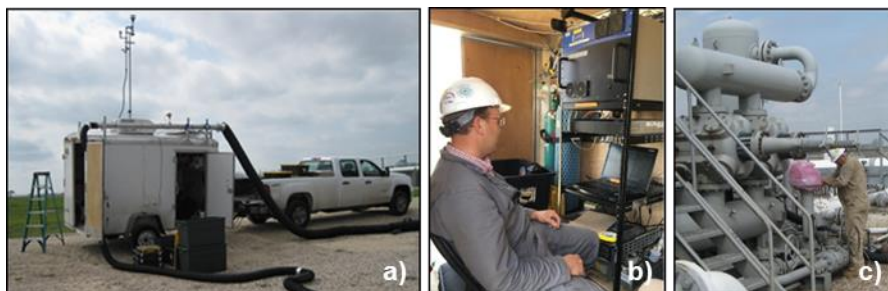


**Figure B-2.** Photographs of the high flow sampling system in operation: a) entire system, b) interior of the trailer, and c) bagging a pneumatic device vent for sampling.

## 2.2 Detailed System Description

### 2.2.1 Locating Leaks

Leak locations were detected with a FLIR GF320 optical gas imaging camera and/or a Bascom Turner Gas Rover (see Appendix A for details on FLIR screening). The Bascom Turner Gas Rover is a handheld instrument used to measure methane concentrations. It can detect methane in air at 10 ppm or greater. The Gas Rover is generally able to detect smaller emission sources than the FLIR camera, but the camera is better able to pinpoint the exact source of emissions.

After locating a leak, it was flagged, given an identification number, and then the leak rate was quantified with the high flow sampling system.

### 2.2.2 Isolating Leaks for Measurement

The high flow system's sampling duct was constructed of 13 cm diameter conductive ducting in 8-m lengths. Aluminum foil tape was used to seal the duct connections. In most cases, an antistatic polymer bag was wrapped around the component and the duct inlet. This isolated the sample from surrounding air and ensured that all of the leaking gas was entrained into the sampling duct. Metal clips and aluminum foil tape were used to aid in this process. In some cases, leaking components could be inserted into the end of the sampling duct, allowing for all leaking gas to be entrained without bagging. In all cases, after connecting the duct to the leaking component, a Bascom Turner Gas Rover was used to measure methane all around the leaking component, sample duct, and bag to ensure that all leaking gas was entrained in the duct.

### 2.2.3 Sample Flow System

An explosion-proof vacuum blower pulled a high volume of gas (between 0.5 and 2.5 m<sup>3</sup> min<sup>-1</sup>) from the sampled component, through the sample duct, and through a flow measurement tube. A manual flow damper was used to adjust the flow if needed. A Fox Thermal Instruments Model FT1 mass flow meter was used to measure flow. The flow meter was housed in a 3 m long, 11 cm diameter stainless steel tube with a stainless-steel flow conditioner at the upstream end. The flow meter was positioned 1.7 m from the upstream end of the tube.

One shortcoming of all mass flow measurements is that the measured flow depends on the composition of the gas sampled. This was compensated for by correcting flows for the methane concentration in the sample gas. However, non-methane organic compounds in emitted gas were not measured and could have resulted in a flow bias, especially for components with high emission rates of gas with high concentrations of non-methane organics, such as liquid storage tanks (Hendler et al., 2009).

For example, emissions were measured from a leaking thief hatch on a liquid storage tank at a compressor station. The average sample gas methane concentration during this measurement was 135,895 ppm, while the ambient methane concentration was less than 100 ppm, and the sample flow rate was 1.27 m<sup>3</sup> min<sup>-1</sup> (mass flow at standard conditions of 0 °C and 1 atm). The flow was corrected based on the methane concentration (MKS, 2017) to 1.21 m<sup>3</sup> min<sup>-1</sup>. With and without the correction, the methane emission rate was 1.96 g s<sup>-1</sup> and 2.06 g s<sup>-1</sup> (368 and 387 SCFH), respectively, a difference of 5%. However, liquid storage tank emissions likely contained significant amounts of non-methane hydrocarbons, which were not measured. If the sample gas consisted of the measured methane concentration, 20% propane, 10% ethane, and remainder air, the corrected flow rate would be 0.86 m<sup>3</sup> min<sup>-1</sup>, and the corrected emission rate of methane would be 1.40 g s<sup>-1</sup> (263 SCFH), a difference of 40%.

### 2.2.4 Methane Measurement

A Los Gatos Research (LGR) Ultraportable Greenhouse Gas Analyzer was used to measure methane concentrations in sample gas. Sample lines leading to and from the analyzer were composed either of PFA tubing or Tygon 2475 high-purity tubing. The analyzer detects methane concentrations of up to 10% in air. It detects up to 1000 ppm with a low-concentration laser and greater than 1000 ppm with a separate high-concentration laser. The results were recorded from both lasers for all samples. When the methane concentration in sample gas exceeded 10%, the analyzer flow was diluted with methane-free air to keep within the analyzer's range. Methane-free air was generated with a custom-built air scrubber system, and the system was tested daily to ensure air produced by the system contained less than 0.2 ppm methane. The flow into the analyzer was measured, as well as the flow rate of methane-free dilution air, with Alicat mass flow controllers. The calibration of the mass flow controllers was checked with a NIST-traceable flow standard prior to each measurement campaign.



### **2.2.5 Correction for Background Methane**

The methane concentration in sample gas was equal to the ambient methane concentration in the air being pulled into the high flow sampling duct plus any methane added from the leaking component. To correct for ambient methane, the ambient methane concentration was measured through a PTFE filter and a 0.5 cm line composed of Tygon 2475 high-purity tubing. The inlet of this line was positioned as close to the sample duct inlet as possible. A LGR Multiport Inlet Unit allowed the methane analyzer to switch between analyzing sample gas and analyzing air from the background line. Usually, the system was programmed to measure sample gas for three minutes and then background air for two minutes. Data for the first minute was discarded after each valve switch. The background methane concentration was subtracted from the sample gas concentration prior to calculating emission rates.

### **2.2.6 Sampling Intervals**

All measurement data was sampled once every 5 s and stored data as 20 s averages. In most cases, emissions from each measured component were quantified for 8-12 min. If the emission rate was variable, or as an occasional test of emission stability, the measurement time was extended. A 10-min sampling time resulted in about ten separate 20-sec emission rate measurements.

### **2.2.7 Measurement System Calibrations**

The calibration of the methane analyzer was checked daily at four or five points along its measurement range, including points within the range of both methane lasers. The analyzer was also periodically checked at 15-20 points to ensure its response was linear across its range. The scrubber system mentioned above was used to generate methane-free air, and NIST-traceable compressed gas standards or an ultra-high purity methane cylinder was diluted to generate methane at specific concentrations. Alicat mass flow controllers were used to control and measure flows in the calibration system. The calibration of all mass flow controllers was checked with a NIST-traceable flow standard prior to each measurement campaign.

A mass flow controller was used to add methane from an ultra-high purity methane cylinder to the upstream end of the high flow sampling duct daily to verify the performance of the high flow measurement system. Methane was added at two different flow rates between 0.1 and 30 L min<sup>-1</sup>. As a blank test, the emission rate was measured daily while the high flow duct was not sampling any emission source.

The Fox FT1 mass flow meter was calibrated at the factory annually, and its flow was checked prior to each measurement campaign with a Pacer DA420 anemometer. Wind speed output of the Pacer anemometer was converted to mass flow by multiplying the speed by the orifice size and correcting for temperature and ambient pressure.

### **2.2.8 Meteorological Measurements**

Basic meteorology was measured during all measurement periods from a retractable 6 m pole attached to the measurement trailer. A New Mountain NM150WX was used to measure temperature, relative humidity, barometric pressure, GPS location, and GPS heading. A Campbell CS300 was used to measure solar radiation. A Gill WindSonic was used to measure wind speed and direction, and wind direction was automatically corrected based on the GPS heading. All meteorological measurements were checked against NIST-traceable standards annually.



## 2.2.9 Data Collection, Processing, and Storage

All measurement data was collected with a Campbell Scientific CR1000 data logger. Sample names, times, and all other notes were recorded electronically throughout each measurement day. At the end of each day, all collected data and notes were uploaded to an automatically archived, cloud-based server. All collected data and generated final results were processed in Microsoft Excel. Every 30 days all data was backed up in three locations, including a cloud-based server, a local hard drive, and a separate local hard drive that was disconnected from the internet except during archival operations.

## 2.2.10 Safety

All external components of the high flow system were grounded to the trailer (all components were conductive), and the trailer was attached to an earth ground. All components that came into contact with sample gas were antistatic and/or explosion proof, including all pumps, flow controllers, and flow meters. The interior of the trailer was not rated for environments that may be rich in flammable gases, so the trailer was kept 10 m or more from potential sources of flammable gas, and the generators that powered the trailer were kept 20 m or more from flammable gas sources. Additionally, a natural gas monitor was mounted in the trailer to provide a warning if combustible gas concentrations in the trailer built up to dangerous concentrations.

## 3.0 DETECTION LIMITS

### 3.1 Method Detection Limit

The method detection limit of the high flow system was calculated as (a) three times the standard deviation of a set of 20-s emission measurements when the instrument was not measuring any emission source (i.e., a blank) (EPA, 2016), and (b) three times the standard deviation of a set of 20-s emission measurements when the system was sampling a very low emission rate generated with a mass flow controller ( $1.1 \times 10^{-3}$  SCFH). Method detection limits calculated using (a) and (b) were  $2.3 \times 10^{-4}$  and  $1.0 \times 10^{-4}$  SCFH, respectively.

**Figure B-3** shows emission rate data from (a) and (b), which were collected outside the laboratory in Vernal, Utah, distant from oil and gas industrial facilities, but in the vicinity of urban and agricultural sources of methane. Gaps in the emission rate data shown in **Figure B-3** are from periods when the ambient (background) methane concentration was measured. It is expected, but cannot be confirmed, that the variability in blank values observable in **Figure B-3** was due to variation in ambient methane concentrations. The blank variability shown in **Figure B-3** corresponds to a variability in methane concentration of  $\pm 35$  ppb.

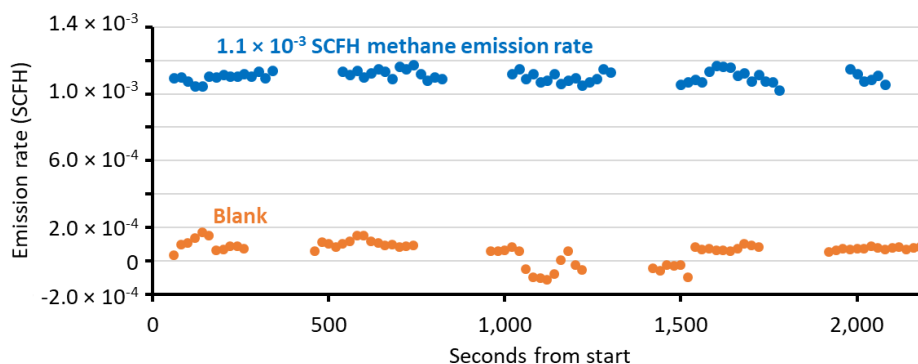


**Figure B-3.** Methane emission measurement data from a detection limit test, including blank measurements and measurements of a  $1.1 \times 10^{-3}$  SCFH emission rate produced with a mass flow controller.

### 3.2 Practical Detection Limit in Field Conditions

Industrial gas facilities have many methane emission sources and variable ambient methane levels. Because the high flow measurement system does not measure background methane and methane in sample gas simultaneously, short-term variations in ambient methane are not adequately corrected for in emission measurements, leading to a decrease in measurement precision (but not accuracy) at industrial facilities. To assess the practical detection limit (a measure of precision) in field conditions, emission measurement blanks were collected (~10 min each) at natural gas compressor stations ( $n = 14$ ). These data were used to calculate practical detection limits for G&B stations as described above. These values are shown in **Table B-1**.

**Table B-1.** Statistical information for blank emission measurements collected outside the laboratory and at G&B stations, in units of SCFH. Values shown were calculated from 20 s data.

SCFH	Lab Blank	Compressor Stations	Compressor Stations (no outliers)
Average	$4.8 \times 10^{-5}$	$7.5 \times 10^{-3}$	$8.6 \times 10^{-3}$
Median	$7.0 \times 10^{-5}$	$2.2 \times 10^{-3}$	$2.4 \times 10^{-3}$
Std. Deviation	$7.8 \times 10^{-5}$	$7.9 \times 10^{-2}$	$3.0 \times 10^{-2}$
Detection Limit	$2.3 \times 10^{-4}$	0.23	$9.0 \times 10^{-2}$
95% Conf. Interval	$1.6 \times 10^{-5}$	$4.7 \times 10^{-3}$	$1.8 \times 10^{-3}$

In addition to having higher detection limits (a measure of precision), emission measurement blanks collected at compressor stations had higher average and median values than the laboratory blank (**Table B-1**). In other words, the sample duct had higher methane concentrations than the background measurement line. It was found that sample methane concentrations remained higher than ambient methane for at least 30 min after sampling strongly leaking components, indicating that residual methane remained in the sample flow path. It is not clear whether this residual methane was in the sample duct, the sample line from the duct to the analyzer, or the switching unit. Assuming the residual methane in the sample line is released at a steady rate, it likely had only a small impact on calculated detection limits.

A few of the blank samples ( $n = 2$ ) were statistical outliers, determined as 10-min average blanks that were higher or lower than 1.5 times the interquartile range. These outliers were either the result of high methane in the sample line prior to the blank measurement or highly variable background methane. With these outliers removed, the practical detection limit was lowered by an order of magnitude (**Table B-1**). A histogram of all field blank values is shown in **Figure B-4**.

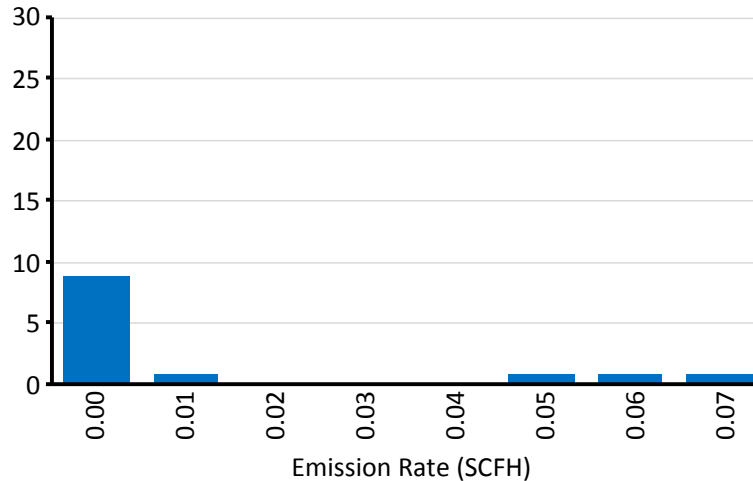


**Figure B-4.** Histogram of methane emission rate for all emission measurement blanks collected at field sites (outliers included). 10-min averages are shown. Values shown on the x-axis are the lower-most bound of each bin.

### 3.3 Detection Limit Sensitivity Analysis

Sensitivity analysis was conducted to determine the effect of using different values for non-detects. The analysis included the scenarios presented in **Table B-2**.

**Table B-2.** Non-detect sensitivity analysis scenarios

Detection Limit	Values less than DL set to:		
	1/2 DL	DL	0
No DL	Unadjusted Value		
0.09 scf/hr	0.045	0.09	0
0.23 scf/hr	0.115	0.23	0

When no DL was applied, the unadjusted values included negative emission rates and small positive emission rates

Results were not sensitive to the various DL scenarios. The difference in average emission rates by component type for the different scenarios was less than 0.5% except for connectors, which had a difference of 1.5%. For data analysis, non-detects were assigned the value of one half the 0.09 scf/hr DL, or 0.045 scf/hr.

## 4.0 CALIBRATION RESULTS

**Table B-3** provides a summary of the results of calibration checks performed on field measurement days.

**Table B-3.** Summary of field calibration results. Zero indicates the analyzer response when methane-free air was sampled. The analyzer's low laser was used for methane concentrations less than 1000 ppm, and the high laser was used for concentrations greater than 1000 ppm.

	Zero (ppm)	Low Laser (% Recovery)	High Laser (% Recovery)	High Flow System (% Recovery)
<b>Average</b>	0.10	101.0	99.7	104.1
<b>Count</b>	49	67	86	95
<b>95% Conf. Interval</b>	0.04	0.8	1.0	1.2

## 5.0 MEASUREMENT RANGE

The method detection limit of  $2.3 \times 10^{-4}$  SCFH is, by definition, the lower end of the measurement range for the high flow sampling system. The maximum flow rate of the sample duct was about  $2,500 \text{ L min}^{-1}$ , and was limited by the flow producible by the blower. Thus, the maximum methane emission rate the system could measure was  $2,500 \text{ L min}^{-1}$  methane, or 5,727 SCFH. A larger blower, or two blowers in series, could perhaps double the flow rate, leading to a maximum of 11,454 SCFH, eight orders of magnitude higher than the method detection limit. The highest emission rate measured was a thief hatch on a liquid storage tank at a G&B station, which had a methane emission rate of 1,288 SCFH. **Figure B-5** presents a histogram of all emission samples collected by the high flow system ( $n = 649$ ).

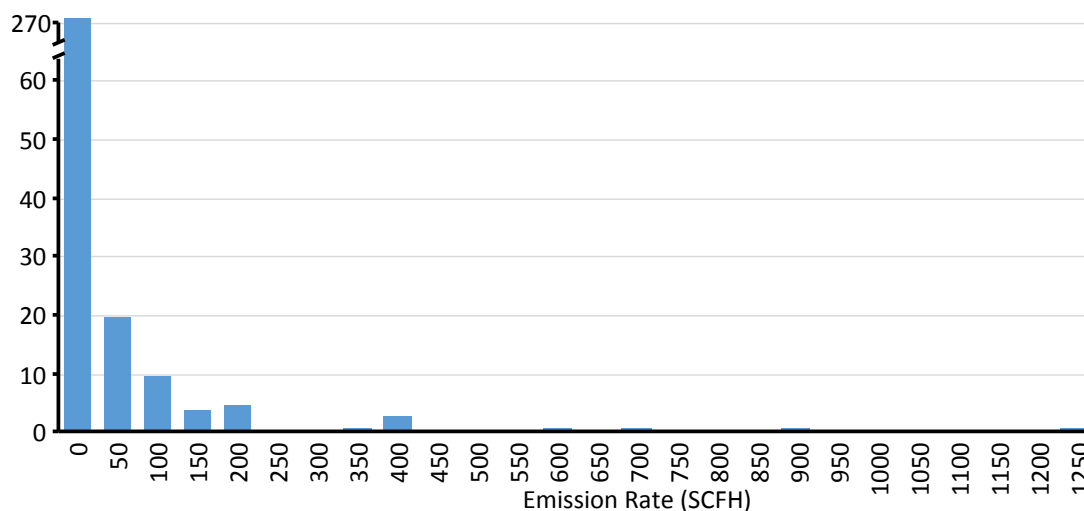


**Figure B-5.** Histogram of methane emission rate for all emission measurement samples that have been collected by the high flow system. Note the change in scale at the top of the y-axis. Values shown on the x-axis are the lower-most bound of each bin.

## 6.0 SAMPLE VARIABILITY

Variability in measured emissions can be due either to instability in the measurement system, short-term variability in background methane, or actual variability in methane emission rates. **Figure B-6** shows emission rates from four G&B station components and emissions regulated with a mass flow controller, and **Table B-4** provides summary statistics for the same dataset. Relative standard deviation, shown in **Table B-4**, is a measure of variability relative to the sample average. The variability in emission rates generated by the mass flow controller is caused by the measurement system and the mass flow controller itself and was 0.68 at an emission rate of 42.5 SCFH. When we used the mass flow controller to generate an emission rate of 0.4 SCFH, the relative standard deviation of the measurements was 1.23. The relative standard deviation of the  $1.1 \times 10^{-3}$  SCFH emission mentioned above was 3.05. The relative standard deviations of emissions from the components shown in **Table B-4** are in the same range as those for emissions generated with a mass flow controller, with the exception of the pressure relief valve.

**Table B-4.** Statistical information for emission measurements from four G&B station components and emissions regulated with a mass flow controller over 35 min. Relative standard deviation was calculated as the standard deviation divided by the average, multiplied by 100. Values shown were calculated from 20 s data.

	Mass Flow Controller	Rod Packing Vent (high)	Pneumatic Controller	Rod Packing Vent (low)	Pressure Relief Valve
Average	42.5	928	12.8	45.2	4.82
95% Conf. Interval	0.07	2.03	0.04	0.09	0.28
Relative Std. Deviation	0.68	1.05	1.38	0.89	18.7

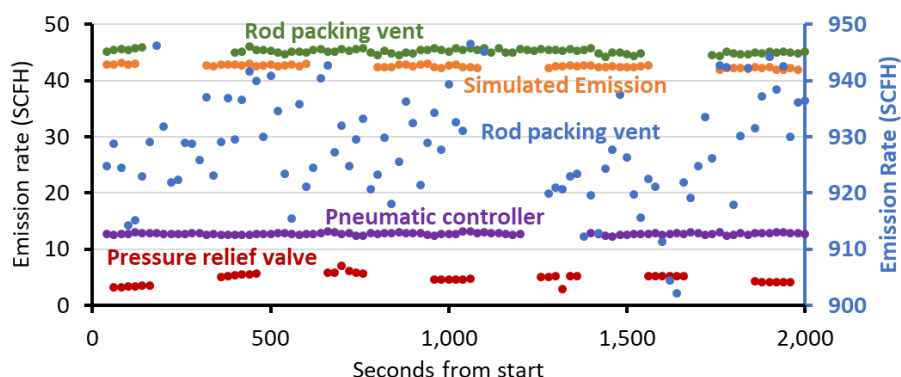


**Figure B-6.** Methane emissions over 35 min from three G&B station components and simulated emissions regulated with a mass flow controller. The y-axis for emissions from the rod packing vent shown in blue is on the right side.

## 7.0 REFERENCES

- Allen, D.T., Torres, V.M., Thomas, J., Sullivan, D.W., Harrison, M., Hendler, A., Herndon, S.C., Kolb, C.E., Fraser, M.P., Hill, A.D., 2013. Measurements of methane emissions at natural gas production sites in the United States. *Proc. Natl. Acad. Sci. U. S. A.* 110, 17768-17773.
- CFR, 2016. CFR Title 40, Part 98, Subpart W, Section 98.234, <https://www.gpo.gov/fdsys/pkg/CFR-2011-title40-vol21/pdf/CFR-2011-title40-vol21-sec98-234.pdf>.
- EPA, U.S., 1995. Protocol for equipment leak emission estimates. United States Environmental Protection Agency, Research Triangle Park, NC, <https://www3.epa.gov/ttnchie1/efdocs/equiplks.pdf>.
- EPA, U.S., 2016. Definition and Procedure for the Determination of the Method Detection Limit, Revision 2. United States Environmental Protection Agency, Washington, D.C., [https://www.epa.gov/sites/production/files/2016-12/documents/mdl-procedure\\_rev2\\_12-13-2016.pdf](https://www.epa.gov/sites/production/files/2016-12/documents/mdl-procedure_rev2_12-13-2016.pdf).
- Hendler, A., Nunn, J., Lundeen, J., 2009. VOC emissions from oil and condensate storage tanks: Final report prepared for Texas Environmental Research Consortium. Texas Environmental Research Consortium, [http://www.mcilvaineconomy.com/Decision\\_Tree/subscriber/articles/Emissions\\_From\\_Oil\\_and\\_Condensate\\_Storage\\_Tanks\\_Final\\_Report.pdf](http://www.mcilvaineconomy.com/Decision_Tree/subscriber/articles/Emissions_From_Oil_and_Condensate_Storage_Tanks_Final_Report.pdf).

- Howard, T., Ferrara, T.W., Townsend-Small, A., 2015. Sensor transition failure in the high flow sampler: implications for methane emission inventories of natural gas infrastructure. *J. Air Waste Manage. Assoc.* 65, 856-862.
- Johnson, D.R., Covington, A.N., Clark, N.N., 2015. Methane emissions from leak and loss audits of natural gas compressor stations and storage facilities. *Environ. Sci. Technol.* 49, 8132-8138.
- MKS, 2017. Flow Measurement & Control, <https://www.mksinst.com/docs/UR/FLOWfaq.aspx>.
- Ravikumar, A.P., Wang, J., McGuire, M., Bell, C.S., Zimmerle, D., Brandt, A.R., 2018. Good versus Good Enough? Empirical tests of methane leak detection sensitivity of a commercial infrared camera. *Environ. Sci. Technol.*
- Subramanian, R., Williams, L.L., Vaughn, T.L., Zimmerle, D., Roscioli, J.R., Herndon, S.C., Yacovitch, T.I., Floerchinger, C., Tkacik, D.S., Mitchell, A.L., 2015. Methane emissions from natural gas compressor stations in the transmission and storage sector: Measurements and comparisons with the EPA greenhouse gas reporting program protocol. *Environ. Sci. Technol.* 49, 3252-3261.



---

# **APPENDIX C**

## **Component Classification and Count Protocol**

---

# APPENDIX C

## COMPONENT CLASSIFICATION AND COUNT PROTOCOL

### 1.0 INTRODUCTION

Component classification and counts were completed at four gathering and boosting (G&B) stations in the Gulf Coast area. Component counting was conducted during each of four separate field campaigns, and after each campaign the counting and classification procedure was refined. As a result, an organized and reliable methodology was developed for classifying and counting components at natural gas G&B stations. The purpose of this appendix is to describe the final refined component classification and counting protocol developed and employed for purposes of this study. In general, this protocol explains the methods used to:

- Separate major equipment units by identifying isolation boundaries,
- Identify components, and assign them to a major equipment category,
- Classify components into major component specific categories, and
- Disaggregate components into various subcategories

Details of the component classification and counting protocol are discussed in the following sections, and figures referenced in each section are provided at the end of this document, unless noted otherwise.

### 2.0 COMPONENT COUNT PROTOCOL

#### 2.1 Component Classification by Equipment Type

At each G&B station, individual components were classified and counted on nine major types of equipment: compressors, separators, dehydrators, coalescers, slug catchers, yard piping, tanks, gathering/discharge lines, and ancillary equipment (e.g. fuel and instrument gas skids, methanol skids). Components were counted on all operating equipment (i.e., pressurized with gas flowing through), as well as some equipment in standby mode (i.e., compressors that were pressurized but not running). A summary of major equipment present at each site is given in **Table C-1**.

**Table C-1.** Major equipment counts for each site. Apart from compressors, only operational and/or pressurized equipment was counted.

Equipment Type	Site 1	Site 2	Site 3	Site 4
Operational Compressors	2-3	1	1	1
Pressurized Compressors	0	1	0	1
Depressurized Compressors	3-4	2	1	0-1
Separators	2	3	3	4
Coalescers	2	1	1	2
Dehydrators	0	1	2	0
Slug Catchers	1	0	0	1
Skids (fuel gas. Methanol)	1	1	1	2
Tanks	0*	10	1	0

\* Tanks at Site 1 were outside the accessible area for the field campaigns

### 2.1.1 Separating Equipment Units

Due to the complexity of the G&B stations' equipment configurations, it was often difficult to assign components to a specific equipment category, depending on their location in the G&B process. For example, a pneumatic valve located between a separator and a dehydrator could be assigned to either piece of equipment. Further, an emergency shutdown (ESD) valve located on the suction line to a compressor could be assigned to the compressor or to yard piping. To address this, each equipment type was given a "boundary" defined by isolation points, and all components within the assigned boundary (including isolation devices) were included in the component count for that equipment. For this study isolation points were defined as: **any device (e.g., isolation valve), process, or configuration that separates a specific equipment unit, either spatially or operationally, from other units in the G&B process.**

An example of a spatial separation would be a separator with both inlet and discharge lines coming from or returning to the ground prior to advancing to the next equipment unit in the process. Similarly, gathering lines were physically separated from station operations (Figure C-1).



**Figure C-1.** Examples of spatial separation: a) gathering lines separated from other equipment, b) slug catcher liquid lines returning to the ground

Operational separations were typically identified by an isolation device (e.g., manual valve, ESD) that would make the equipment non-operational if activated. A common example encountered during this study was a manual valve or ESD located on the suction and discharge lines of compressors, as shown in **Figure C-2** below. In this scenario, both the suction and discharge line ESDs, and all components in-between (i.e., on compressor skid) were counted as part of the compressor.

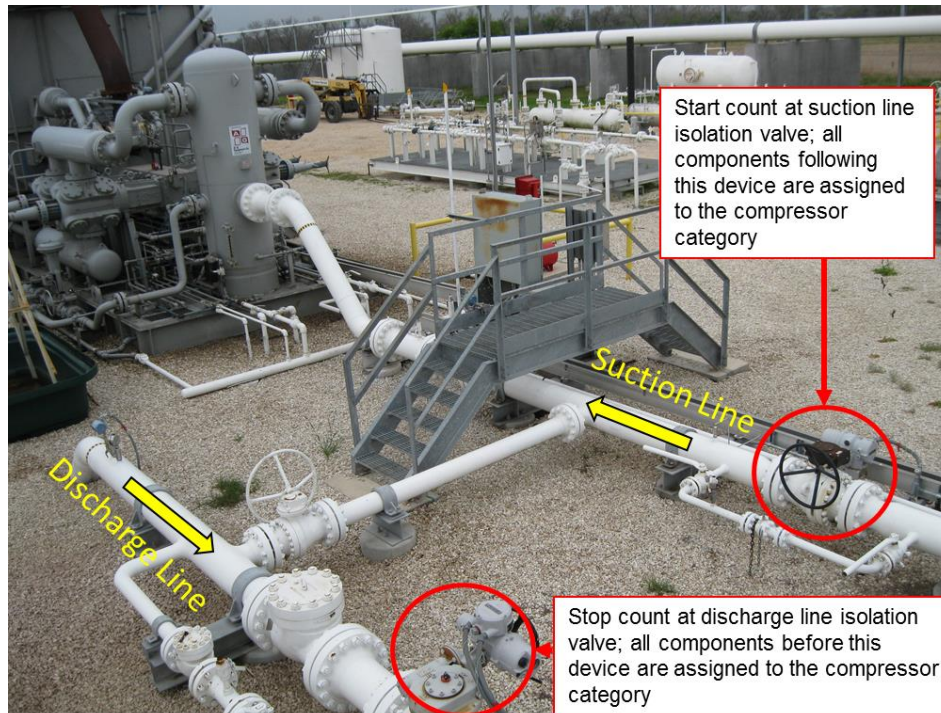


**Figure C-2.** Example of operational separation: Isolation valves on compressor suction and discharge lines

It should be noted that even following the above isolation methodology, assigning components to their respective equipment was not trivial for some equipment configurations. In situations where a component could not be confidently assigned to a specific equipment unit, the yard piping category was used. Other equipment which were included in the yard piping category included i) main header and discharge lines and manifolds to/from compressors (before and after isolation valves), ii) facility-wide ESDs located on isolated segments of pipe, and iii) other isolated segments of process piping or equipment not associated with specific equipment.

## 2.2 Component Classification and Subcategorization

Component types were separated into the following main categories: connectors (flanged and other), valves, pressure relief valves (PRVs), open ended lines (OELs), pneumatic device vents, actuators, meters, gauges, regulators, and compressor vents. The categories of connectors, valves, PRVs, OELs, and pneumatic device vents are consistent with EPA's Greenhouse Gas Reporting Program Subpart W (Tables W-1A and W-1E) (U.S. EPA 2015, U.S. EPA 2016). Meters, gauges, regulators, actuators, and compressor vents were added to the counting protocol due to i) the relatively large number of these components at the sites (actuators, gauges, regulators), ii) the large contribution the components made to measured emissions (compressor vents), or iii) the presence of the category in different sections of Subpart W (meters).

When applicable, classified components were further subdivided based on physical and/or operational characteristics. A summary of major component categories and subcategories is presented in **Table C-2**.

**Table C-2. Component categories used in classification and count protocol**

Major Component Categories	Major Component Subcategories	Component Specifics
Connector	Other or flanged; Size of other connector ( $d < 6"$ , $6" \leq d < 12"$ , $d \geq 12"$ ); Size of flanged connector ( $d=0.5"$ , $0.5" < d < 6"$ , $d \geq 6"$ )	<ul style="list-style-type: none"> <li>Equipment category and location</li> <li>Liquid or gas line</li> <li>Venting, leaking, or both</li> <li>Function (e.g. level, pressure, temperature, ESD, etc.)</li> <li>Make, model, age</li> <li>Operational parameters (e.g. inlet and discharge pressure)</li> <li>Other (visibility limitations)</li> </ul>
Valve	Size (small, large); type (ball, gate, needle); and operating mechanism (manual, pneumatic, electronic)	
Pressure Relief Valve	n/a	
Meter	n/a	
Gauge	n/a	
Regulator	n/a	
Pneumatic Device Vent	Intermittent, continuous low-bleed, continuous high-bleed	
Compressor Vent	Rod packing, distance piece, pocket	

Additional component specifics were documented to support further subcategorizations and/or data analyses, as discussed below:

- Components that were on smaller pieces of equipment located on one of the major equipment types were classified under both pieces of equipment. An example is a valve on a separator/scrubber that was located on a compressor skid.
- Lines carrying gas were counted separately from lines carrying liquid.
- Components within a pneumatic device loop, such as small valves, regulators, filters, control boxes, actuators, and connectors were all counted individually and documented as being associated with a pneumatic device. These components were added into the overall count for the specific piece of equipment on which the device was located.
- All components were classified as: leak, loss (vent), or malfunction. Components categorized as a malfunction were those that were designed to vent, but were confirmed to be malfunctioning during the field event.
- The primary function of each component was also documented. Major component functions include: flow, pressure, level, and temperature control and/or measurement; emergency relief or shutdown; and process metering.
- When available, other information was collected on pneumatic device vents, including make and model, action (snap or throttle), and emission frequency (continuous or intermittent).
- Additional operational information was collected for specific equipment types when available/visible including inlet and discharge pressures, age, and make and model.
- When portions of equipment were covered in thermal insulation, counts were estimated based on visible components. For example, at Site 4 the handles of valves were visible above thermal insulation and were used to estimate the counts of covered components: large valves were assumed to have three flanged connectors, and small valves were assumed to have two other connectors.

## 2.3 Component Specific Details

Detailed descriptions of various component types and classification and subcategorization procedures are discussed in the following sections. Figures containing examples of component classification and counting scenarios are provided at the end of this document.



### 2.3.1 Connector, Other

Examples of other connectors and counts are shown in **Figure C-3**. These components connect piping or tubing together (e.g., **Figure C-3f** and **g**), connect piping/tubing to other components (e.g., **Figure C-3b**), or connect piping/tubing to equipment (e.g., **Figure C-3h**, network of components connected to a separator). This category includes all non-flanged connections, such as threaded (e.g., **Figure C-3c**) and compression (e.g., **Figure C-3e**) fittings.

- Other connectors were subdivided based on the diameter of tube/pipe that was being connected:  $d = 0.5"$ ,  $0.5" < d < 6"$ , and  $d \geq 6"$ . Connectors on tubing less than 0.5" were seen infrequently and not counted.
- Threaded or compression connections that connected tubing/piping to a component (regulators, meters, valves) were counted as individual connectors, and **not** part of the connected component. In other words, emissions from these connections were classified as connectors, not emitting regulators, meters, valves, etc.
- Connectors (threaded, compression) located within a pneumatic loop were counted individually. If a connector within a pneumatic loop was leaking, it was classified as a connector, as opposed to a pneumatic device (e.g., **Figure C-3b** and **e**).
- Connectors (threaded, compression) that were part of a larger component and not used to connect tubing/piping or other components were **not** counted as separate connections. For example, a grease fitting on a large valve would not be included in the connector count. Emissions from these fittings were included as part the larger component.

### 2.3.2 Connector, Flanged

Examples of flanged connectors and counts are shown on **Figure C-4**. These components connect lengths of pipe together (e.g., **Figure C-4b**), connect other large components to pipes (e.g., valve in **Figure C-4a**), or cap pieces of equipment (e.g., **Figure C-4d**) with a ring of bolts.

- Flanged connectors were subdivided based on the diameter of the flange:  $d < 6"$ ,  $6" \leq d < 12"$ ,  $d \geq 12"$ .
- Flanges that were part of a larger component (e.g. valves) were counted separately. For example, a large valve that has three separate flanges (see **Figure C-4a**) would contribute three flanges to the total flanged connector count.

### 2.3.3 Valves

Examples of valves and counts are shown in **Figures C-5** to **C-8**. The function of a valve is to control flow and/or pressure through the line. The field sites had valves that could be operated manually, pneumatically, electronically, or a combination of these three mechanisms. Manual valves were categorized as those that require a person to physically turn a handle or wheel to open or close the valve (**Figures C-5** and **C-6**). Pneumatic valves were actuated (opened/closed, throttled) and controlled by pneumatic (e.g. instrument/fuel gas) means (**Figure C-7**). Electronic valves seen in this study could be controlled either electronically or manually (**Figure C-8**). Often pneumatic and electronic valves could also be controlled manually; but they were categorized as pneumatic/electronic not manual.

#### Manual Valve

- Manual valves were subdivided based on size and type. Valves that could be turned with one hand were classified as small, valves that could not easily be turned with one hand were classified as large.



- Small manual valves were identified as ball, needle, or gate valves (**Figure C-5**); large manual valves were identified as ball or gate valves (**Figure C-6**).
- Small manual valves located within pneumatic device loops were classified as individual valves and counted towards the total valve population. However, these valves were noted as being associated with a pneumatic device.

### **Pneumatic Valve**

- In pneumatic valves, the size of the flow passage is controlled by a signal from the pneumatic controller.
- Pneumatic valves were identified by an instrument or fuel gas supply line, examples are shown in **Figure C-7**.
- Note that pneumatic valves were counted separately from pneumatic controllers and actuators, despite being part of the same pneumatic system. At the sites visited, the valve-portion of the pneumatic loop was not designed to vent (unlike actuators and controllers); therefore, any emissions coming from a pneumatic valve were classified as a leak.

### **Electronic Valve**

- Electronic valves were present only at one site, and functioned as emergency shutdown valves (**Figure C-8**).

### **2.3.4 Pressure Relief Valves (PRV)**

Examples of PRVs and component counts are shown on **Figure C-9**. The function of a PRV is to protect equipment from being subjected to pressures the equipment is not designed to handle. The PRV is designed to open when a certain pressure is exceeded, relieving the unsafe pressure. Many PRVs encountered in this study had a pipe or stack attached to their outlet side to route any emissions to a higher elevation (see **Figure C-9**). All components on pipes/stacks after PRVs are at atmospheric pressure and any emissions that appear to come from them are due to a malfunction (or activation) in the upstream PRV, therefore:

- Components on pipes/stacks following PRVs were **not** counted.
- Open pipes/stacks following PRVs were **not** categorized as open-ended lines (OEL).

### **2.3.5 Meters**

Examples of meters are shown on **Figure C-10**. In this protocol, meters are defined as instruments that measure the rate or usage of an operational parameter, such as cumulative gas flow. Most meters in this study were identified by digital read-outs of parameters being measured.

- Meters were commonly found on gathering/discharge lines. For example, SCADA (supervisory control and data acquisition) systems at G&B stations typically have multiple meters associated with them.
- Small connections (threaded, compression) and valves connected to meters were counted individually, and therefore included in the site-wide count.
- Subdivision by meter type (e.g., ultrasonic, orifice) was not performed, however examples of types of meters encountered in this study are shown on **Figure C-10**.

### **2.3.6 Gauges**

Examples of gauges are shown on **Figure C-11**. The purpose of a gauge is to instantaneously measure an operational parameter (e.g., pressure, temperature). Gauges do not provide

information on the rate or usage of a parameter. At G&B stations, gauges can be analog (dial) or electronic, and usually measure pressure, temperature, or volume (level).

- For a gauge to be classified as leaking, the emissions had to come from the gauge itself (e.g., cracked glass, top of gauge), not the connectors that attached the gauge to pipes or equipment.
- Gauges were divided into categories based on type of measurement: pressure, temperature, level (i.e., site glass).
- Many pneumatic devices have gauges on the fuel gas line. These gauges were included in the site-wide count, but also identified as part of a pneumatic device.

### 2.3.7 Regulators

Examples of regulators and counts are shown on **Figure C-12**. For this study, regulators were defined as devices that reduce the inlet pressure of gas to smaller output pressure. At G&B stations regulators are commonly found on the fuel gas supply lines on pneumatic devices. These regulators reduce the fuel gas pressure to the required pneumatic device input.

- Many different types of pressure regulators were encountered during this study, some of which were designed to vent while others were not. If there was uncertainty on whether emissions from a regulator should be classified as a leak or vent, site operators were asked to confirm.
- Regulators were only classified as leaking or venting if the emission was confirmed to be sourced from the regulator (e.g. damaged seals, rusted/cracked housing, vent ports, etc.). Leaks from threaded or compression connections attaching tubing/pipe to the regulators did not qualify as a leak from a regulator.
- Many pneumatic devices have multiple regulators in series on their fuel/instrument gas lines. These regulators were counted individually and included in the site-wide count, but also identified as part of a pneumatic device.

### 2.3.8 Pneumatic Filters

Filters are commonly found on pneumatic devices to filter the instrument/fuel gas supplied to the device. Examples of filters are shown in **Figure C-13**. Like regulators, many different types of filters were encountered during this study. Most filters are designed to vent, but only when maintenance is required or a malfunction occurs in the pneumatic system. In most cases, emissions came from threaded connections attaching tubing to the filter, and not the filter body. In this situation, the leak was classified as a connector, as opposed to a leak from the filter.

### 2.3.9 Pneumatic Devices

Examples of pneumatic devices are shown on **Figure C-14**. Pneumatic devices are used to operate mechanical devices, like valves, with compressed air or natural gas. When a signal is sent to the pneumatic device controller that a change in system parameters (e.g., pressure, level, or flow) is needed, the device will reposition a valve (open/close, throttle) to achieve the desired system condition. Compressed gas contained in the actuator diaphragm is released, or actuates, to operate the valve. In other words, the energy of compressed gas in the actuator is converted into mechanical energy to reposition a valve.

Pneumatic components (controllers, actuators, EDSs) encountered in this study were all operated by compressed natural gas. All components (e.g., connectors, regulators, valves) within a pneumatic device loop were counted individually and added to the site-wide component count.

- Pneumatic devices were categorized by what was being controlled (pressure, level, flow) and venting frequency (intermittent or continuous).
  - Intermittent bleed vents were further divided by the venting action (snap or throttle)
  - Continuous bleed vents were identified as low (< 6 scf/hr) or high (>6 scf/hr) bleed based on measured emission rate
- Small components on the pneumatic device such as connectors, valves, regulators, gauges, filters, and PRVs were included in the site-wide count, but identified as part of a pneumatic device.
- As previously discussed, pneumatic device controllers (**Figure C-15**) and actuators (**Figure C-16**) were counted and measured separately, despite being part of the same pneumatic system. This is because actuators and controllers, even if in the same pneumatic loop, could have separate vents or leaks.
- Actuators are found on liquid lines for devices controlling level, and on gas lines for devices controlling flow/pressure.
- Emissions from pneumatic device controllers and actuators are classified as vents unless the component is malfunctioning (e.g., leak from valve stem of actuator, pneumatic device vent stuck open).

It should be noted that venting frequency and/or venting action could not be identified on all pneumatic devices in this study. This is due to a variety of factors, including the condition of the pneumatic device (missing labels, age), complexity of process equipment, or minimal observed venting rate or frequency. The following methods were used to identify the various pneumatic device characteristics:

- Check for a snap or throttle label inside the control box
- Observe device with FLIR optical imaging camera
- Listen for intermittent actuation
- Monitor emission rate with methane sensor/high flow, look for intermittent actuation
- Ask site operators
- Monitor pressure gauges on the control box. If the gauges are functioning properly, the pressure should occasionally drop to zero if snap acting, or the pressure should hover around a certain point if throttling. However, this is **not** a definitive way to identify venting action.
- Take note of make and model, check manufacturer specs

### 2.3.10 Compressor Vents

Examples of compressor vents are shown in **Figure C-17**. Compressors are designed to vent to prevent dangerous buildup of pressure in the rod housing of compressor throws. Compressor vents were divided into three categories: distance piece vents (DPV), rod packing vents (RPV), and pocket vents. These categories are discussed further below:

#### Distance Piece Vents

- DPVs vent from the top of compressor throws and are typically identified by a small section of open tubing or hose (see **Figure C-17**).
- All compressors measured in this study had one DPV for each throw (four DPVs per compressor). Although not encountered during this study, it should be noted that DPVs can also be manifolded together and routed to a separate venting or capture location.

## Rod Packing Vents

- RPVs are piped from the bottom of a compressor's throw, often manifolded to RPVs from other throws, and typically routed to the lower front of the compressor skid where the emissions are vented (see **Figure C-17**). Like DPVs, the purpose of RPVs is to vent gas that escapes around rod packing seals from within a compressor throw.
- RPVs are also called Lower Packing Vents, since they allow liquids (e.g., condensation) to drain from the compressor throws to a sump below the compressor skid. Consequently, the effluent end of RPVs are typically routed down and to the front of the compressor skid.
- Emissions could not be measured from RPVs on individual compressor throws in this study; all RPVs were manifolded in some way and routed to a separate effluent vent location. At the four field sites, compressors had one or two RPV effluent vent locations (where measurements were collected), depending on how the compressor rod packing was piped. Compressors with all four RPVs manifolded together had one effluent vent location. Compressors with two effluent vent locations had two RPVs manifolded and routed per effluent vent.

## Pocket vents

- Pocket vents are small vents located at the end of the compressor throws. They are typically identified as small tubing with a downward-facing open end (**Figure C-17**).
- Emissions from pocket vents were often not large enough to be visible with the FLIR (OGI) camera. This study measured four pocket vents in the first field campaign. Emissions from these vents were all less than 0.09 scf/hr. Therefore, pocket vents were not measured after Field Campaign 1.

In addition to classifying and counting compressor components, the following ancillary data was collected for each compressor, when possible:

- Compressor mode (operating, standby/pressurized, off)
- Inlet and discharge pressure
- Make, model, and horsepower
- Construction date
- Maintenance schedule
- Operating hours



### CONNECTOR, OTHER (NON-FLANGED CONNECTOR)

These components connect piping or tubing together (e.g., Figures 1f and 1g), connect piping/tubing to other components (e.g., Figure 1b), or connect piping/tubing to equipment (e.g., Figure 1h, nest of components connected to a separator). This category includes all non-flanged connections, such as threaded (e.g., Figure 1c) and compression (e.g., Figure 1e) fittings.

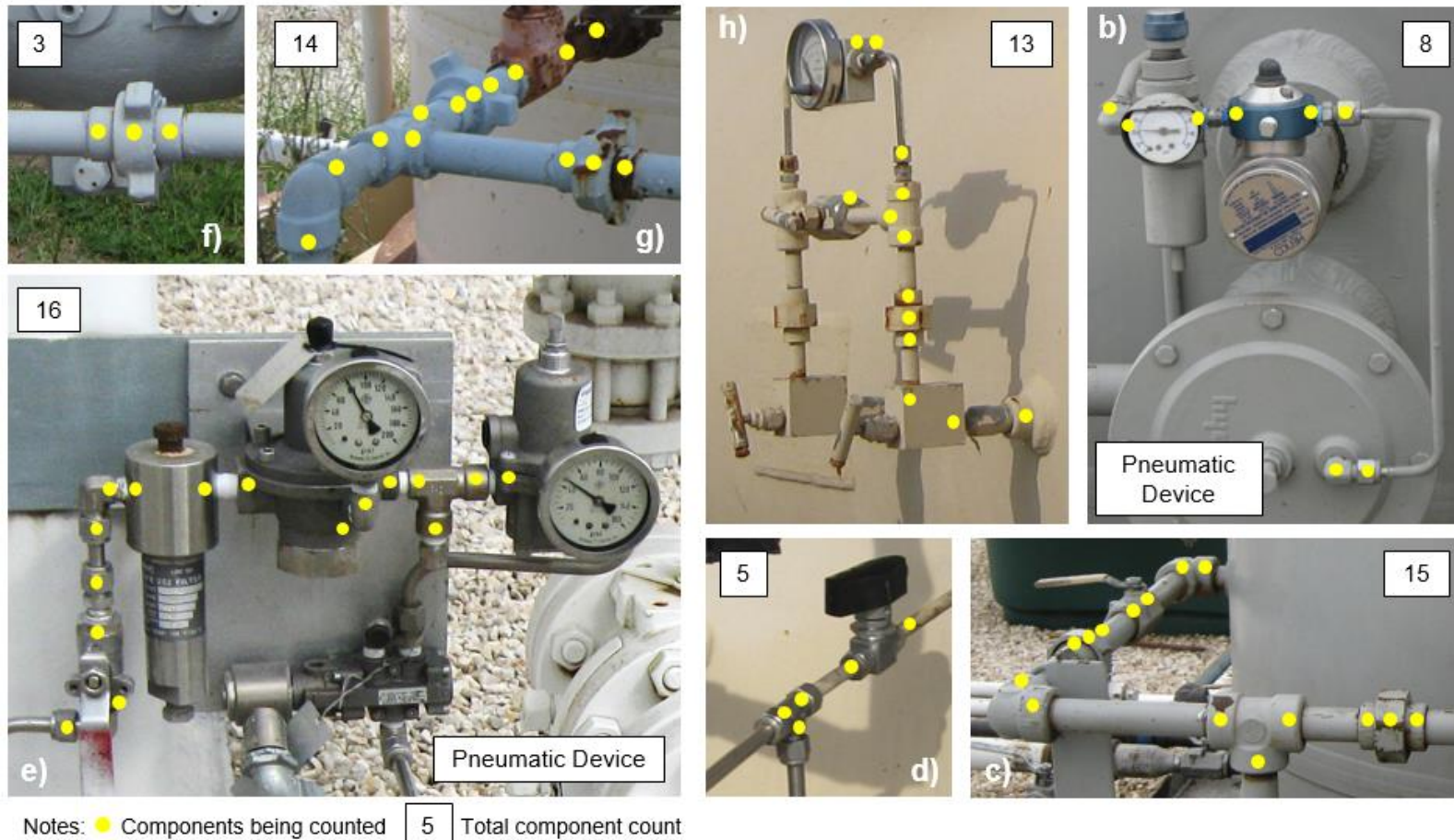


**Figure C-3.** Other connector examples

## CONNECTOR, FLANGED

These components connect lengths of pipe together (e.g., Figure 2b), connect other large components to pipes (e.g., valve in Figure 2a), or cap pieces of equipment (e.g., 2d) with a ring of bolts.



Notes: ● Components being counted

5 Total component count

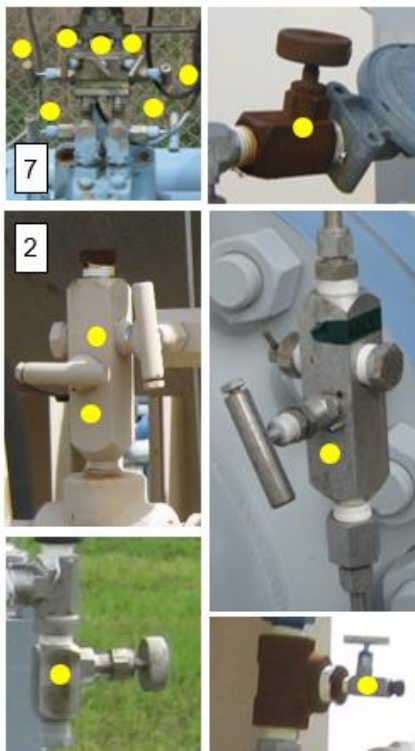
**Figure C-4.** Flanged connector examples



## MANUAL VALVE, SMALL

The function of a valve is to control flow through the line. Small manual valves are subdivided into three categories: ball, needle, and gate valve. Other types of valves may also be present at G&B sites and can be classified as "other" or additional subcategories can be added. These valves are small enough to be turned with one hand.

### NEEDLE VALVES



### GATE VALVES



### BALL VALVES



Notes: ● Components being counted

5 Total component count

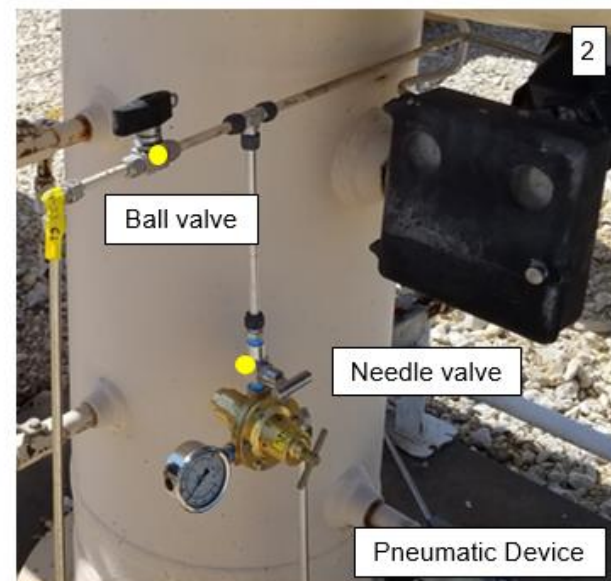


**Figure C-5.** Small manual valve examples

## MANUAL VALVE, LARGE

The function of a valve is to control flow through the line. Large manual valves are subdivided into two categories: ball and gate. These valves require two hands to turn and are usually connected to piping with flanged connectors.

Large ball valves may not have the handle attached, but can still be identified by the valve body.

### BALL VALVES



### ACTUATOR VALVE STEM



### GATE VALVES



Notes: ● Components being counted ● Valves with no handle attached 5 Total component count

**Figure C-6. Large manual valve examples**



### **PNEUMATIC VALVE – Emergency Shutdown (ESD)**

The function of a valve is to control flow through the line. ESDs can usually be identified by a long, cylindrical valve with small tubing, connections, valves, regulators, and/or filters. These small components supply fuel gas, which is used to power the ESD actuator.



**Figure C-7.** *Pneumatic valve examples*

## **ELECTRONIC VALVE – Emergency shutdown (ESD)**

The function of a valve is to control flow through the line. An electronic valve operates off of electricity instead of fuel gas. Notice there is conduit running into the valves in the photographs, but no  $\sim\frac{1}{2}$ " fuel gas lines

The example valves are both electronic and big manual gate valves. These valves function as ESDs.

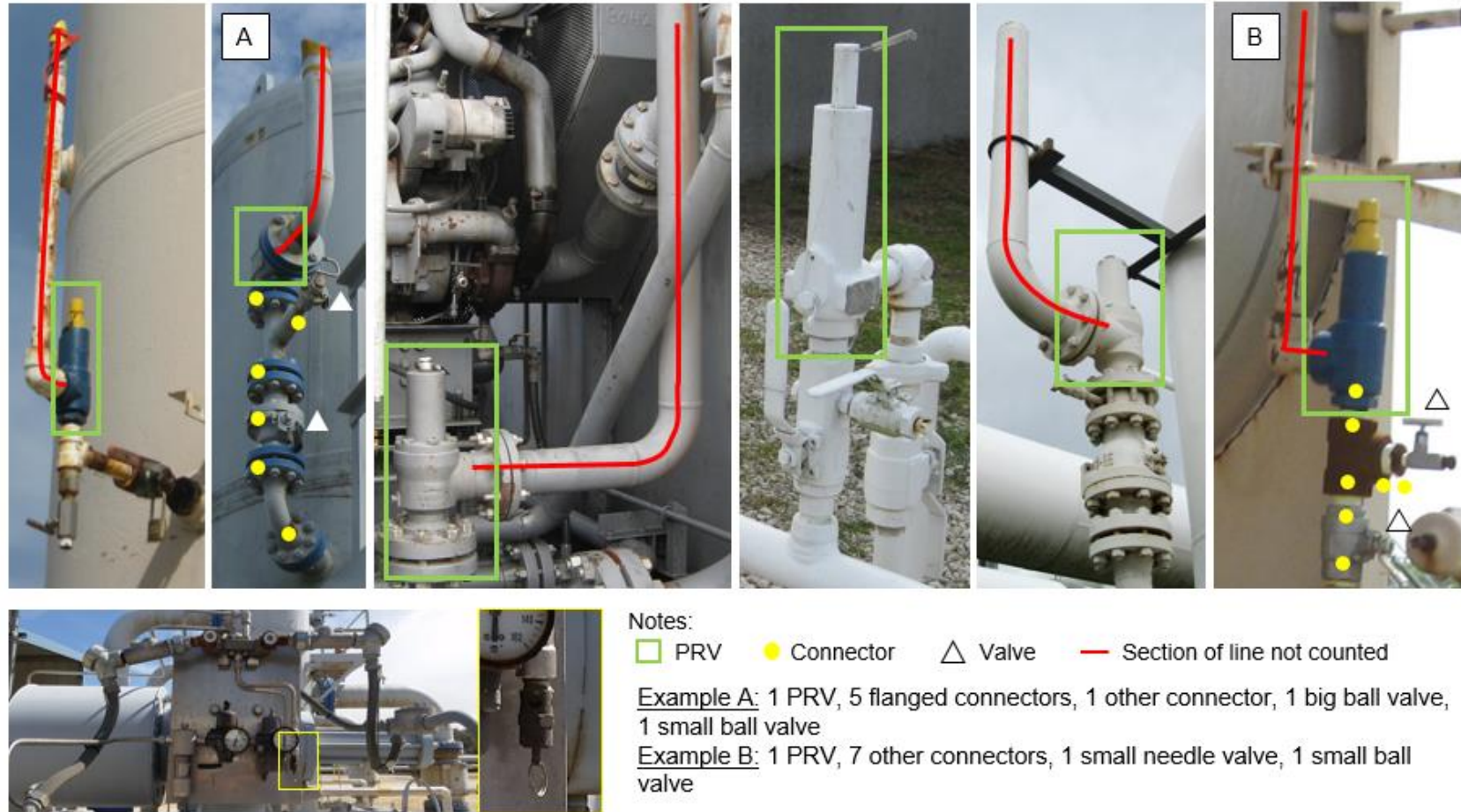


**Figure C-8.** *Electronic valve examples*



## PRESSURE RELIEF VALVE (PRV)

The function of a PRV is to protect equipment from being subjected to pressures the equipment was not designed to handle. The PRV is designed to open when a certain pressure is exceeded, relieving the excess/unsafe pressure. Any emissions coming from piping, valves, stacks, etc. following a PRV are considered to be emissions from a malfunctioning PRV.



Small PRVs may be present on pneumatic devices.

**Figure C-9.** Pressure relief valve examples

## METER

Meters are defined as instruments that measure the rate or usage of an operational parameter, such as cumulative gas flow. Different types of flow meters include: orifice, venturi, annubar, and ultrasonic. Small needle valves and threaded connectors on meters were included in the site-wide component count.



Note: ● Components being counted

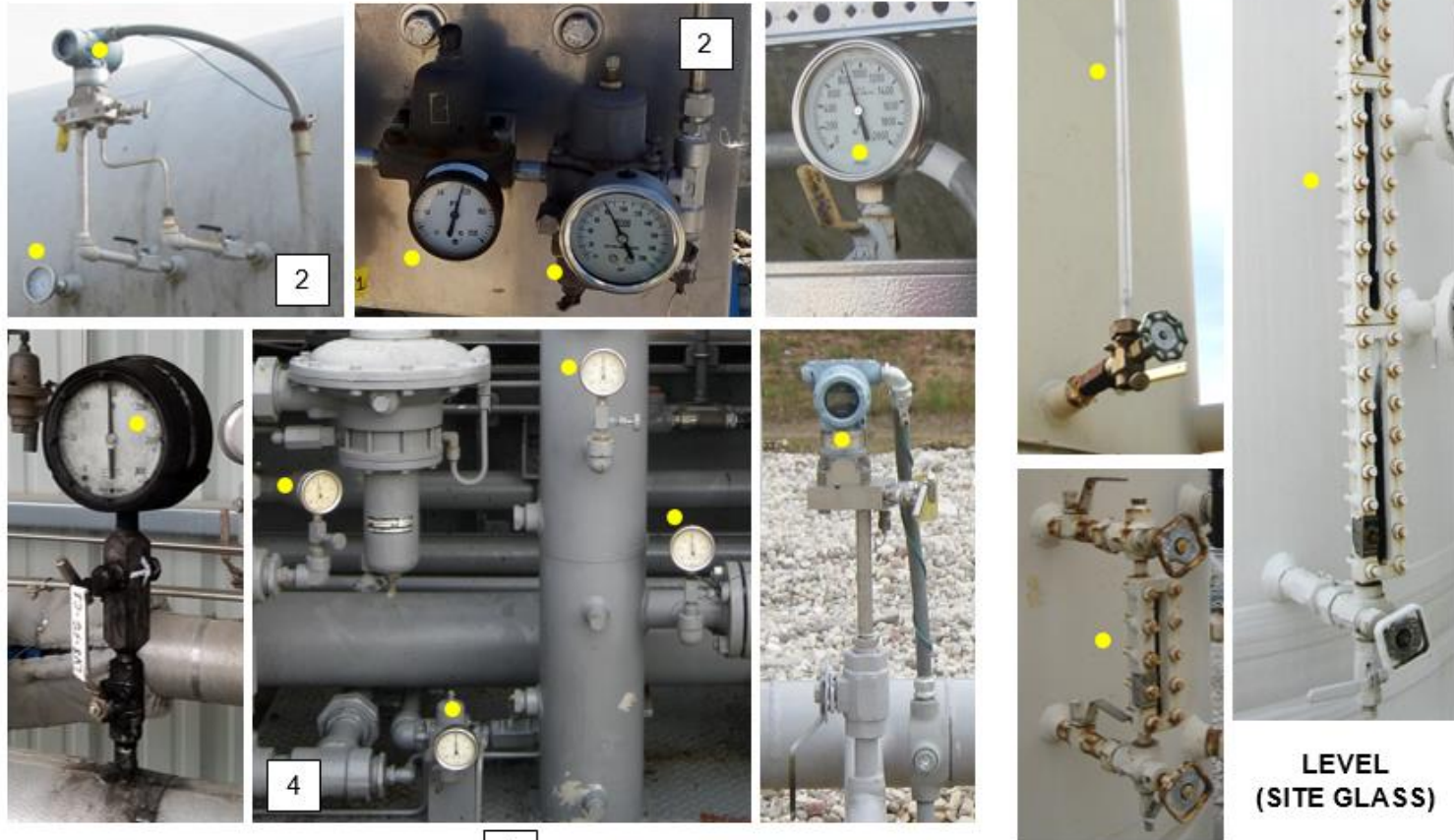
**Figure C-10.** Meter examples



## GAUGE

The purpose of a gauge is to instantaneously measure an operational parameter; gauges do not provide information on the rate or usage of a parameter. At G&B stations, gauges can be analog (dial) or electronic, and usually measure pressure, temperature, or volume (level).

## PRESSURE AND TEMPERATURE

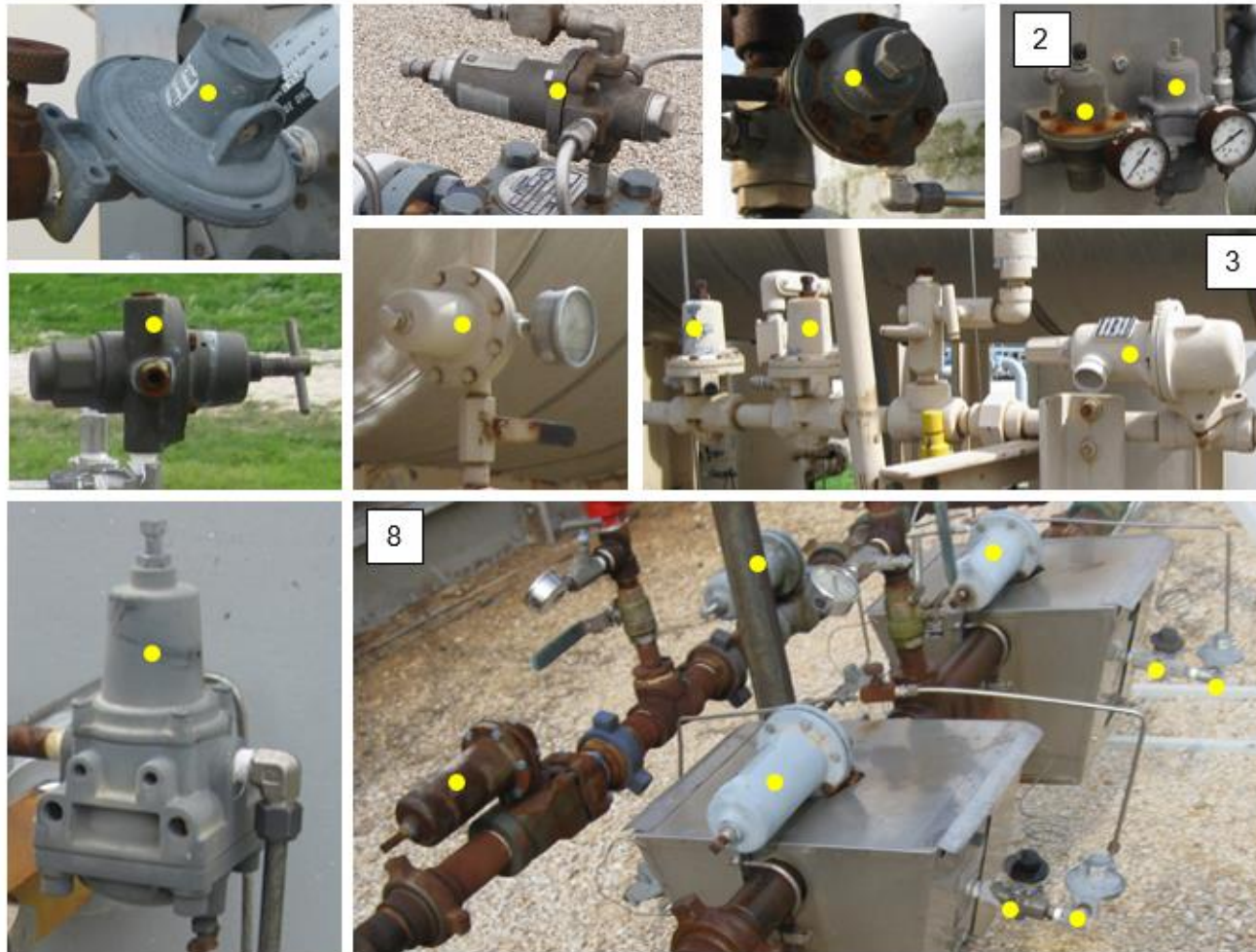


Notes: ● Components being counted	5	Total component count
-----------------------------------	---	-----------------------

**Figure C-11. Meter examples**

## REGULATOR

The function of a regulator is to reduce inlet pressure to a selected outlet pressure.



Notes: ● Components being counted

5

Total component count

**Figure C-12. Regulator examples**

## FILTER

Filters are commonly found on pneumatic devices to filter the fuel gas supplied to the device.



*Figure C-13. Filter examples*



## PNEUMATIC DEVICE

Pneumatic devices are used to operate mechanical devices, like valves, with compressed air or natural gas. When a signal is sent to the pneumatic device controller that a change in system parameters (e.g., pressure, level, or flow) is needed, the device will open or close a valve to achieve the desired system condition. The device actuates, or releases gas, to operate the valve.

### FLOW CONTROL




### LEVEL CONTROL



### PRESSURE CONTROL



Note:  Fuel gas supply line

**Figure C-14.** Pneumatic device examples

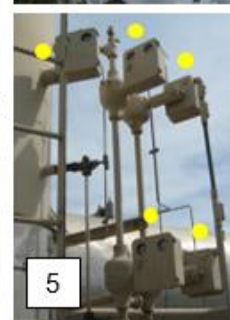
## PNEUMATIC DEVICE CONTROLLER

Pneumatic device controllers, such as the examples below, control the actuation of pneumatic devices. Controllers are supplied by fuel gas and also occasionally electricity. Controllers can be intermittent bleed with snap or throttle action, low continuous bleed (<6 scf/hr), or high continuous bleed (>6 scf/hr).

### DIGITAL POSITIONER/DIGITAL VALVE CONTROLLER



### FLOAT SWITCH



Notes: ● Components being counted

5

Total component count

**Figure C-15.** Pneumatic device controller examples



## ACTUATOR

Actuators contain compressed gas, which is released when a signal is received from the pneumatic device controller, to operate a control valve when the component actuates.



*Figure C-16. Actuator examples*



## COMPRESSOR VENTS

Compressors are designed to vent to prevent dangerous buildup of pressure. Compressor vents were divided into 3 categories for this protocol: distance piece vents (DPV), rod packing vents (RPV), and pocket vents. RPVs are piped from the bottom of the throw, follow the small tubing from the bottom of the throw to the vent.

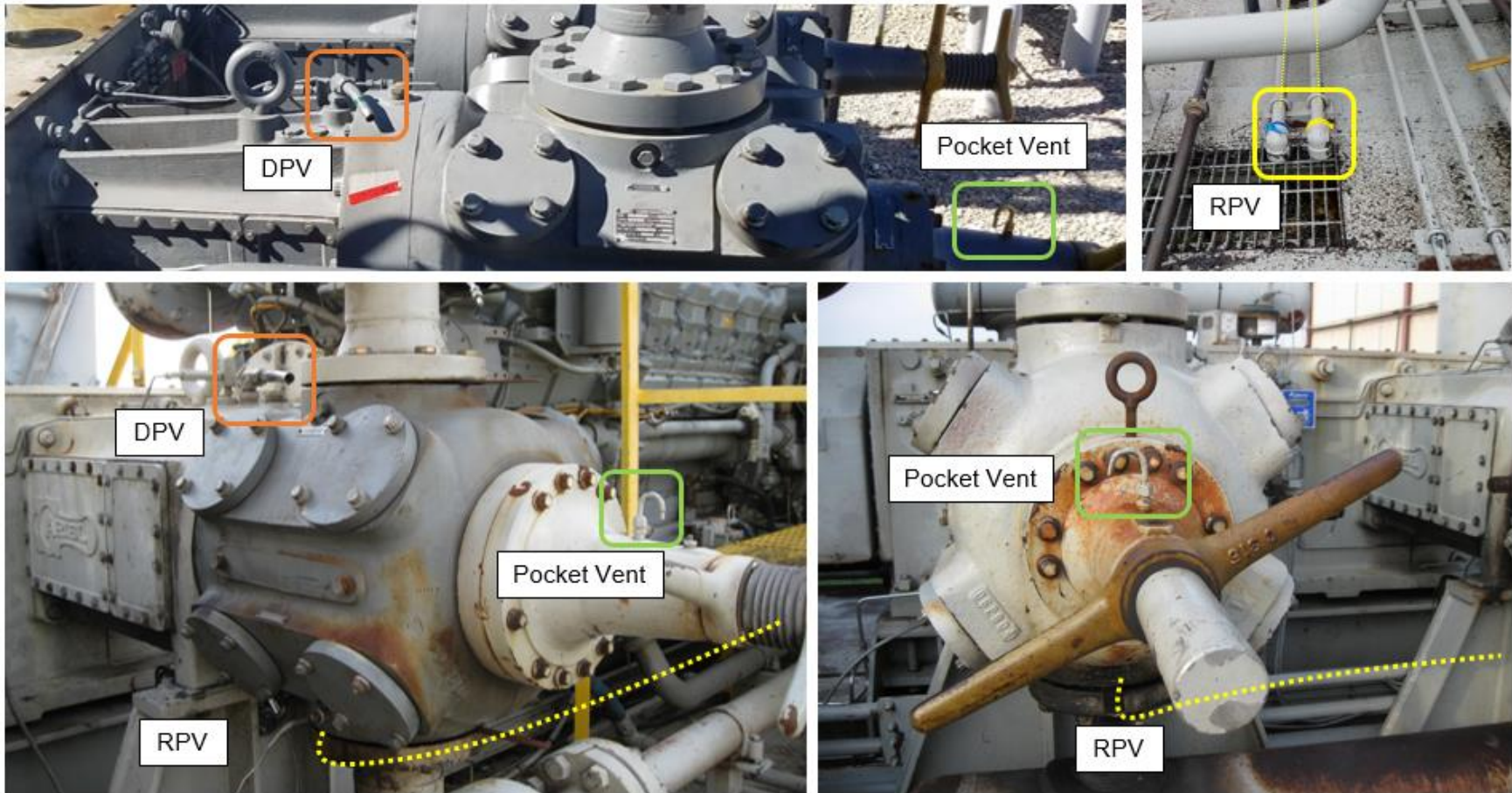


**Figure C-17.** Compressor vent examples

### **3.0 REFERENCES**

U.S. EPA, 2016. Mandatory Greenhouse Gas Reporting Subpart W – Petroleum and Natural Gas Systems, 40 C.F.R. §98.232.

U.S. EPA, 2015. Mandatory Greenhouse Gas Reporting Subpart W – Petroleum and Natural Gas Systems, 40 C.F.R. §98.232.

---

# **APPENDIX D**

## **OP-FTIR Spectrometry Procedures, Equipment and Specifications**

---

## APPENDIX D

### OP-FTIR SPECTROMETRY PROCEDURES, EQUIPMENT, AND SPECIFICATIONS

#### 1.0 BASIC PRINCIPLES OF OPEN-PATH SPECTROSCOPY

The RAM2000™ OP-FTIR was operated with a corner-cubed prismatic retro-reflector, oriented to accept prevailing winds through an open-air optical path. A beam of light spanning a range of wavelengths in the mid-infrared portion of the electromagnetic spectrum was propagated from the transmitter portion of the OP-FTIR instrument. Methane, ethane and carbon monoxide present in the air crossed the beam path, interfered with modulated infrared energy from a silicon carbide (SiC) glower source, became energetically excited by the resonant frequency of the source, and caused the beam to divest of relative energy.

The retro-reflector bent the source energy back to a mercury/cadmium/telluride detector in the OP-FTIR optics chamber, where a Michelson Interferometer achieved further modulation by splitting the returning beam of radiation into two paths, and recombined them in a way to generate an interference from the phase difference. The phase difference, and thus the interference, was dependent on the wavelengths present in the beam. In one of the paths, the radiation was reflected off a moving mirror, resulting in an intensity variation which was measured as a function of the path difference between the two mirrors. The result was an interferogram.

The interferogram obtained from a monochromatic beam was a simple cosine wave. The broadband interferogram was a sum of cosine waves (the Fourier series) for each spectral component as a function of mirror-beam-path separation. A spectrum (in optical frequency units) was obtained by performing a Fourier transform upon the interferogram. Interferograms were created at a chosen rate of 32 signal-averaged scans per one sample frame. Resultant absorbance spectra were compared to reference spectra using multi-component regression algorithms. Concentrations were path-averaged and path-integrated.

Compounds were identified and quantified via a computer-based spectral search involving sequential, compound-specific analyses and comparison to the system's internal reference spectra library. The most widely employed technique for analyzing FTIR spectral data is the multi-component classical least squares (CLS) technique. Any gaseous compound which absorbs the infrared (IR) region is a potential candidate for monitoring using this technology.

The Minimum Detect Levels (MDL) were algorithmically calculated values that defined the minimum methane concentration, within six sigma statistical confidence. Upon completion of a time-lapsed sampling session, all frames (samples) were averaged per analyte (methane/ethane/carbon monoxide) by the software. A mean MDL for each analyte was calculated based upon the full sampling session. According to the manufacturer, the range of detection limits for a 100-meter separation between the sensor and retroreflector was from 0.10 to 15 ppb for most infrared active chemicals.

Concentrations of analytes were reported only if the time-weighted mean concentration was found to be in excess of two times the software calculated mean MDL. The maximum detected concentration, observed at any given time during sampling history, was only reported if the maximum was found to be at least two times the software-calculated-mean MDL. As a result of these ultra conservative steps, the concentration values for methane (mean or max), were only

reported if the results were beyond a 12 sigma statistical confidence range above the MDL. As a result, the possibility of having a false positive concentration was null.

## **2.0 OP-FTIR AND RETROREFLECTOR SET UP**

The upwind and downwind locations were determined in relation to the physical properties of the compressors and gas gathering lines. The optical beam path between the OP-FTIR spectrometer and the retroreflector was oriented perpendicular to prevailing wind direction as much as possible.

Downwind setup locations for the OP-FTIR and retroreflector were restricted to areas that were free of traffic flow and were oriented such that the infrared beam was unobstructed by facility equipment or buildings. Each retroreflector array consisted of thirty-seven 2.5-inch hollow reflector cubes consisting of three mutually perpendicular mirrors that bend infrared light back to its exact point of origin and, as such, reduced the divergence of the beam on its return path back to the detector. The spectrometer was adjusted so that the sighting scope (located between the spectrometer and telescope) displayed crosshairs at the upper left corner of the retroreflector mirror. A range finder or measuring wheel was used to measure the distance from the spectrometer to the retroreflector. The instruments required a round trip beam path for the measurement so it was necessary to multiply the distance by a factor of two.

Since the OP-FTIR system contained a liquid nitrogen cooling unit, liquid nitrogen was added to the spectrometer prior to measurement. Once the spectrometer system was engaged and the nitrogen cooling began, the OP-FTIR detector was allowed to cool for 20 minutes. Hotter ambient temperatures required a longer cooling time.

## **3.0 BACKGROUND (UPWIND) SAMPLING**

Background or upwind samples were collected and evaluated to determine the possibility of upwind emitting sources contributing to emission levels at the study site. Upwind sampling locations were chosen as close to the sample area as possible and were free of wind obstacles to the extent possible. At least one-hour of upwind measurements was gathered at each location.

## **4.0 METEOROLOGICAL DATA TO SUPPORT EMISSION FLUX CALCULATIONS**

A controlled stream of gas-phase SF<sub>6</sub> was released during OP-FTIR measurement periods. The OP-FTIR spectrometer detected and quantified the SF<sub>6</sub> plume along with methane and ethane (target compounds) to distinguish between thermogenic and biogenic methane sources. Since the SF<sub>6</sub> emission rate was known, the emission rate of other compounds were scaled based on the ratio of their concentrations to the measured SF<sub>6</sub> concentration.

Cylinders containing 99% pure SF<sub>6</sub> were utilized in conjunction with a 0-10 L min<sup>-1</sup> mass flow controller to control the release of SF<sub>6</sub> from the cylinder. After the mass flow controller, the SF<sub>6</sub> traveled through a 50-m length of inert tubing to a tripod and was released from the end of the tubing at the tripod.

All meteorological measurements were collected at 6m above ground level concurrent with, and using the same instrumentation as, measurements collected for the high flow sampling program (See Appendix B) and all measurements were recorded with a Campbell Scientific CR1000 data logger.

Flow rates of the SF<sub>6</sub> mass flow controller used to release the tracer were checked at least monthly against a BIOS dry gas meter, and the dry gas meter was calibrated at least annually against a NIST-traceable standard.

---

# **APPENDIX E**

## **Plume Visualization**

---



# APPENDIX E

## PLUME VISUALIZATION

### 1.0 INTRODUCTION

A user-friendly data visualization tool was developed in Microsoft Excel to conservatively estimate the extent of the plume generated by measured emissions from compressors. An output table of results can be generated and used to create additional figures in other programs like Python.

### 2.0 PLUME VISUALIZATION MODEL

The Gaussian air dispersion model was used to visualize measured methane emission rates as methane plumes (**Equation D-1**). The Gaussian air dispersion model is a steady-state model; therefore, the resulting plume is a conservative visualization of the methane emissions measured in the field.

$$C(x, y, z) = \frac{Q}{2\pi u \sigma_y \sigma_z} \times \left[ \exp - \left( \frac{y^2}{2\sigma_y^2} \right) \right] \left[ \exp \left( \frac{-(z-H)^2}{2\sigma_z^2} \right) + \exp \left( \frac{-(z+H)^2}{2\sigma_z^2} \right) \right] \quad (\text{Equation D-1})$$

Where:

C = Concentration of methane in the air (mg/m<sup>3</sup>)

Q = Rate of chemical emission (mg/s)

u = Wind speed in the x-direction (m/s)

$\sigma_y$  = Standard deviation in the y-direction (m)

$\sigma_z$  = Standard deviation in the z-direction (m)

y = Distance along axis horizontal to wind direction (m)

z = Distance along vertical axis (m)

H = Effective stack height (m)

The visualization package calculates  $\sigma_y$  and  $\sigma_z$ , based on input parameters including date and time, site location, sky cover, and land surface cover. A screenshot of the main page of the tool is shown in **Figure D-1**. Up to three different emission sources can be input; the resulting plumes are calculated and plotted. A total plume is also generated, which sums individual plumes and plots a “total” plume.

#### 2.1 Inputs

The user enters the following input data:

1. Source strength (mg/s); up to three sources. If the sources are emitting from different locations the distances between the sources can be input into the model. Source locations must be in x-y coordinate form, where the x-direction is parallel to the wind direction, and y-direction is horizontal to the wind direction.
2. Effective stack height (same for all sources)

3. Date (MM/DD/YY) and time (military) of emission.
4. Source location (latitude and longitude) and time zone. This information, along with date and time is used to calculate the solar elevation angle. The solar elevation angle is calculated using the NOAA Solar Calculations (NOAA, 2010)
5. Sky cover. Based on options in a dropdown menu.
6. Landscape. Options include rural or urban.
7. Stability class. The Pasquill Stability Class is chosen from a dropdown menu. The tool is designed to help the user determine the stability class (see the next Section 2.2 Stability Class).
8. Wind speed (m/s) and height of wind speed measurement (m). If sky cover and wind speed are unknown, websites that have historical weather data such as Weather Underground may be useful.
9. Receptor height (m). The most conservative height is equal to the effective stack height
10. Plume grid spacing (delta X and Y) (m). The tool calculates plume concentrations for a set number of grid spaces; therefore, if a larger plume area is desired the delta X and/or delta Y values need to be increased
11. Initial X and Y coordinates (m). This is the starting location along the plume that the user wants to view. The default Initial Y is 0 m. Due to the equations used to calculate  $\sigma_y$  the Initial X must be greater than 0. The default value is 0.01 m

Source Inputs		Source 1	Source 2	Source 3	Output concentration at given location	
Source Strength, Q (mg/s)		2681	392	107	Distance from source parallel to wind (m)	5
Effective Stack Height, H (m)		2	2	2	Distance from source perpendicular to wind (m)	5
X Coordinate of Source (m)		0	5.02	10.03	Concentration (mg/m3)	1.5E+11
Y Coordinate of Source (m)		0	-14.14	-28.27		

Site Inputs		6/6/2017	Sky Cover Options 1) Any amount of high, thin clouds 2) <50% cover by middle clouds 3) <50% cover by low clouds (base <7,000 ft) 4) >50% cover by middle clouds 5) >50% cover by low clouds (base <7,000 ft)
Date (MM/DD/YY)		9	
Time (military)		29.7314	
Latitude (+ to N)		-96.7314	
Longitude (+ to E)		-7	
Time Zone	See Time Zone Table	4	See Sky Cover Options
Sky Cover Type		Rural	
Landscape			

Solar Elevation Angle (deg)		56.72	Use to determine Stability Class
Stability Class		D	Determine from site conditions

Measured Wind Speed (m/s)		2.036	10 m is standard Calculated from reference wind speed and stability class
Wind Speed Measurement Height (m)		10	
Effective Wind Speed (m/s)		1.599	

Plume Calculation Inputs		2	Set z = H for most conservative scenario
Receptor Height (z)		500	
delta X (m)		200	
delta Y (m)		0.01	Default to 0.01, must be greater than zero
Initial X (m)		0	Default to zero
Initial Y (m)		25000	
Final X (m)		6000	
Final Y (m)			

Adding Plumes		Source 1	Source 2	Source 3
Adjusted X (m)		0	0	0
Adjusted Y (m)		0	0	0

**Generate output spreadsheet**

$$C(x, y, z) = \frac{Q}{2\pi u \sigma_y \sigma_z} \times \left[ \exp\left(-\frac{y^2}{2\sigma_y^2}\right) \right] \left[ \exp\left(-\frac{(z-H)^2}{2\sigma_z^2}\right) + \exp\left(-\frac{(z+H)^2}{2\sigma_z^2}\right) \right]$$

C = Concentration of the chemical in air. [M/L<sup>3</sup>]  
 Q = Rate of chemical emission. [M/T]  
 u = Wind speed in x direction. [L/T]  
 σ<sub>y</sub> = Standard deviation in y direction. [L]  
 σ<sub>z</sub> = Standard deviation in z direction. [L]  
 y = Distance along a horizontal axis perpendicular to the wind. [L]  
 z = Distance along a vertical axis. [L]  
 H = Effective stack height. [L]

Figure D-1. Screenshot of tool main page

## 2.2 Stability Class

If needed, the visualization tool offers guidance for determining the atmospheric stability class based on the site conditions. The stability class guide is shown in **Figure D-2**.

- 1) Determine daytime insolation based on the solar elevation angle and sky cover. The solar elevation angle is calculated by the tool and output to the main page of the tool.
- 2) Find the atmospheric stability class based on the daytime insolation and surface wind speed. The surface wind speed is calculated by the tool based on the measured wind speed, wind speed measurement height, and landscape input by the user.

## Determine Stability Class

### 1. Find Daytime Insolation

Sky Cover	Solar Elevation Angle (degrees)			
	> 60	≤60 but >35	≤35 but >15	Nighttime (≤15)
1) Any amount of high, thin clouds	strong	moderate	slight	*
2) <50% cover by middle clouds	strong	moderate	slight	*
3) <50% cover by low clouds	strong	moderate	slight	*
4) >50% cover by middle clouds	moderate	slight	slight	*
5) >50% cover by low cloud	slight	slight	slight	*

### 2. Find Atmospheric Stability Class

Surface wind speed at a height of 10 m (m/s)	Daytime Insolation			Nighttime *	
	Strong	Moderate	Slight	Thinly overcast or ≥4/8 low cloud cover	≤3/8 cloud cover
<2	A	B	B	F	F
2 to 3	B	B	C	E	F
3 to 5	B	C	C	D	E
5 to 6	C	D	D	D	D
>6	C	D	D	D	D

Notes:

Assume neutral class (D) for all overcast conditions

Night is defined as the period from one hour before sunset to one hour after sunrise

**Figure D-2.** User guide to determine atmospheric stability class

## PLUME VISUALIZATION RESULTS

### 2.3 Output Concentration at a Given Location

The user can check the concentration of the final plume at any location in the generated figure. In the main page there is a location for the user to input a distance from the source in the x- and y-directions. The corresponding concentration is returned.

### 2.4 Total Plume Output

A screenshot of the Excel-calculated total plume for measured emissions from three compressors at Site 1, during Field Campaign 2 is shown in **Figure D-3**. Conditional formatting is used to color the plume based on methane concentration from grey at < 0.001 mg/m<sup>3</sup> (less than background concentrations) to dark red at > 100 mg/m<sup>3</sup>.

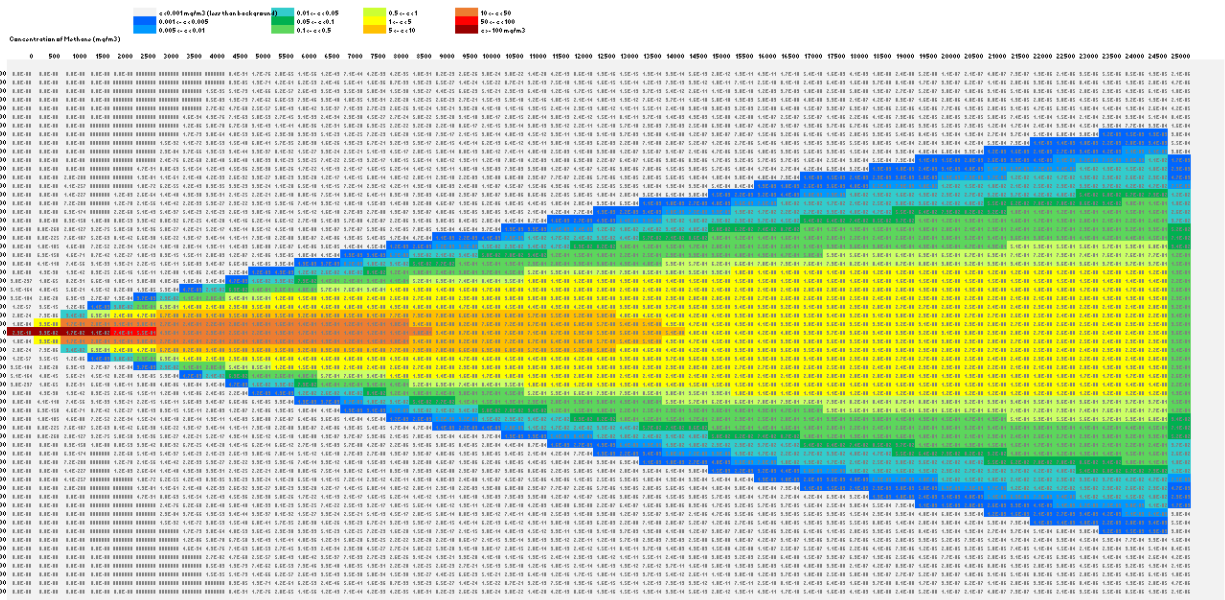


**Figure D-3. Output figure - Estimated methane plume from compressor emissions, Site 1, Field Campaign 2, 9 am**

### 3.0 REFERENCES

NOAA, 2010. NOAA Solar Calculations

---

# **APPENDIX F**

## **Emission Factors**

---



# APPENDIX F

## EMISSION FACTORS

Emission factors (EF) were developed for the small number of sites (four) visited in this study. The EFs presented are not assumed to be nationally representative. Population EFs for leaking and venting components, respectively, are presented in **Tables F-1** and **F-2**. Leaker EFs are presented in **Table F-3**. EFs from USEPA Subpart W are provided for comparison. EF calculation details can be found in Section 2.4.3; the equations used to calculate EFs are repeated here.

$$\text{Population } EF_{i,leak} = \frac{\sum ER_{i,measured,leak}}{N_{i,screened \text{ population}}} \quad \text{Equation 2-1}$$

$$\text{Population } EF_{i,vent} = \text{Average}(ER_{i,measured,vent}) \quad \text{Equation 2-2}$$

$$\text{Leaker } EF_i = \text{Average}(ER_{i,measured,leak}) \quad \text{Equation 2-3}$$

Where:

$ER_{i, measured, vent}$  = Measured methane emission rate of leaking component type  $i$  (scf/hr)

$ER_{i, measured, vent}$  = Measured methane emission rate of venting component type  $i$  (scf/hr)

$N_{i, screened \text{ population}}$  = Total number of component type  $i$  screened with the FLIR during field campaigns

**Table F-1. Population emission factors – Leaking components**

Component	EPA 2015 <sup>a</sup>	This Study		
	Pop. EF (scf/hr/comp)	Pop. EF (scf/hr/comp)	Component Population Count	Total Measured Emissions (scf/hr)
Valve	0.121	0.042	6,393	266
Connector	0.017	0.003	43,575	119
Open-Ended Line	0.031	-	-	0
Pressure Relief Valve	0.193	1.41	385	544

<sup>a</sup> From Table W-1A, USEPA Subpart W, 2015 update

**Table F-2. Population emission factors – Venting components**

Component	EPA 2015 <sup>a</sup>	This Study		
	Pop. EF (scf/hr/comp)	Pop. EF (scf/hr/comp)	Sample Count	Stdev of Emission Rate (scf/hr)
Low Continuous Bleed Pneumatic Device Vents	1.39	3.6	8	1.60
High Continuous Bleed Pneumatic Device Vents	37.3	38.1	8	26.9
Intermittent Bleed Pneumatic Device Vents	13.5	12.8	85	23.9
Pneumatic Pump	13.3	8.8	3	4.88
Compressor Distance Piece Vent	-	30.3	80	51.2
Compressor Rod Packing Vent	-	165.1	28	242

<sup>a</sup> From Table W-1A, USEPA Subpart W, 2015 update

**Table F-3. Leaker emission factors**

Component	EPA 2016 <sup>a</sup>	This Study		
	Leaker EF (scf/hr/comp)	Leaker EF (scf/hr/comp)	Measurement Count	Stdev (scf/hr)
Valve	4.9	9.14	23	15.3
Flange	4.1	5.24	8	8.45
Connector (other)	1.3	3.21	24	6.65
Open-Ended Line	2.8	-	0	-
Pressure Relief Valve	4.5	68.0	8	145
Pump Seal	3.7	-	0	-
Other	4.5	3.53 <sup>b</sup>	14	6.17

<sup>a</sup> From Table W-1E, USEPA Subpart W, 2016 update

<sup>b</sup> Other category contains regulators, gauges, meters

Using the density of methane (19.17 g/ft<sup>3</sup>), the measured methane emissions from the four facilities can be converted from volumetric flow rate (scf/hr) to mass flow rate (kg/hr). The mass flow rate ranged from 3.11 kg/hr (Site 3, FC2) to 36.2 kg/hr (Site 1, FC1).

**Table F-4. Mass flow rates**

Measured emissions - kg CH <sub>4</sub> /hr				
Field Campaign	Site 1	Site 2	Site 3	Site 4
1	36.2	12.5	9.25	11.2
2	11.5	3.89	3.11	5.52
3	5.69	14.1	8.58	18.5
4	6.67	8.13	4.19	20.6

---

# **APPENDIX G**

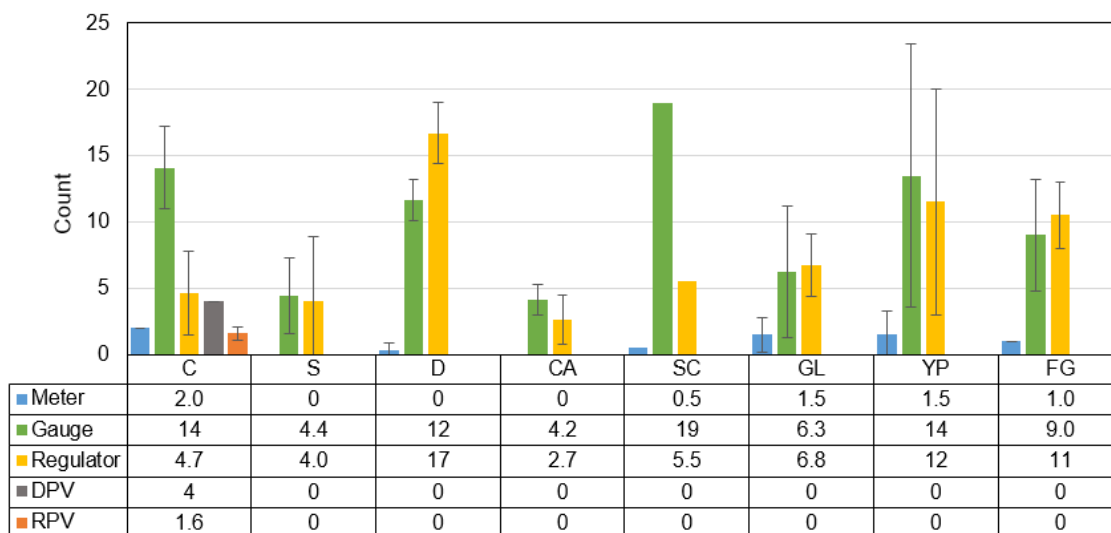
## **Additional Component Count Results**

---

## APPENDIX G

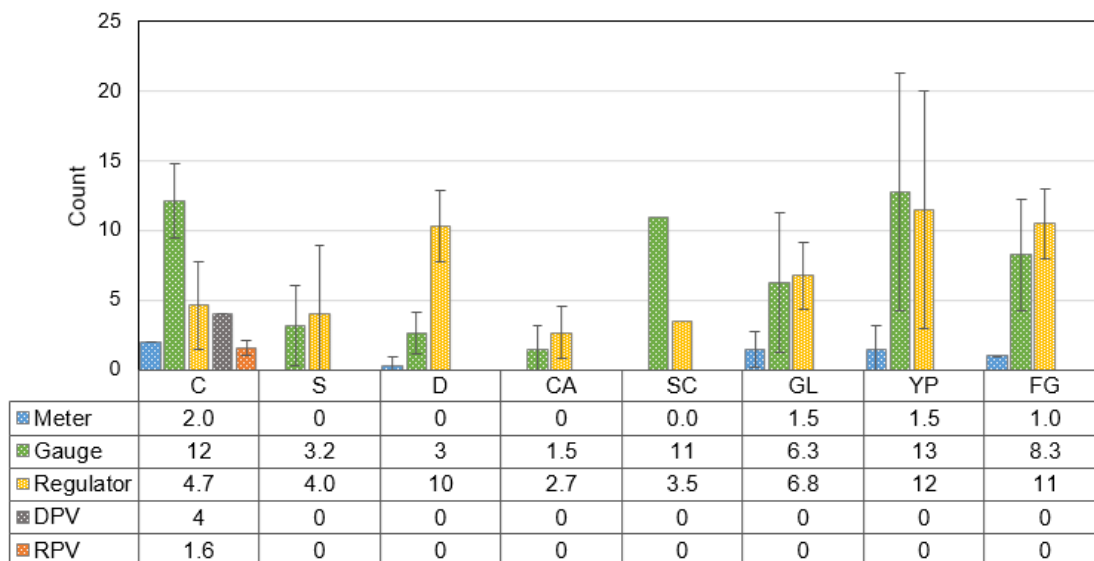
### ADDITIONAL COMPONENT COUNT RESULTS

Component counts for component categories not presented in Section 3.1 (meters, gauges, regulators, DPVs and RPVs) are shown in **Figures G-1** and **G-2**.



Error bars are standard deviations. Abbreviations: DPV = distance piece vent, RPV = rod packing vent, C = compressor, S = separator, D = dehydrator, CA = coalescer, SC = slug catcher, GL = gathering line, YP = yard piping, FG = fuel gas skid

**Figure G-1.** Average component count by equipment type for additional component categories, including gas and liquid lines



Error bars are standard deviations. Abbreviations: DPV = distance piece vent, RPV = rod packing vent, C = compressor, S = separator, D = dehydrator, CA = coalescer, SC = slug catcher, GL = gathering line, YP = yard piping, FG = fuel gas skid

**Figure G-2.** Average component count by equipment type for additional component categories, only gas lines